Identification of feedback mechanisms from horizontal cells to cone photoreceptors in the mouse retina using two-photon calcium imaging and pharmacology

Dissertation

zur Erlangung des Grades eines

Doktors der Naturwissenschaften

der Mathematisch-Naturwissenschaftlichen Fakultät

und

der Medizinischen Fakultät

der Eberhard-Karls-Universität Tübingen

vorgelegt von

Robin Kemmler

März – 2014

Tag der mündlichen Prüfung:	18. Juni 2014
Dekan der Math.-Nat. Fakultät:	Prof. Dr. W. Rosenstiel
Dekan der Medizinischen Fakultät:	Prof. Dr. I. B. Autenrieth
1. Berichterstatter:	Prof. Dr. Thomas Euler
2. Berichterstatter:	Prof. Dr. Frank Schaeffel
Prüfungskommission:	Prof. Dr. Thomas Euler
	Prof. Dr. Frank Schaeffel
	Prof. Dr. Matthias Bethge
	Prof. Dr. Marlies Knipper

Ich erkläre, dass ich die zur Promotion eingereichte Arbeit mit dem Titel „Identification of feedback mechanisms from horizontal cells to cone photoreceptors in the mouse retina using two-photon calcium imaging and pharmacology“ selbstständig verfasst, nur die angegebenen Quellen und Hilfsmittel benutzt und wörtlich oder inhaltlich übernommene Stellen als solche gekennzeichnet habe. Ich versichere an Eides statt, dass diese Angaben wahr sind und dass ich nichts verschwiegen habe. Mir ist bekannt, dass die falsche Abgabe einer Versicherung an Eides statt mit Freiheitsstrafe bis zu drei Jahren oder mit Geldstrafe bestraft wird.

Tübingen, den _____ _____

Datum Unterschrift

Acknowledgement

I particularly thank **Prof. Dr. Thomas Euler** and **Dr. Timm Schubert** for the excellent supervision and continuous support of this project. I am especially grateful for having had the opportunity to present this project on various international conferences and exchange myself with other experts of this field.

I thank **Prof. Dr. Matthias Bethge** and **Prof. Dr. Frank Schaeffel** for being part of my thesis advisory committee, and **Prof. Dr. Frank Schaeffel** for his agreement to evaluate this thesis as a second referee.

I thank our collaborators **PD Dr. Karin Dedek** and **Dr. Konrad Schultz** from Oldenburg for their contribution to this project by performing the electron microscopy experiments.

I thank **Prof. Dr. Maarten Kamermans** for helpful discussions and proof-reading of the manuscript.

Many thanks go to **Dr. Thomas Baden** who helped me especially with Igor Pro programming and who offered me the possibility to teach in his “TReND”-project in Uganda.

I thank **Dr. “Steven” Chang** for his help with programming the light stimulation protocols and **Dmytro Velychko** for giving me advice in case of theoretical problems with data analysis.

Many thanks to **Valeska Botzenhardt**, **Dr. Tobias Breuninger**, **Gordon Eske**, **Katrin Franke**, **Manoj Kulkarni**, **Miro Rezac**, **Dr. Tao Wei** and **Antje Wielinski** for always being there in case of problems, and for your friendship.

Last but not least I am very grateful to **Antonia v. Saint Paul** and my family and friends for their warm support during all these years.

Table of Contents

Table of Figures

Abbreviations

AAV	adeno-associated virus
AMPA	α-amino-3-hydroxy-5-methyl-4-isoxazolepropionic acid
BC	bipolar cell
Ca^{2+}	calcium ion
CBX	Carbenoxolone
cGMP	cyclic guanosine monophosphate
CNGC	cyclic nucleotide-gated channel
cone	cone photoreceptor
eCFP	enhanced cyan fluorescent protein
ERG	electroretinography
FRET	fluorescence/Förster resonance energy transfer
GABA	γ-aminobutyric acid
GDP	guanosine diphosphate
G-Protein	GTP-binding protein
GTP	guanosine triphosphate
Gz	Gabazine (SR-95531)
HC	horizontal cell
hemichannel	hemi-gap junction channel
HEPES	4-(2-hydroxyethyl)piperazine-1-ethanesulfonic acid
iGluR	ionotropic glutamate receptor
IS	inner segment
LCoS	liquid crystal on silicon display
LED	light-emitting diode

M-opsin/cone	medium wavelength-sensitive opsin/cone
Na^+	sodium ion
NBQX	6,7-dinitroquinoxaline-2,3-dione
NCX	sodium-calcium exchanger
OPL	outer plexiform layer
OS	outer segment
PMCA	plasma membrane Ca^{2+}-ATPase
PMT	photomultiplier tube
rod	rod photoreceptor
SD	standard deviation
SEM	standard error of the mean
S-opsin/cone	short wavelength-sensitive opsin/cone
TPMPA	(1,2,5,6-Tetrahydropyridin-4-yl)methylphosphinic acid
VGCC	voltage-gated calcium channel

1 Abstract (English)

In neurons, transmitter release from axon terminals is directly linked to the calcium level (Thoreson, 2007; Jackman et al., 2009). Thus, one key mechanism to control transmitter release is to modulate presynaptic calcium by synaptic feedback (reviewed in Kamermans and Fahrenfort, 2004). "Traditional" GABAergic feedback but also more unconventional mechanisms like ephaptic and pH-mediated feedback are found in many parts of the central nervous system (reviewed in Voronin, 2000; Chesler, 2003). However, little is known if these mechanisms operate in parallel to control transmitter release – that is, form a complex feedback system –, and if so, to what extent they fulfil distinct functions. An excellent system to study such feedback mechanisms is the photoreceptor synapse in the retina.

This study investigated how the glutamatergic output of cone photoreceptors (cones) in the mouse retina is shaped by different feedback mechanisms from postsynaptic GABAergic horizontal cells using a combination of two-photon calcium imaging and pharmacology at the level of individual cone axon terminals. I provide evidence that ephaptic feedback sets the cone output gain by defining the basal calcium level, a mechanism that may be crucial for adapting cones to the ambient light level. In contrast, pH-mediated feedback did not modulate the cone basal calcium level, but affected the size and shape of light-evoked cone calcium signals in a contrast-dependent way: low contrast light responses were amplified, whereas high contrast light responses were reduced. Finally, I provide functional evidence that GABA shapes light-evoked calcium signals in cones. Because we could not localize ionotropic GABA receptors on cone axon terminals using electron microscopy, this suggests that GABA may act through GABA auto-receptors on horizontal cells, thereby possibly modulating ephaptic and/or pH-mediated feedback.

Taken together, the results of my thesis suggest that at the cone synapse, ephaptic and pH-mediated feedback may fulfil distinct functions to adjust the output of cones to changing ambient light levels and stimulus contrasts, and the efficacy of these feedback mechanisms is likely modulated by GABA release in the outer retina. Such an intricate feedback system at the first synapse of our visual system could be important for reliable information transfer from one neuron to the next. It is possible that similarly complex synapses with different feedback mechanisms also play a role in other parts of the nervous system.

Abstract (German)

Die Transmitter-Freisetzung aus den Axonendigungen von Nervenzellen wird direkt durch die intrazelluläre Kalziumkonzentration kontrolliert (Thoreson, 2007; Jackman et al., 2009). Daher stellt die Modulation des präsynaptischen Kalziumniveaus durch synaptische Rückkopplung (Feedback) einen Schlüsselmechanismus dar, um die Transmitter-Freisetzung zu kontrollieren (Review: Kamermans and Fahrenfort, 2004). „Traditioneller" GABAerger Feedback, aber auch unkonventionelle Mechanismen wie ephaptischer und pH-vermittelter Feedback, kommen in vielen Teilen des zentralen Nervensystems vor (Review: Voronin, 2000; Chesler, 2003). Es ist jedoch nicht bekannt, ob diese Mechanismen zur Kontrolle der Transmitter-Freisetzung parallel arbeiten (möglicherweise mit jeweils unterschiedlichen Funktionen) und wenn ja, ob sie damit ein komplexes Feedbacksystem bilden. Die Photorezeptorsynapse in der Retina bietet eine ausgezeichnete Möglichkeit, um solche Feedbackmechanismen zu untersuchen.

In dieser Studie wurde untersucht, wie das glutamaterge Ausgangssignal von Zapfenphotorezeptoren (Zapfen) in der Mäuseretina durch die verschiedenen Feedbackmechanismen kontrolliert wird, die von den postsynaptischen, GABAergen Horizontalzellen ausgehen. Dazu wurden lichtinduzierte Kalziumsignale in individuellen Zapfen-Axonendigungen mittels der Zweiphotonenmikroskopie gemessen und gleichzeitig unterschiedliche Feedbackmechanismen selektiv mit Pharmaka blockiert. Die so gewonnenen Daten deuten darauf hin, dass der ephaptische Feedback die Verstärkung des Zapfen-Ausgangssignals bestimmt, indem er das Ruhe-Kalziumniveau definiert. Dieser Mechanismus könnte entscheidend daran beteiligt sein, Zapfen an die Umgebungshelligkeit anzupassen. Im Gegensatz dazu veränderte der pH-vermittelte Feedback das Ruhe-Kalziumniveau nicht; er modulierte jedoch Größe und Form der lichtinduzierten Kalziumsignale in einer kontrastabhängigen Weise: Lichtantworten auf kleinere Kontraste erschienen verstärkt, während Lichtantworten auf größere Kontraste abgeschwächt wurden. Außerdem zeigt es sich, dass auch GABA die lichtinduzierten Kalziumantworten in Zapfen moduliert. Da wir mit Hilfe von Elektronenmikroskopie keine ionotropen GABA-Rezeptoren auf Zapfen-Axonendigungen finden konnten, aktiviert GABA vermutlich GABA-Autorezeptoren auf Horizontalzellen und kann dadurch den ephaptischen und/oder den pH-vermittelten Feedback modulieren.

Zusammengefasst deuten die Ergebnisse meiner Arbeit darauf hin, dass der ephaptische und der pH-vermittelte Feedback unterschiedliche Funktionen besitzen, um das Ausgangssignal der Zapfen an sich verändernde Umgebungsbedingungen (Helligkeit, Kontraste) anzupassen. Die Wirksamkeit dieser Feedback-Mechanismen wird dabei wahrscheinlich zusätzlich über GABA-Ausschüttung in der äußeren Retina moduliert. Es ist anzunehmen, dass ein solch komplexes Feedbacksystem an der ersten Synapse

unseres visuellen Systems für die zuverlässige Informationsweitergabe von den Photorezeptoren an die postsynaptischen Neurone äußerst wichtig ist. Ähnlich komplexe Synapsen mit unterschiedlichen Feedbackmechanismen könnten auch in anderen Teilen des Nervensystems eine Rolle spielen.

2 Introduction

Vision is the main means by which humans sense their environment. This is illustrated by the fact that visual information processing occupies approximately 50% of our brain (Van Essen, 2004). Light from the outside world is projected by the eye's optical system onto the photoreceptor layer in the retina. The photoreceptor cells convert the incoming stream of photons into electrochemical signals. These signals are then transmitted to different microcircuits within the retina where important features of the visual scene like brightness, contrast, "colour" and movement of objects are extracted. Finally, the different pieces of visual information are sent in an encoded form via the axons of the ganglion cells, the output neurons of the retina, to higher centres of the central nervous system (reviewed in Wässle, 2004). There, the information is "bound together" to form an overall perception.

Our visual system functions over a range of ambient light levels covering at least ten orders of magnitude (Rodieck, 1998), a range that considerably exceeds the operating range of neurons. The neurons' responses to visual stimuli therefore have to be adjusted to the ambient light level – a process referred to as light adaptation. Adaptation ensures that small light signals are amplified and can be "extracted" from the noise, whereas large light signals are attenuated to prevent saturation of the neurons' responses. Many of the mechanisms that contribute to light adaptation already occur at the level of the photoreceptors. Besides intrinsic adaptive mechanisms, i.e. at the level of the transduction cascade, these cells receive feedback from postsynaptic horizontal cells. This feedback is considered an important factor in controlling the gain of the photoreceptors' output signal as a function of prevailing ambient light level and stimulus contrasts.

This thesis focuses on the feedback from horizontal cells to cone photoreceptors in the mouse retina. The mouse is an increasing popular model to study visual information processing because of the availability of genetic tools to selectively label cell types (reviewed in Huberman and Niell, 2011), e.g. cone photoreceptors (Wei et al., 2012). Since many visual processing steps are conserved among species, e.g. between mice and humans, it has thus become possible – using the mouse retina as a model system – to gain insight into the synaptic interactions that underlie our vision.

2.1 Structure of the mammalian retina

The mammalian retina (Figure 1) harbours five neuronal cell classes, i.e. photoreceptors, horizontal cells, bipolar cells, amacrine cells, and ganglion cells (reviewed in Wässle, 2004). The cells are organized in a

laminar way, with the somata located in *nuclear layers* and synaptic connections between cells located in *plexiform layers*. The somata of the photoreceptor cells reside in the outer nuclear layer (ONL), those of the bipolar, horizontal and amacrine cells in the inner nuclear layer (INL), and those of the ganglion cells, together with some so-called "displaced" amacrine cells, in the ganglion cell layer (GCL). The synapses between photoreceptors, bipolar and horizontal cells are situated in the outer plexiform layer (OPL), those between bipolar, amacrine and ganglion cells in the inner plexiform layer (IPL). After transduction of light into electrical signals by the photoreceptors, the visual information is transmitted to the bipolar cells and finally to the output neurons of the retina, i.e. the ganglion cells (vertical pathway). On its way through the retina, the information is importantly modified by lateral interactions provided by horizontal cells in the outer retina and amacrine cells in the inner retina (lateral pathway). In addition, the physiological function of the retinal neurons is supported by glial Müller cells (Newman and Reichenbach, 1996).

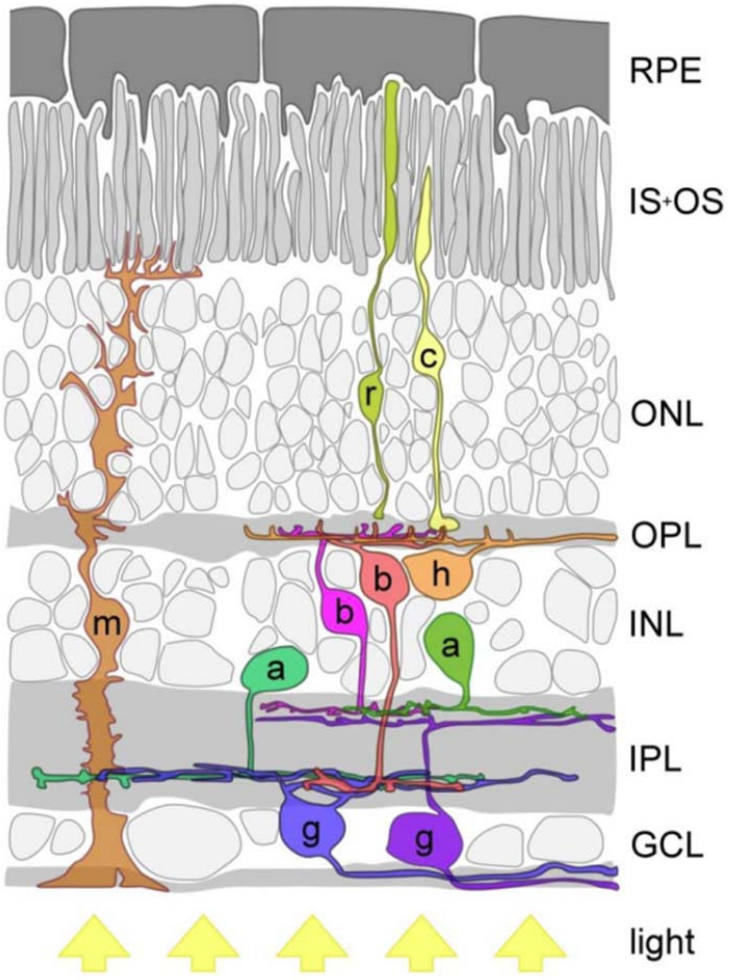

Figure 1: Schematic structural organization of the mammalian retina
The mammalian retina has a layered structure and is composed of the retinal pigment epithelium (RPE), outer nuclear layer (ONL), outer plexiform layer (OPL), inner nuclear layer (INL), inner plexiform layer (IPL) and ganglion cell layer (GCL). The retina hosts rod (r) and cone (c) photoreceptors, horizontal cells (h), bipolar cells (b), amacrine cells (a), ganglion cells (g) and specialized glia, the Müller cells (m). Photoreceptors consist of an outer segment (OS), an inner segment (IS), a soma, an axon and a synaptic terminal – the latter which connects with horizontal and bipolar cell dendrites. The outer segment is invaginated into the RPE. Note the inverted structure of the mammalian retina: light enters the tissue from the ganglion cell side and thus has to pass all the layers, before reaching the light-sensitive outer segments of the photoreceptors. Modified from Euler et al. (2009).

2.2 Photoreceptors (rods and cones)

2.2.1 Classification

Vertebrate photoreceptors can be divided by morphology and function into rods and cones (Luo et al., 2008). Rods are very light sensitive but slow and rather noisy; they mediate vision at dim illumination (e.g. “starlight”; scotopic vision), whereas cones are less light sensitive but fast and overall provide a better signal-to-noise ratio compared to rods; they mediate vision during daylight (photopic vision). At twilight, both rods and cones are thought to contribute to vision (mesopic vision).

Rods and cones are quite similar in structure (reviewed in Mustafi et al., 2009): They consist of four compartments (Figure 2), i.e. an outer segment, an inner segment, a soma, an axon and a synaptic terminal – each of them subserving different functions: The *outer segment* contains the visual pigment for transducing the incoming light energy into a cellular response using a sophisticated biochemical machinery (see 2.2.2). The *inner segment* contains the metabolic machinery (i.e. mitochondria) to meet the high energy demand of photoreceptors. The soma with the nucleus is involved in gene expression. The *axon and axon terminal* are concerned with relaying the light signals generated in the outer segment to the postsynaptic neurons, namely bipolar and horizontal cells.

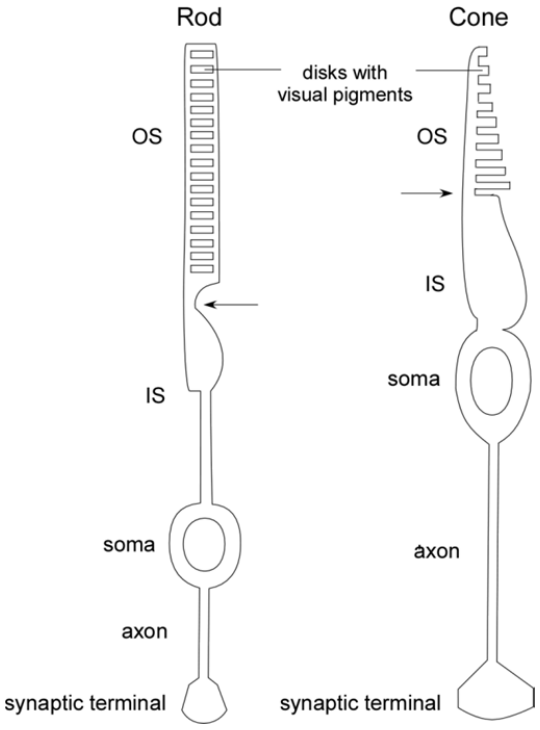

Figure 2: Morphology of rod and cone photoreceptors
Rods and cones can be subdivided into an outer segment (OS), an inner segment (IS), a soma, an axon and a synaptic terminal. Outer and inner segments are connected by a thin intracellular “bridge”, the so-called cilium (arrow). The outer segments contain membranous disks, in which the visual pigments for light reception are embedded. In rods, these membranous disks are pinched off from the plasma membrane, whereas cones possess open disks formed by invaginations of the cell membrane.

For light reception, photoreceptors possess visual pigments embedded in the membranous disks of the outer segment. Visual pigments in vertebrate photoreceptors generally consist of the light-absorbing 11-*cis* retinal that is incorporated in a transmembrane protein, i.e. the opsin. The opsin tunes the spectral sensitivity of the retinal (reviewed in Stenkamp et al., 2002). Rods possess only one type of opsin, the rhodopsin. In contrast, cones in most mammals (including the mouse) use two different types of (cone) opsins (reviewed in Jacobs, 1993): Cones in the mouse expressing the S- (short wavelength-sensitive) opsin have a high sensitivity to blue light (peak sensitivity at ~360 nm), whereas those expressing the M- (medium wavelength-sensitive) opsin (M-cones) have a high sensitivity to green light (peak sensitivity at ~510 nm) (Jacobs et al., 1991). Human cones express, in addition to S- and M-opsins, a third spectral type of opsin, an L- (long wavelength-sensitive) opsin. Comparing the activity between different spectral types of cones forms the basis of colour vision. Humans are therefore trichromats who can distinguish between blue, green and red hues – in contrast to mice which are dichromats.

Like in most mammals, cones represent only a small percentage of the total photoreceptor population in mice (<3%; (Jeon et al., 1998)). Thus, studying the function of cones in the mouse is greatly facilitated by using (transgenic) animals in which cones are selectively labelled (Wei et al., 2012).

2.2.2 Phototransduction

Photoreceptors use a biochemical amplification cascade to transduce light into a reliable cellular response, i.e. a depolarization in darkness and a hyperpolarization upon light stimulation. The membrane potential of photoreceptors is modulated by light in a graded way: the brighter the light, the bigger the light-induced hyperpolarization. Depending on the incoming light intensity, the balance between synthesis and degradation of the cyclic nucleotide cGMP in the outer segment is changed (Figure 3). cGMP gates non-selective cation channels (cyclic nucleotide-gated channels, CNGCs) (Yau and Nakatani, 1984).

In darkness, cGMP synthesis (mediated by the enzyme guanylate cyclase) is favoured over cGMP degradation (mediated by the enzyme phosphodiesterase) and thus cGMP levels are high. As a consequence, CNGCs mediate a continuous influx of cations such as Na^+ and Ca^{2+} into the outer segment, thus depolarizing the photoreceptor. The depolarization is electrotonically relayed to the synaptic terminal, which, as a consequence, continuously releases glutamate in darkness (see 2.6).

Light stimulation activates the phototransduction cascade and thereby tips the balance between cGMP synthesis and degradation towards degradation (Hodgkin and Nunn, 1988). In more detail (reviewed in Burns and Baylor, 2001), photons arriving in the photoreceptor's outer segment trigger the isomerization of 11-*cis* retinal to all-*trans* retinal, thereby changing the conformation of the covalently-bound opsin (a prototypical G-Protein coupled receptor). This activates the G-protein transducin (by exchanging GDP for GTP) and subsequently the enzyme phosphodiesterase. The phosphodiesterase in turn hydrolyses cGMP and therefore the CNGCs close. As a consequence, the photoreceptor hyperpolarizes and reduces glutamate release from the synaptic terminal. The phototransduction cascade is terminated by inactivation of all active elements in the signalling cascade (reviewed in Fu and Yau, 2007). The "light-consumed" form of retinal, i.e. all-*trans*-retinal, is recycled in the retinal pigment epithelium and transported back to the outer segments to finally reform functional visual pigments (reviewed in Steinberg, 1985).

Mechanistically, phototransduction is very similar in rods and cones. However, some functional differences between rods and cones can be explained by quantitative differences at some steps during the cascade. For example, rods are more light sensitive than cones and respond even to single photons (Baylor et al., 1979), as they use a longer photon integration time and higher phototransduction gain. Cones, in contrast, use a shorter photon integration time and lower phototransduction gain and thus have a higher temporal resolution, which enables them to respond better to fast changes in the visual environment (moving objects).

Phototransduction in both rods and cones is subject to modulation by Ca^{2+}. The reduction of Ca^{2+} influx through CNGCs during light triggers multiple intrinsic inhibitory feedback pathways within the outer segment of the photoreceptors (reviewed in Pugh et al., 1999). This avoids photoreceptor saturation and thus keeps the photoreceptors responsive over a broad range of ambient light levels. Cones adapt to background light much more dramatically than rods (Nakatani and Yau, 1988; Matthews et al., 1990) and therefore remain functional also at very bright ambient light levels. Besides intrinsic light adaptive processes within the photoreceptors, postsynaptic horizontal cells help to adjust the operating range of the photoreceptors to the ambient light (Burkhardt, 1995) by modulating the activity of the voltage-gated calcium channels (VGCCs) in the output structure of the photoreceptors, i.e. the axon terminal (reviewed in Kamermans and Fahrenfort, 2004).

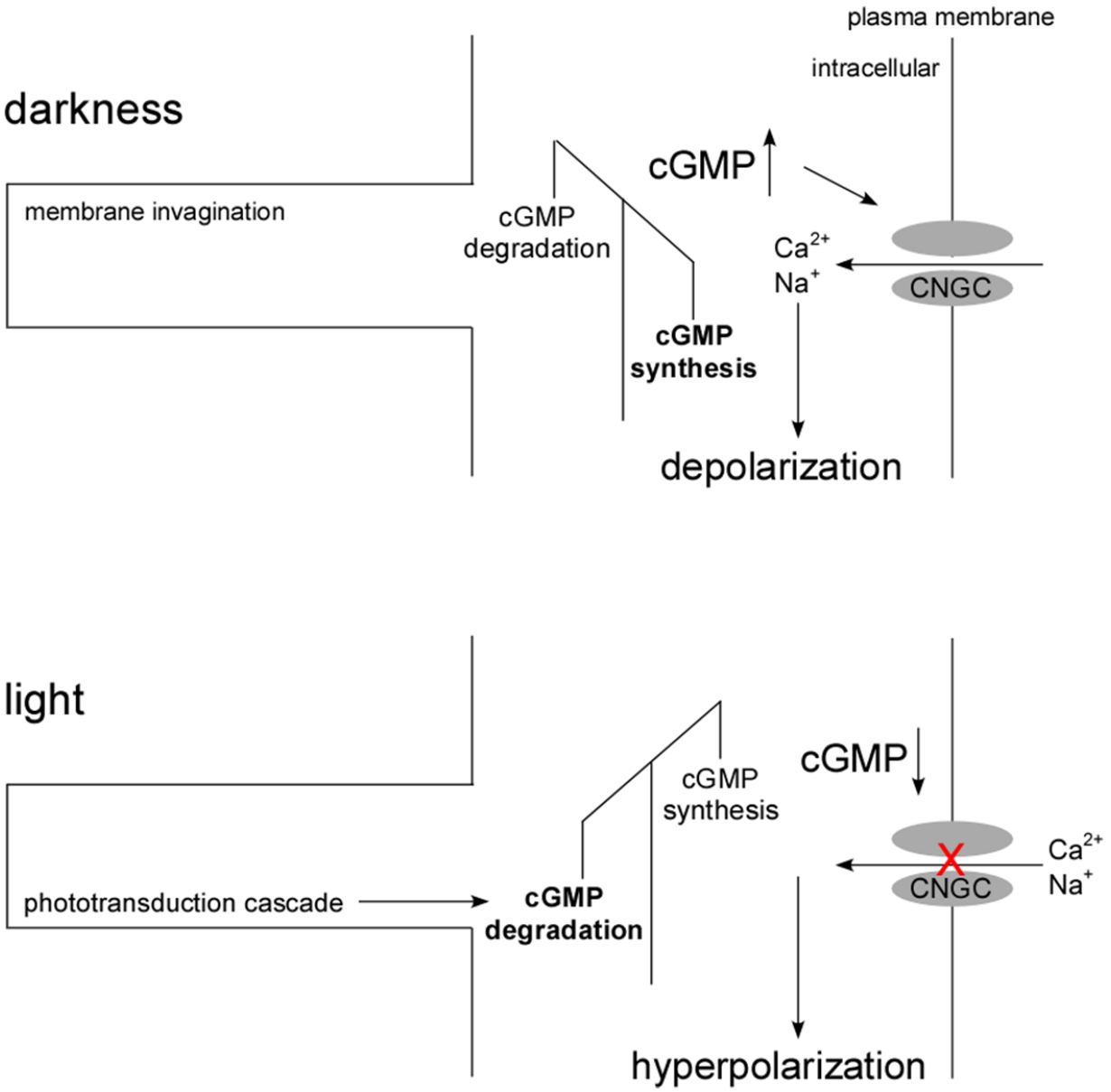

Figure 3: Phototransduction cascade

In darkness, there is a high level of the cyclic nucleotide cGMP in the outer segment of photoreceptors. cGMP opens cyclic nucleotide-gated channels (CNGCs), which mediate an influx of Na^+ and Ca^{2+} into the outer segment, thus depolarizing the photoreceptor. Upon light stimulation, the phototransduction cascade is initiated (for details, see text), which reduces the cGMP level. As a consequence, CNGCs close, which results in a hyperpolarization. This hyperpolarization is relayed to the synaptic terminal, where glutamate release is reduced.

2.3 Horizontal cells

2.3.1 Classification

Horizontal cells, which are postsynaptic to the photoreceptors, have been morphologically classified into axon-less (A-type) and axon-bearing (B-type) horizontal cells (Figure 4A) (Smith, 2008). A-type horizontal cells have a dendritic arbour forming synapses exclusively with cones; B-type horizontal cells, in contrast, use a dendritic arbour to contact cones (cat: ~100), and, in addition, an axon terminal system to connect with rods (cat: ~2000) (Kolb, 1974). Despite their differential synaptic connectivity, the horizontal cell dendritic arbour and axon terminal system effectively receive a mixture of rod and cone inputs because of extensive rod-cone coupling (Tsukamoto et al., 2001), and signal transmission via the axon that connects the two compartments (Trümpler et al., 2008). Most mammals possess both horizontal cell types; however, in the mouse and in other rodents only a B-type has been described (Figure 4B) (Peichl and Gonzalez-Soriano, 1994). The cone-to-horizontal cell ratio, however, is similar in the species with and without A-type cells (Peichl and Gonzalez-Soriano, 1994).

Mouse horizontal cells contact all cones within their dendritic field, and each individual cone is contacted by several horizontal cells (Schubert et al., 2010). Because horizontal cells are extensively coupled by gap junctions consisting of Connexin 57 (Shelley et al., 2006; Janssen-Bienhold et al., 2009), they form a large network, and therefore the receptive field of a horizontal cell is larger than its dendritic field. Importantly, the amount of coupling is modulated by light via neuromodulators including dopamine (Lankheet et al., 1990; Hampson et al., 1994; Xin and Bloomfield, 1999; He et al., 2000), adjusting the horizontal cell's response properties and strength of feedback to the photoreceptors dependent on the ambient light level (see 2.7.1).

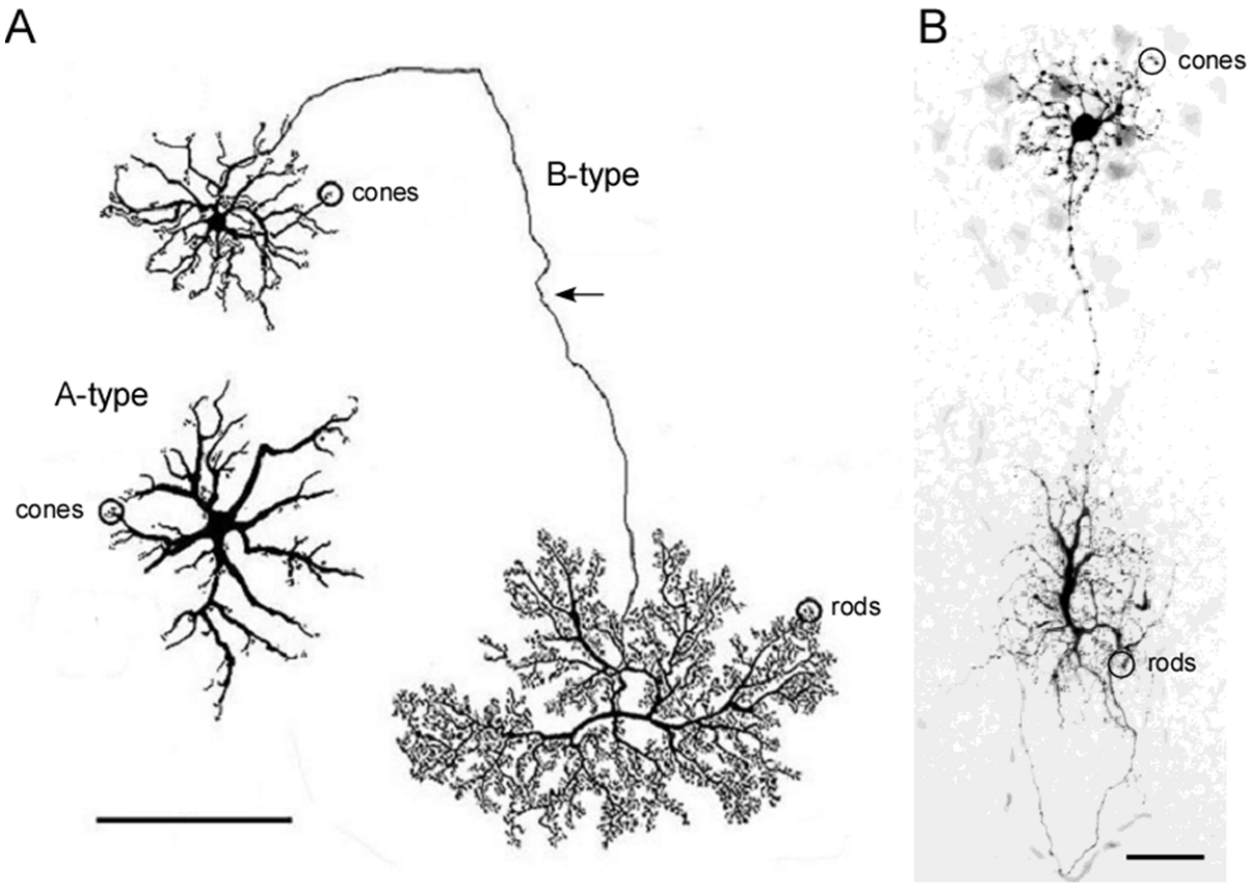

Figure 4: Morphology of horizontal cells
A Golgi-stained horizontal cell types in the cat: The A-type has a large and sparse dendritic tree contacting exclusively cones. The B-type, in contrast, consists of two compartments that are linked by an axon (arrow), i.e. a dendritic tree to connect with cones (it is smaller and bushier than the dendritic tree of the A-type cell), and an axon terminal system to connect with rods. Scale bar: 100 µm. Modified from Kolb (1974). ***B*** Neurobiotin-injected horizontal cell in the mouse. Note that mice possess only a single type of horizontal cell that corresponds to the B-type (compare with *A*). Scale bar: 20 µm. Modified from He et al. (2000).

2.3.2 Functions

Horizontal cells form sign-conserving synapses with the photoreceptors, as they express ionotropic glutamate receptors of the AMPA/kainate type (Schubert et al., 2006; Ströh et al., 2013). Therefore, they hyperpolarize in response to light increments and depolarize to light decrements. Horizontal cells in turn provide feedback to photoreceptors and feed-forward to bipolar cells; the mechanisms underlying horizontal cell feedback to cones are in the focus of this thesis. As horizontal cells form a large coupled network, they sample light signals from many photoreceptors and thus can provide an estimate of the

ambient light level. This ambient light level is subtracted from local changes in light intensity by feeding back to the photoreceptors, thereby contributing to the generation of the antagonistic centre-surround receptive field structure of retinal neurons (see 2.7.1). Such a subtractive mechanism operates in different domains (reviewed in Thoreson and Mangel, 2012): *(i)* in the *spatial* domain, subtraction of the mean light level from local contrasts contributes to contrast enhancement (Ratliff and Hartline, 1959), *(ii)* in the *temporal* domain, subtraction of on-going changes in the ambient light level (e.g. during the course of the day) adjusts the operating range of retinal neurons to dimmer or brighter conditions (light adaptation) (Burkhardt, 1995), and *(iii)* in the *spectral* domain, subtraction of the ambient light level with changing spectral distribution has been suggested to contribute to a phenomenon called colour constancy, i.e. objects appear to have the same colour irrespective of (limited) spectral changes in illumination (Vanleeuwen et al., 2007).

Noteworthy, horizontal cells appear to play a role in generating colour opponency, as has been described in the primate: Here, S-cones display – besides a "blue" centre – a "yellow" surround, as they receive inhibitory feedback from a specific type of horizontal cell that is preferentially driven by M- and L-cones (Packer et al., 2010); such a colour opponency-generating mechanism involving horizontal cell to photoreceptor feedback has been recently confirmed in a non-primate species, the rabbit (Mills et al., 2014).

2.4 Bipolar cells

The output signal of the photoreceptors – after adjustment by the horizontal cells – represents the input signal to the bipolar cells. In the mammalian retina, there are ~12 different bipolar cell types (reviewed in Masland, 2012), relaying the photoreceptor signal to the inner retina, where they form glutamatergic synapses with amacrine and ganglion cells. Bipolar cells are mainly classified based on *(i)* their light sensitivity range: rod bipolar cells contact rods, whereas cone bipolar cells contact dominantly cones (Wu et al., 2000). *(ii)* the "sign" of their response: OFF-bipolar cells *conserve* the photoreceptor signal, as they express ionotropic glutamate receptors of the AMPA/kainate type (Euler et al., 1996). Consequently, they – like the photoreceptors – hyperpolarize to stimuli that are brighter than the background light level, and depolarize to stimuli that are darker than the background light level. ON-bipolar cells, in contrast, respond in the reverse way, as they express the *sign-inverting* metabotropic glutamate receptor mGluR6 (Masu et al., 1995). Dividing the photoreceptor signal into an ON- and OFF channel is crucial, as it doubles the dynamic range of retinal neurons and therefore helps to improve the

encoding of visual information. *(iii)* their temporal properties: depending on the type of dendritic and axonal receptors, and the network interactions with horizontal and amacrine cells, bipolar cells respond to light e.g. in a more transient or sustained manner (DeVries, 2000; Eggers and Lukasiewicz, 2011 (review)). *(iv)* their spectral preference: selective connectivity to specific cone types tunes bipolar cells to a specific "colour" (Haverkamp et al., 2005; Breuninger et al., 2011).

Bipolar cells are best excited by small spots of light illuminating their receptive field centre, which approximately corresponds to their dendritic field size. Illuminating their receptive field surround in addition, inhibits the centre response (centre-surround antagonism) (see 2.7.1) (Barlow, 1953; Kuffler, 1953; Werblin and Dowling, 1969; Dacheux and Miller, 1981) – a mechanism that enhances the neural representation of contrast (Ratliff and Hartline, 1959). Horizontal cells significantly contribute to the formation of the bipolar surround, especially indirectly by feedback to the photoreceptors (see 2.7.2), but possibly also directly by feed-forward input to the bipolar cells (reviewed in Wu, 1992). Amacrine cells further complement the bipolar cell surround by an inner retinal component (Cook and McReynolds, 1998; McMahon et al., 2004; Ichinose and Lukasiewicz, 2005). The relative contribution of horizontal *vs.* amacrine cells to the bipolar cells' receptive field surround varies dynamically with background intensity and type of stimulus (Ichinose and Lukasiewicz, 2005). In summary, each type of bipolar cell represents a distinct information channel that is concerned with different aspects of the visual scene. Such parallel processing at the bipolar cell level is fundamental to generate (postsynaptic) ganglion cells that respond to specific features of the visual scene (see 2.5.2) (reviewed in Masland, 2012).

2.5 The inner retina

Although this thesis focuses on the outer retina comprising photoreceptors and horizontal cells, it is necessary to outline the processing steps downstream to the bipolar cells; here, amacrine and ganglion cells are involved.

2.5.1 Amacrine cells

Amacrine cells represent the retinal cell class with the most morphological and probably also functional diversity: in the mammalian retina, there are ~30 morphologically identified types of amacrine cells (reviewed in Masland, 2012), but so far only some of them have been well described at the functional

level. Amacrine cells are mostly inhibitory interneurons, using generally GABA or glycine and often an additional co-transmitter or -modulator (Marc et al., 1995). They are driven by bipolar cells and other amacrine cells, and provide feedback inhibition to bipolar cells as well as feed-forward inhibition to ganglion cells. Most cell types use their dendrites for synaptic input and output, which suggests an extensive amount of dendritic processing. Like the horizontal cells in the outer retina, amacrine cells are involved in lateral signal processing and thus contribute to the centre-surround structure of the visual system (see 2.7.1). Amacrine cells help to create ganglion cell types that encode specific features of the visual scene. The best studied amacrine cell types are *(i)* the AII cells involved in funnelling rod bipolar signals into cone pathways (reviewed in Bloomfield and Dacheux, 2001), *(ii)* the A17 cells mediating reciprocal feedback inhibition and gain control of rod bipolar cells (reviewed in Schubert and Euler, 2010), *(iii)* the dopaminergic amacrine cells involved in adjusting the signal processing of retinal neurons to the ambient light level (Herrmann et al., 2011), *(iv)* the A1 polyaxonal amacrine cells supporting the segregation of object motion from background motion (Ölveczky et al., 2003), and *(v)* the starburst amacrine cells involved in the detection of motion direction (directional selectivity) (Euler et al., 2002).

2.5.2 Ganglion cells

Ganglion cells are the output neurons of the retina and they receive excitatory input from bipolar cells and inhibitory input from amacrine cells. In the mammalian retina, there are ~20 types of ganglion cells, based on morphological and functional characteristics (reviewed in Masland, 2012). Their dendritic field size determines the sampling area of photoreceptor signals and thus the spatial resolution (visual acuity). Ganglion cells represent feature detectors extracting information about e.g. the absolute light level (brightness) (reviewed in Berson, 2003), contrast (Demb et al., 1999), “colour” (Dacey and Lee, 1994), and motion and its direction (Barlow and Levick, 1965). They encode the retinal output into spike trains and project via their axons, forming the optic nerve, to different parts of the brain. Ganglion cells that contribute to the conscious perception of our world project to the lateral geniculate nucleus, a structure in the thalamus which in turn relays the visual information to the visual cortex. Other major projection areas are the pretectum which is involved in controlling the pupil size, and the superior colliculus which mediates eye movements (reviewed in Wässle, 2004).

2.6 The photoreceptor synapse

Photoreceptors transmit the visual information to horizontal and bipolar cells. For that, they use a specialized synapse, i.e. the ribbon synapse. In a ribbon synapse, neurotransmitter-filled vesicles are tethered to a presynaptic plate, the so-called ribbon. The photoreceptor ribbon synapse meets two important demands (reviewed in Sterling and Matthews, 2005): *(i)* it transduces the light intensity-dependent graded changes in membrane potential into graded changes in glutamate release so that the representation of different light intensities is maintained at postsynaptic sites, and *(ii)* in darkness, it maintains high rates of glutamate release from the synaptic terminal.

Figure 5 shows the characteristic triadic structure of a cone synaptic terminal, the cone pedicle: it is contacted centrally by one ON-cone bipolar cell dendrite and two horizontal cell dendrites; OFF-cone bipolar cells make flat contacts at the terminal base (Haverkamp et al., 2000). In general, each cone is contacted by at least one member of any given bipolar cell type, and thus already at the first synapse of the visual system, the photoreceptor signal is split and fed into different information channels which are concerned with different aspects of the visual scene (reviewed in Wässle, 2004) (see 2.4).

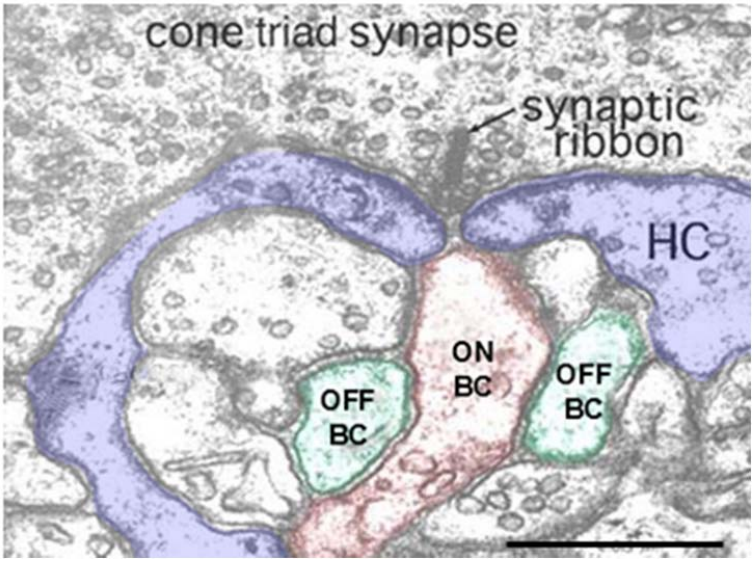

Figure 5: Ultrastructure of the cone synapse
Electron micrograph of synaptic contacts in the cone axon terminal triad from the primate. Each cone forms multiple output synapses with postsynaptic bipolar cells (BC) and horizontal cells (HC). Shown is one synapse. Glutamate release occurs close to the ribbon. Once horizontal cells have integrated and processed the cone signals, they feed back to the cones by different hypothesized mechanisms. Scale bar: 0.5 µm. Modified from Kolb (1970).

Photoreceptors are coupled to each other forming homotypic, i.e. rod-rod and cone-cone, as well as heterotypic, i.e. rod-cone gap junctions (Raviola and Gilula, 1973). In the case of cone-cone coupling, the responsible protein is Connexin 36; for rod-cone coupling, the opposed protein partner in rods is still unknown (Feigenspan et al., 2004). Electrical coupling enhances the signal to noise ratio in photoreceptors, and mediates the interaction between rod and cone pathways at a very early retinal level. However, coupling between photoreceptors naturally comes at the cost of local chromatic information, spatial resolution, and detecting very dim light signals. The dependency of coupling between photoreceptors (and other retinal neurons) on the circadian rhythm (Ribelayga et al., 2008) and light adaptation state (reviewed in Bloomfield and Volgyi, 2009) ensures the "right" amount of coupling to meet the demands of the prevailing illumination condition.

Synaptic transmission from photoreceptors to postsynaptic cells is Ca^{2+} dependent and vesicular (Schmitz and Witkovsky, 1997). In darkness, photoreceptors are depolarized, meaning that VGCCs, likely of the L-type, are open in the synaptic terminal (Taylor and Morgans, 1998; Morgans et al., 2005) (Figure 6). Ca^{2+} influx triggers the fusion of glutamate-filled vesicles docked at the distal end of the ribbon with the plasma membrane, thereby releasing glutamate. Glutamate acts on glutamate receptors on horizontal and bipolar cells and is then taken up from the synaptic cleft via glutamate transporters into photoreceptors (Rauen and Kanner, 1994; Pow and Barnett, 2000) or Müller cells (Rauen et al., 1998). Glutamate release is influenced by Ca^{2+} influx through the VGCCs into the photoreceptor terminal, Ca^{2+} release from internal stores (e.g. endoplasmic reticulum), Ca^{2+} buffering and Ca^{2+} extrusion, but also by the rate of vesicle replenishment (reviewed in Thoreson, 2007). Importantly, horizontal cells modulate the activity of the VGCCs responsible for glutamate release by different hypothesized feedback mechanisms, and by that change the photoreceptor output (see 2.7.2).

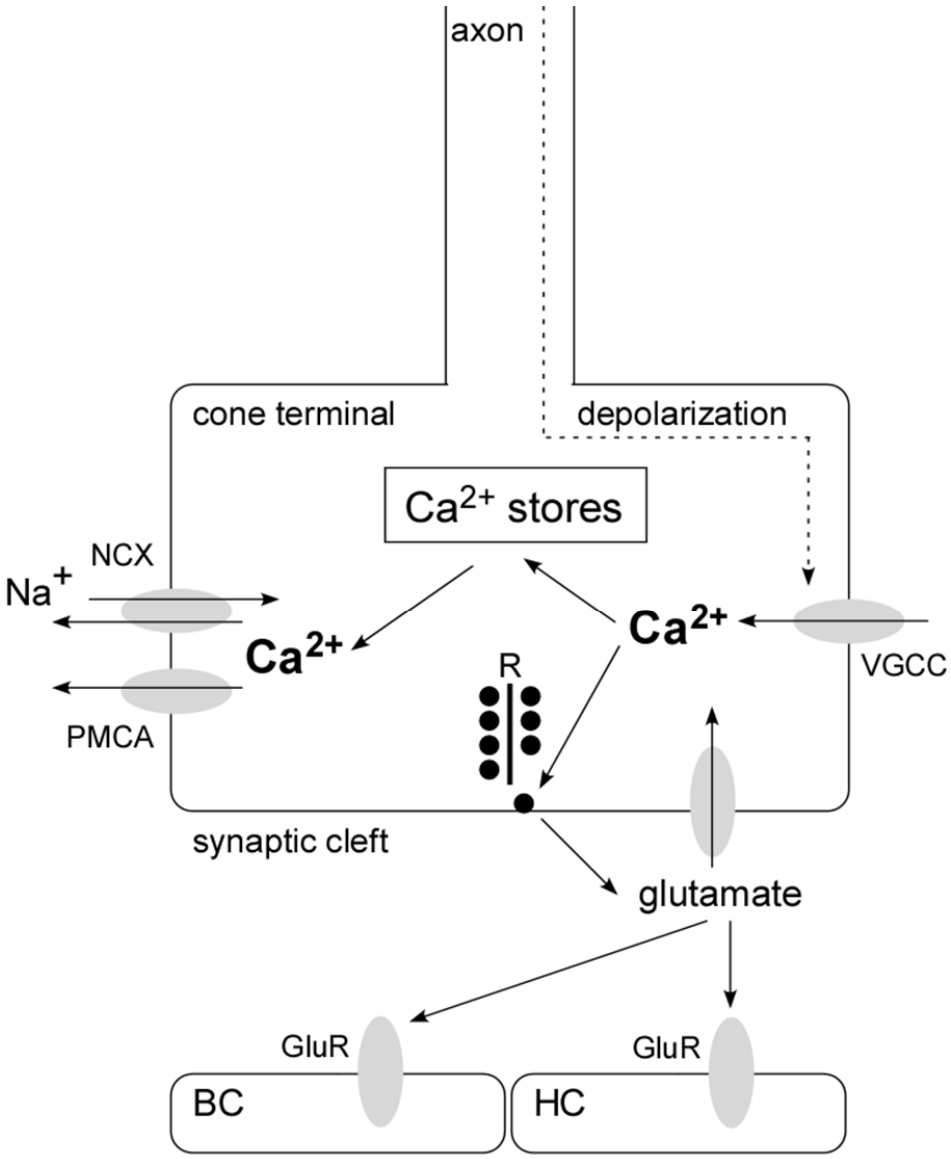

Figure 6: Synaptic transmission at the cone axon terminal
In darkness, photoreceptors are depolarized, which activates voltage-gated Ca^{2+} channels (VGCCs) in the synaptic terminal, leading to an influx of Ca^{2+} ions. Ca^{2+} mediates the fusion of glutamate-filled vesicles at the ribbon (R) with the plasma membrane, thereby releasing glutamate. Glutamate activates glutamate receptors (GluR) on bipolar (BCs) and horizontal cells (HCs), and is then removed from the synaptic cleft by glutamate transporters back into the photoreceptors or into Müller cells (not shown). Ca^{2+} in the synaptic terminal also triggers Ca^{2+} release from the endoplasmic reticulum (Babai et al., 2010; Wei et al., 2012), and is extruded by sodium-calcium exchangers (NCX) or plasma membrane Ca^{2+}-ATPases (PMCA) (Johnson et al., 2007).

2.7 Horizontal cell feedback

2.7.1 Contribution of horizontal cells to the antagonistic centre-surround receptive field organization of retinal neurons

In general, retinal neurons have an antagonistic centre-surround receptive field organization, i.e. ON-ganglion cells are excited by light falling onto their receptive field's centre and inhibited by illumination of their receptive field's surround; OFF-ganglion cells respond in the inverse way (Barlow, 1953; Kuffler, 1953; Werblin and Dowling, 1969; Dacheux and Miller, 1981). Antagonistic receptive fields represent the elementary building blocks for processing spatial information in the visual system, and the convergence of cells with adjacent antagonistic receptive fields into higher-order visual cells generates more complex receptive fields for highly specific feature detection (e.g. selective responses of cells to objects with a specific orientation, orientation selectivity) (Hubel and Wiesel, 1962). The major synaptic interactions responsible for the formation of antagonistic centre-surround receptive fields in the retina are *(i)* horizontal cell to photoreceptor feedback (see 2.7.2), *(ii)* horizontal cell to bipolar cell feed-forward (Yang and Wu, 1991; Fahey and Burkhardt, 2003), and *(iii)* amacrine cell to bipolar cell feedback and amacrine cell to ganglion cell feed-forward (reviewed in Lukasiewicz, 2005). What evidence supports the notion that horizontal cells contribute to the generation of an inhibitory receptive field surround of retinal neurons?

Already in the 1950s, Hartline and co-workers discovered that neighbouring photoreceptor units in the compound eye of the horseshoe crab interact with each other in an antagonistic way (Hartline et al., 1956; Hartline and Ratliff, 1957). Later on, it was shown that in the vertebrate retina this newly introduced principle called "lateral inhibition" is mediated by the horizontal cells, based on two important observations: *(i)* Hyperpolarizing horizontal cells by current injection (and thereby simulating light stimulation) evoked a response in neighbouring cones with opposite polarity compared with the response to light falling onto the cones' receptive field centre. *(ii)* Stimulating cones with large-diameter light flashes (and thereby strongly hyperpolarizing horizontal cells) elicited a response in cones that was smaller than their response to small-diameter light flashes (Baylor et al., 1971). The effects of lateral interactions in the outer retina provided by the horizontal cells cannot only been observed in photoreceptors but also at the level of bipolar and ganglion cells (Toyoda and Kujiraoka, 1982; Mangel, 1991): For example, when horizontal cells are hyperpolarized by current injection, the responses of

nearby ganglion cells to centred spot stimuli are reduced (because by that, the ganglion cells' antagonistic surround is strengthened), a finding suggesting that horizontal cells contribute to surround antagonism of bipolar and ganglion cells (Mangel, 1991).

The surround of bipolar and ganglion cells is modulated by the ambient light level and is thus highly dynamic (reviewed in Thoreson and Mangel, 2012). The strength of their inhibitory surround is increased at brighter light levels, thereby keeping the cells responsive over a broad range of ambient light levels (Barlow et al., 1957; Zhang and Wu, 2009). This observation suggests that also the strength of feedback from horizontal cells to photoreceptors – thought to be mainly responsible for the inhibitory surround of bipolar and ganglion cells – is increased at brighter conditions. In line with this notion, the size of the horizontal cell network is reduced by closing gap junctions at brighter light levels (Xin and Bloomfield, 1999). This increases the responses of horizontal cells to light stimuli (because the responses are less "diluted" in a smaller network) (Teranishi et al., 1983), which probably evokes larger feedback signals to the photoreceptors. In conclusion, the antagonistic centre-surround receptive field organization of retinal neurons is not only useful to process visual information on a spatial scale, i.e. to reduce the responses to uniform areas of illumination and increase the responses to light-dark borders (contrast enhancement), but also to adjust the gain of neurons dependent on the ambient light level (light adaptation).

2.7.2 Hypothesized mechanisms for inhibitory horizontal cell to cone feedback

Horizontal cell to photoreceptor feedback is one of the major synaptic mechanisms underlying the antagonistic receptive field organization of retinal neurons. By which mechanism(s) horizontal cells feed back to the photoreceptors, however, has remained a mystery for many decades. Verweij and co-workers approached this question by recording the changes in a cone's whole-cell current as an *estimate* for its Ca^{2+} current to large-diameter flash stimulation using the goldfish retina as a model system (Verweij et al., 1996). They found that eliciting horizontal cell feedback by large-diameter light flashes shifts the activation function of the cone Ca^{2+} current to more negative potentials, leading to an increase in the cone Ca^{2+} level and putative increase in glutamate release (Thoreson, 2007; Jackman et al., 2009) (Figure 7). As the effect of horizontal cell feedback opposes the intrinsic cone response to light, which is a reduction in the terminal Ca^{2+} level and thus glutamate release, the signal from horizontal cells is usually referred to as "inhibitory feedback". It is noteworthy that horizontal cell feedback has

pronounced effects on the cone Ca^{2+} level and therefore glutamate release but typically not on the cone membrane potential (Kraaij et al., 2000) – with some exceptions for certain experimental conditions and/or species. Such feedback-induced modulation of the cone Ca^{2+} current has been also described in other species including newt (Hirasawa and Kaneko, 2003) and monkey (Verweij et al., 2003). Interestingly, horizontal cell feedback to rods appears to be mediated by similar mechanisms as to cones (Thoreson et al., 2008; Babai and Thoreson, 2009).

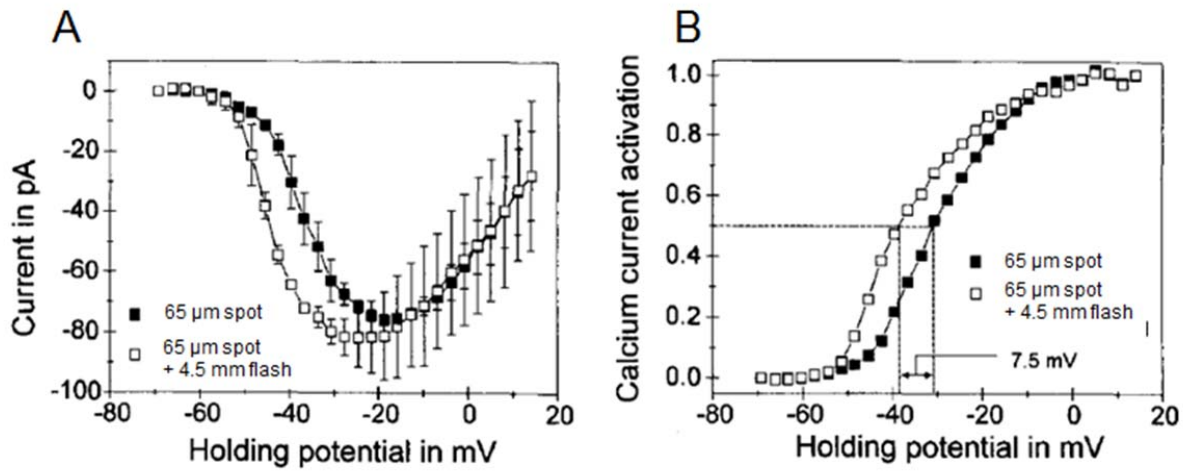

Figure 7: Horizontal cell feedback modulates the cone Ca^{2+} current activation function
Cones in the goldfish retina were voltage-clamped in the whole-cell mode at different potentials and stimulated with large-diameter flashes (4.5 mm) to elicit horizontal feedback under conditions where the direct light responses were saturated with a small-diameter spot (65 µm) centred onto the recorded cones. ***A*** The whole-cell current was leak-subtracted to get an estimate for the Ca^{2+} current and then plotted as a function of cone membrane potential. Large flash stimulation (resulting in horizontal cell feedback) increased the Ca^{2+} current in cones, and this effect was maximal when the membrane potential of the cone ranged between ~ -50 mV and ~ -20 mV. ***B*** Estimates of the half-maximum activation potentials of the cone Ca^{2+} current with and without horizontal cell feedback. Horizontal cell feedback shifts the cone Ca^{2+} current activation range to more negative potentials (by ~7.5 mV), thus increasing the cone Ca^{2+} level and glutamate release. Modified from Verweij et al. (1996).

How exactly horizontal cells feed back to cones has been intensively debated for decades. There are three major hypotheses how they modulate cone output: ephaptic, pH-mediated and GABAergic (Figure 8). It is noteworthy that these hypotheses are based on experiments involving different animal species (e.g. non-mammalian *vs.* mammalian), experimental conditions (e.g. light adaptation state (mesopic *vs.* photopic)), tissue preparation (whole mount *vs.* slices) and electrical recordings (microelectrode *vs.* patch-clamp) (reviewed in Kamermans and Spekreijse, 1999). All three mechanisms are expected to affect the activity of the VGCCs in the cone terminal and therefore modulate glutamate release.

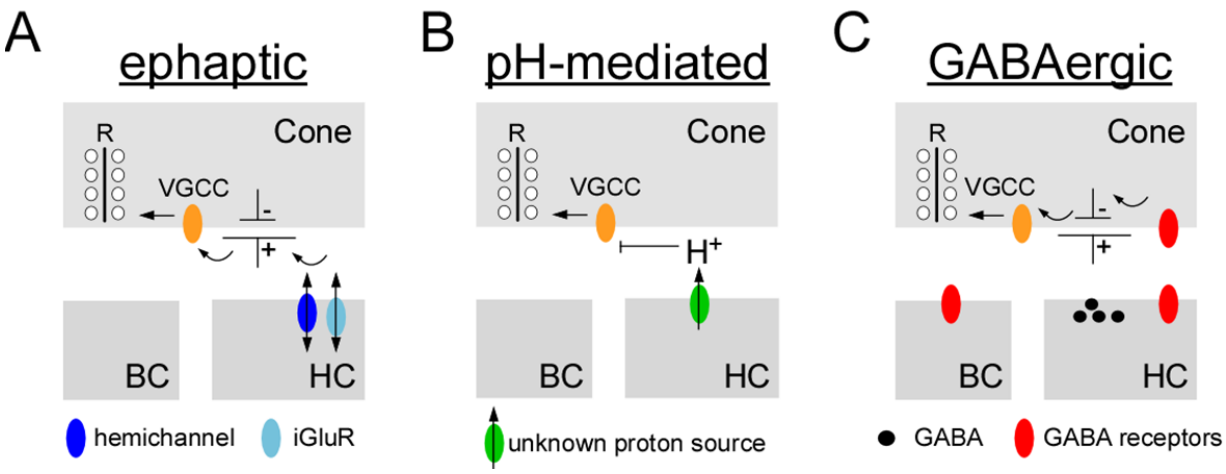

Figure 8: Three hypotheses for inhibitory horizontal cell to cone feedback
A Ephaptic feedback is mainly based on current flowing through hemi-gap junction channels (hemichannels) and ionotropic glutamate receptors (iGluRs) on horizontal cell dendrites (HC). This current flow locally changes the cone terminal membrane potential and thus modulates the activity of VGCCs. ***B*** pH-mediated feedback is based on pH-changes in the synaptic cleft, which modulate the activity of VGCCs (VGCCs are pH-sensitive). ***C*** GABAergic feedback is based on GABA release from horizontal cells, which activates putative GABA receptors in the cone terminal, thereby modulating the cone membrane potential and, thus, the activity of VGGCs. R, ribbon; BC, bipolar cell.

2.7.3 Ephaptic feedback hypothesis

Communication between neurons is based on "classical" *chemical synapses* (e.g. glutamatergic transmission between photoreceptors and horizontal cells), *electrical synapses* (e.g. gap junctions between photoreceptors), or *ephaptic interactions*. "Ephaptic" (Greek: to touch) interactions describe the observation that currents flowing through the intersynaptic space can influence the activity of neighbouring neurons (reviewed in Kamermans and Fahrenfort, 2004), a type of neural communication that was proposed to occur in many parts of the central nervous system, including hippocampus, cerebellum and retina (reviewed in Vroman et al., 2013). A prerequisite for ephaptic interactions to have a significant impact on neighbouring neurons is a high resistance of the intersynaptic space; the synaptic terminal of photoreceptors appears to be an appropriate morphological correlate for creating such a high intersynaptic resistance because of its highly convoluted structure (reviewed in Vroman et al., 2013). It is noteworthy that ephaptic effects are highly local, in contrast to the "field effects" generated by the synchronous activity of neurons, e.g. in the hippocampus (reviewed in Jefferys, 1995).

In the 1980s, it was proposed that horizontal cells provide feedback to cones using ephaptic interactions (Byzov and Shura-Bura, 1986) – a hypothesis that was eventually experimentally tested by Kamermans and co-workers using the fish retina as a model: Based on immunohistochemical (Kamermans et al., 2001), pharmacological (Kamermans et al., 2001; Fahrenfort et al., 2004; Fahrenfort et al., 2005; Fahrenfort et al., 2009) and genetic experiments (Klaassen et al., 2011), they suggested that the key elements in ephaptic horizontal cell to cone feedback are so-called hemi-gap junction channels (hemichannels). Hemichannels consist of the gap junction proteins connexins or pannexins, and act as large current sinks on the horizontal cell dendrites (Figure 8A). Upon light stimulation, cones hyperpolarize, the VGCCs close and thus the Ca^{2+} level and glutamate release from the synaptic terminal are reduced. Accordingly, horizontal cells also hyperpolarize to light because they form a sign conserving synapse with the cones. As a consequence, the current through the hemichannels increases (Sun et al., 2012), leading to a voltage drop in the synaptic cleft, that is more specifically, across the cone membrane (Figure 9). This voltage drop leads to a local depolarization of the cone terminal and thus increases the open probability of the VGCCs. As a result, the cone terminal Ca^{2+} level and, consequently, glutamate release are increased. This increase in glutamate release from the cone terminal by feedback opposes the initial intrinsic cone response to light; thus, ephaptic feedback is – according to this conceptual model – inhibitory. The combined signal, i.e. the intrinsic cone response modulated by horizontal feedback, is relayed to the bipolar cells. In fact, any conductance at the horizontal cell dendrites (e.g. ionotropic glutamate receptors (iGluRs) (Fahrenfort et al., 2005; Fahrenfort et al., 2009)) or even in the cone terminals (e.g. ionotropic GABA receptors (Endeman et al., 2012)) can, in principle, modulate and thereby control the effect ephaptic feedback has on cone output. Because of its electrical nature, ephaptic feedback occurs virtually instantaneous and thus represents a means of controlling the activity of neurons without significant time delays (reviewed in Vroman et al., 2013). Apart from fish, there is also evidence for such a mechanism e.g. in primates (McMahon et al., 2004). The presence of Pannexin 1-formed hemichannels at mouse horizontal cell dendrites strongly suggests that horizontal cell feedback is also based on ephaptic interactions in this species (Kranz et al., 2013).

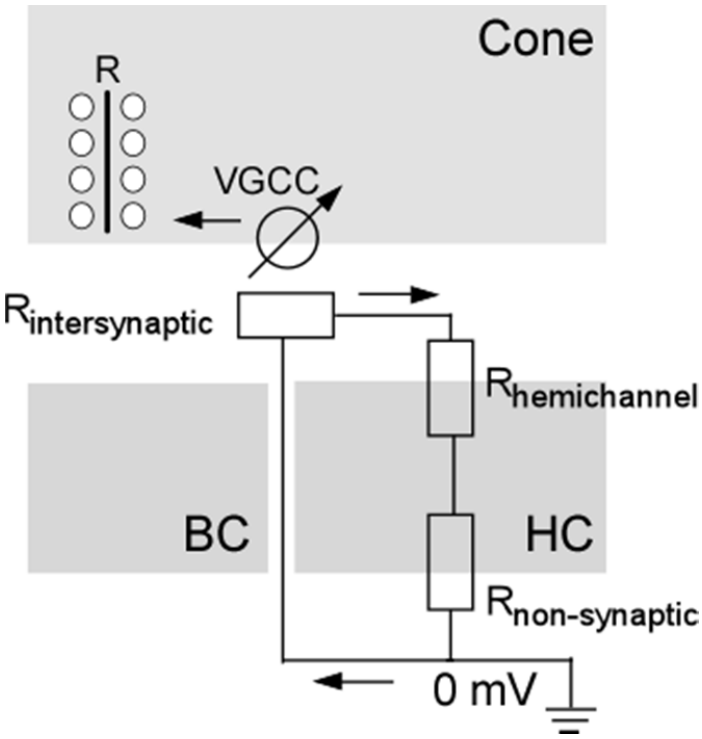

Figure 9: **Ephaptic feedback model**
The circuit underlying ephaptic feedback consists of a series of resistors, i.e. the hemichannel resistance ($R_{hemichannel}$), resistance of the intersynaptic space ($R_{intersynaptic}$), and non-synaptic membrane resistance of the horizontal cell (HC) outside the cone synaptic complex ($R_{non-synaptic}$). The VGCCs in the cone terminal are depicted as a potentiometer, as they measure the transmembrane potential, which is modulated by ephaptic feedback (see text). The direction of current flow is indicated by the arrows. Note that the voltage drop at $R_{intersynaptic}$ is – according to Ohm's law – proportional to $R_{intersynaptic}$ (supposed to be high in the invaginating photoreceptor synapse) and the current. Modified from Kamermans and Fahrenfort (2004).
R, ribbon; BC, bipolar cell.

2.7.4 pH-mediated feedback hypothesis

Horizontal cells have also been hypothesized to provide feedback to photoreceptors by changing the pH in the synaptic cleft. First evidence for this notion was provided by Barnes and co-workers who showed that cone Ca^{2+} currents are modulated by the extracellular pH (Barnes and Bui, 1991; Barnes et al., 1993). Protons directly inhibit the VGCCs by protonation of residues in the channel pore (Chen et al., 1996). The pH-mediated feedback hypothesis proposes that the light-induced hyperpolarization of horizontal cells leads to an alkalinization of the synaptic cleft and a subsequent disinhibition of the VGCCs in the cone terminal; as a consequence, Ca^{2+} influx into and glutamate release from the cone terminal are increased (inhibitory feedback) (Figure 8B). Depolarization of horizontal cells has the opposite effects on synaptic cleft pH and activity of the cone VGCCs. This hypothesis is based on pharmacological experiments using the newt (Hirasawa and Kaneko, 2003) and pH imaging experiments in which the pH has been monitored directly in the synaptic cleft using the fish retina (Wang et al., 2014). How horizontal cells change the synaptic cleft pH has not yet been convincingly resolved. However, there is evidence for the involvement of several factors, including pH-regulating (chloride-bicarbonate and sodium-hydrogen) exchangers (Haugh-Scheidt and Ripps, 1998; Molina et al., 2004), plasma membrane Ca^{2+}-ATPases (PMCAs)

(exchanging intracellular Ca^{2+} for extracellular protons) (Molina et al., 2004; Kreitzer et al., 2007), proton pumps (acidifying the synaptic cleft) (Wang et al., 2014), proton-permeable channels (Brockway et al., 2002; Vessey et al., 2005; Ettaiche et al., 2006; Jonz and Barnes, 2007; Wang et al., 2014), and extracellular carbonic anhydrase (catalysing the conversion of carbon dioxide and water to protons and bicarbonate) (Vessey et al., 2005; Fahrenfort et al., 2009). Importantly, both the ephaptic and pH-mediated horizontal cell feedback mechanisms may be interconnected, as the hemichannels (the key elements of ephaptic feedback) have been demonstrated to be pH-sensitive (Trexler et al., 1999) and suggested to be permeable to protons (Zaniboni et al., 2003; Wang et al., 2014). In line with this notion, it has been proposed that – at least in the fish – hemichannels mediate both a fast ephaptic (time constant ~35 ms) as well as a slower pH-mediated mechanism (time constant ~180 ms) (Kamermans et al., 2013; ARVO abstract). Apart from fish and newt, there is also evidence for pH-mediated feedback to cones in the primate (Davenport et al., 2008) and to rods in the mouse (Babai and Thoreson, 2009).

Interestingly, besides horizontal cells, also photoreceptors were shown to release protons into the synaptic cleft, e.g. concomitantly with vesicular glutamate release (glutamate-filled vesicles are acidic) (DeVries, 2001). Such inhibitory auto-feedback might be important to limit the high rate of steady exocytosis in darkness. Since this inhibitory mechanism does not involve the laterally-operating horizontal cells, it acts on a more local scale and is not expected to contribute to the antagonistic centre-surround receptive field organization of retinal neurons.

2.7.5 GABAergic feedback hypothesis

Besides more unconventional horizontal cell feedback hypotheses involving ephaptic and pH-mediated interactions, there is also a “classical” feedback hypothesis (Wu, 1986), according to which horizontal cells release the inhibitory neurotransmitter GABA when being depolarized by light decrements (Hirano et al., 2011). GABA activates ionotropic GABA receptors in the cone terminal, thereby increasing the influx of chloride ions into the cone. As a consequence, the cone hyperpolarizes, Ca^{2+} influx into and thus glutamate release from the synaptic terminal are reduced, representing inhibitory feedback (Figure 8C). There is functional evidence for such feedback in some species like salamander (Wu, 1986) and turtle (Tatsukawa et al., 2005). However, pharmacological experiments in several species including fish (Verweij et al., 1996), rat (Liu et al., 2013) and primate (Verweij et al., 2003) have failed to demonstrate a direct involvement of GABA in horizontal to cone feedback. Instead, GABA’s role is thought to act as a “neuromodulator” (reviewed in Kamermans and Spekreijse, 1999) not only at potential GABA receptors

on photoreceptors but also at auto-receptors on horizontal cells ("auto-feedback loop") (Liu et al., 2013) and bipolar cells (feed-forward) (Herrmann et al., 2011). In the mouse retina, it is still not clear whether horizontal cells directly feed back to cones via GABA as a transmitter. However, there is growing evidence for GABAergic transmission at the mouse cone-horizontal cell synapse: *(i)* horizontal cells contain GABA (Deniz et al., 2011; Herrmann et al., 2011), *(ii)* horizontal cells express the vesicular GABA transporter (Cueva et al., 2002), and *(iii)* also proteins required for vesicular fusion have been shown to be present in horizontal cells (Hirano et al., 2011).

2.7.6 Excitatory horizontal cell to cone feedback

A few years ago, Jackman and co-workers provided experimental evidence that, apart from the inhibitory mechanisms (discussed in 2.7.2-2.7.5), horizontal cells can also feed back to cones using an excitatory mechanism (Jackman et al., 2011). Such an excitatory feedback has been suggested to be initiated by local Ca^{2+} changes in the horizontal cell dendrites, and thus is expected to act on a more local scale. In contrast, inhibitory feedback represents a more globally operating mechanism (Baylor et al., 1971), as it is thought to be mediated by membrane potential changes in the horizontal cell network. Excitatory feedback might be important to restore the dynamic range of the cones lost by inhibitory feedback on a local scale. The neurotransmitter mediating the excitatory feedback has not yet been found. Furthermore, it remains to be investigated whether such an excitatory feedback can be evoked by actual light stimulation (in Jackman's study, pharmacology was used to mimic light), and whether this positive feedback pathway also exists in the mouse.

2.8 Aims and Contributions

In the mouse retina, there is evidence that horizontal cells may use more than one feedback mechanism as discussed in 2.7: this includes experimental data in favour of GABAergic transmission (Cueva et al., 2002; Herrmann et al., 2011; Hirano et al., 2011), ephaptic feedback via Pannexin 1-formed hemichannels (Kranz et al., 2013) and pH-mediated feedback (Babai and Thoreson, 2009). Because mice possess only a single type of horizontal cell (Peichl and Gonzalez-Soriano, 1994), the presence of multiple feedback mechanisms at a single synaptic site is particularly interesting, hinting at a complex processing of cone input and feedback signals in this interneuron.

The aim of this thesis was to investigate how mouse horizontal cells control the output of the cones, i.e. neurotransmitter release, with presynaptic Ca^{2+} in the cone terminal as the readout. I was especially interested whether the different hypothesized feedback mechanisms modulate different spatial and temporal aspects of the cone output, and how these mechanisms might interact in the mouse. To achieve the goal, the tasks in the project included:

(1) Optimization of tissue preparation to measure intact horizontal cell feedback in the slice at the level of the individual cone axon terminal (see 3.2).

(2) Design of appropriate light stimulus protocols (see 3.5) to measure and dissect the horizontal cell feedback mechanisms in cone axon terminals. I used stimuli that differed in polarity and contrast to analyse if the effects of feedback are dependent on the type of light stimulus.

(3) Simultaneous surround light stimulation and two-photon Ca^{2+} imaging in cone axon terminals to study the effects of laterally-operating horizontal cell feedback on cones ("lateral inhibition" *vs.* "lateral excitation").

(4) Simultaneous light flash stimulation and two-photon Ca^{2+} imaging in cone axon terminals combined with pharmacology to dissect the different feedback mechanisms (ephaptic, pH-mediated and GABAergic). I used local ("puff") and global ("bath") drug applications to study the spatial extent of the different horizontal cell feedback mechanisms (see 3.6).

(5) Quantification of the effects of horizontal cell feedback on different parameters of the cone light response (see 3.7).

(6) Immuno-electron microscopy to study the presence of ionotropic GABA receptors in cone axon terminals as a prerequisite for a *direct* GABAergic horizontal cell to cone feedback mechanism (see 3.8).

I performed all tasks except task (6), which was carried out by Dr. Konrad Schultz and PD Dr. Karin Dedek (Department of Neurobiology, University of Oldenburg).

3 Materials and Methods

Unless stated otherwise, all chemicals were purchased from Sigma-Aldrich (Steinheim, Germany) or Merck (Darmstadt, Germany).

3.1 Animals

For Ca^{2+} imaging experiments (see 3.3), we used adult mice of the transgenic *HR2.1:TN-XL* mouse line. For electron microscopy (see 3.8), C57B6/J mice were used. Animals (4-8 weeks, both genders) were dark-adapted for at least 2 hours, anesthetized with Isoflurane (Baxter, Germany) or CO_2 and killed by cervical dislocation. All procedures were performed in accordance with the law on animal protection (Tierschutzgesetz) issued by the German Federal Government and approved by the institutional committees on animal experimentation of the University of Tübingen and the University of Oldenburg.

3.2 Retinal tissue preparation

Eyes were enucleated and placed in extracellular solution that contained (in mM) 125 NaCl, 2.5 KCl, 2 $CaCl_2$, 1 $MgCl_2$, 1.25 NaH_2PO_4, 26 $NaHCO_3$, 0.5 L-glutamine and 20 glucose, and were maintained at pH 7.4 using carboxygen (95% CO_2/5% O_2). After removing cornea and lens, the retina was isolated from the eye-cup. Since our recordings from cone axon terminals in flat-mounted retina using two-photon microscopy turned out to saturate the photoreceptor light responses, I used retinal slices, in which the laser-evoked effects on photoreceptors are reduced (for details, see 3.3). Slicing the retina, however, has the disadvantage of *(i)* partially destroying the horizontal cell network, which reduces the laterally-operating horizontal cell feedback, and *(ii)* possibly washing out factors required for horizontal cell feedback mechanisms. To work under more "physiological" conditions, I optimized the retinal tissue preparation: *(i)* Horizontal cells in the mouse do not show functional GABA-uptake, meaning that GABA that may be lost during conventional preparation can only be restored by horizontal cell intrinsic *de novo* GABA synthesis from glutamate or glutamine. Thus, to ensure that a potential GABAergic feedback mechanism remained functional *in vitro,* 150 µM pyridoxal 5-phosphate, a co-factor of the GABA-synthesizing glutamic acid decarboxylase (GAD), was added to the extracellular solution (Deniz et al., 2011). *(ii)* Since working with slices of ~200 µm thickness revealed in some cases "spiky" light responses in cones, possibly indicative of impaired horizontal cell feedback (Wei et al., 2012), the slice thickness was increased to ~300 µm, thereby increasing the number of intact horizontal cells. For slicing (for

detailed description, see Wei et al., 2012), retinae were dissected from the eye-cup, cut into halves and put onto filter paper (0.22 µm pore size, Millipore) with the photoreceptor layer facing up. Vertical retinal slices of ~300 µm thickness were cut using a standard technique with a manual retina slicer (Werblin, 1978). Slices attached to the filter paper were stored in carboxygenated extracellular solution in darkness at room temperature and then transferred individually to the recording chamber. The slice in the recording chamber was constantly perfused with carboxygenated extracellular solution at 36°C.

3.3 Imaging light-evoked Ca^{2+} activity in the *HR2.1:TN-XL* mouse line using two-photon microscopy

Optical recordings of light-evoked Ca^{2+} responses in cone axon terminals were performed using the *HR2.1:TN-XL* mouse line, in which cones selectively express the Ca^{2+} indicator TN-XL (Figure 10B) (Wei et al., 2012). TN-XL is a FRET-based indicator that consists of the two fluorophores eCFP and citrine, linked by the Ca^{2+} sensor Troponin C, and therefore allows for ratiometric Ca^{2+} measurements (Figure 10C) (Mank et al., 2006). Using ERG-recordings, Wei and co-workers showed that the cone photoreceptor function is not impaired by the indicator expression. For the optical recordings, we used a custom-built two-photon microscope (Denk et al., 1990) as described earlier (Euler et al., 2009; Breuninger et al., 2011) (Figure 10A). In brief, the system was equipped with a mode-locked Ti/sapphire laser (MaiTai-HP DeepSee; Newport Spectra-Physics) tuned to 860 nm, two detection channels for fluorescence imaging of eCFP (483 BP 32; AHF) and citrine (535 BP 50; AHF) and a 20x water-immersion objective (XLUMPlanFL, 0.95 NA; Olympus). Image acquisition was performed using custom software (CfNT, by Michael Müller, MPI for Medical Research, Heidelberg, Germany) and by taking 128x16 pixel images (at 31.3 Hz frame rate) restricted to the row of cone axon terminals in the outer plexiform layer. Because the scanning laser beam is oriented in an approximately right angle to the surface of the tissue in the retinal slice preparation (Figure 10B), bleaching of the light-sensitive cone outer segments by the scanning laser could be largely avoided (for details, see Wei et al., 2012; Baden et al., 2013b).

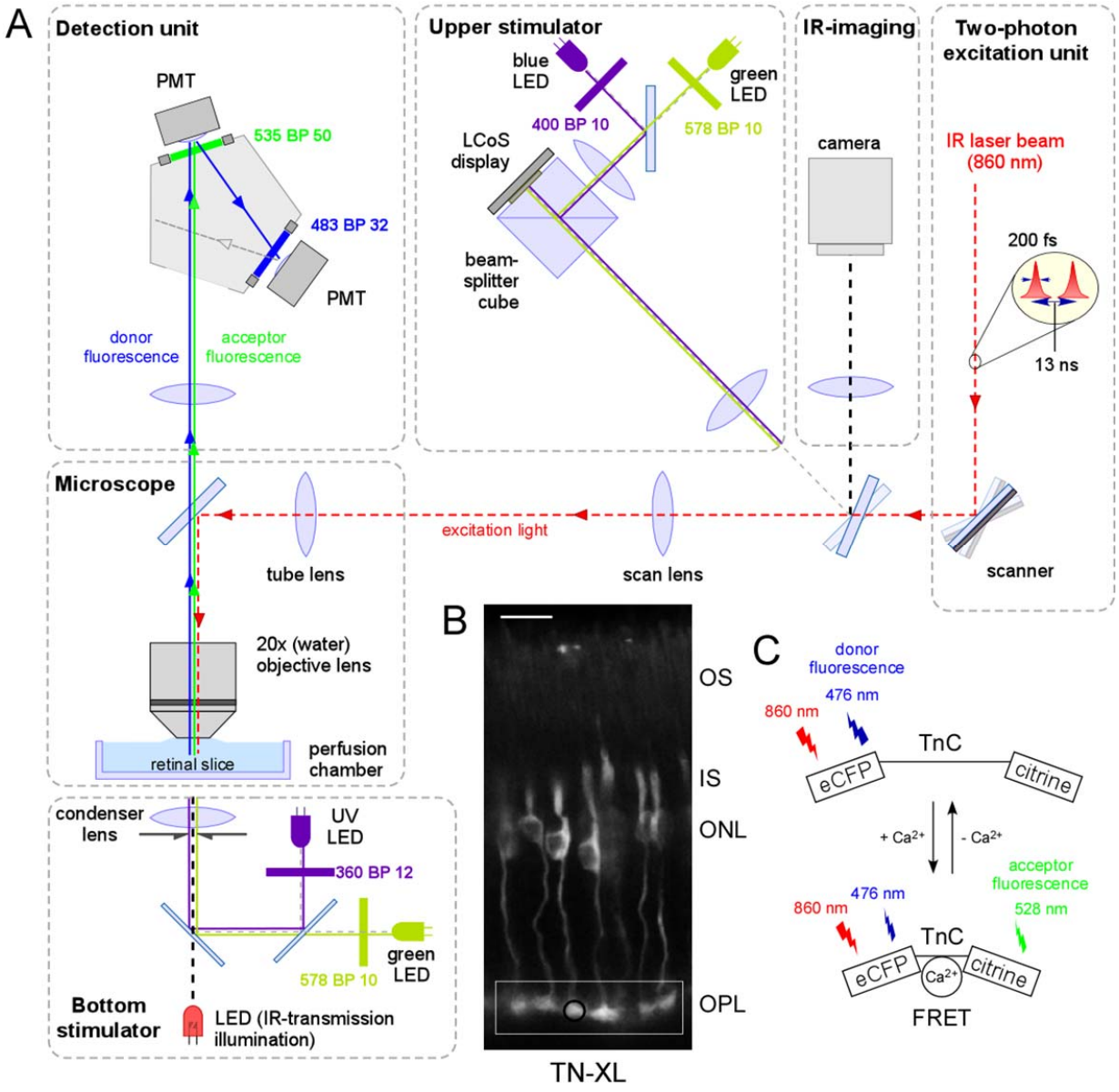

Figure 10: Simultaneous light stimulation and two-photon Ca^{2+} imaging in cone axon terminals

A Cones were stimulated either with spatio-temporally structured light (upper stimulator) or light flashes (bottom stimulator). Simultaneously, the light-evoked changes in Ca^{2+} activity reported by TN-XL (see *B+C*) were measured in cones using two separate channels for the donor and acceptor fluorescence. An infrared (IR) camera was used to judge the quality of the tissue. Modified from Euler et al. (2009); note that the IR camera was actually introduced into the optical path between scan lens and tube lens by means of a movable mirror (not shown here). PMT, photomultiplier tube; LCoS, liquid crystal on silicon display. ***B*** In the *HR2.1:TN-XL* mouse line, cones selectively express the FRET-based Ca^{2+} indicator TN-XL in every compartment except for the outer segment (Wei et al., 2012). Measurements were made at the level of the cone axon terminals (box). Encircled is an individual axon terminal. Scale bar: 10 µm. OS, outer segment; IS, inner segment; ONL, outer nuclear layer, OPL, outer plexiform layer. ***C*** TN-XL consists of the Ca^{2+} sensor Troponin C (TnC) flanked by two fluorophores, i.e. the donor fluorophore eCFP and the

acceptor fluorophore citrine. The laser wavelength was chosen to (in large part) selectively excite eCFP (reviewed in Drobizhev et al., 2011). At low Ca^{2+} levels, the efficiency of FRET between the two fluorophores is low and thus the donor fluorescence measured at the detectors (see *A*) is high. Binding of Ca^{2+} leads to a conformational change in the TN-XL construct, thereby increasing the efficiency of FRET between eCFP and citrine. As a consequence, less donor and more acceptor fluorescence is detected.

3.4 Light stimulators

Dichromatic light stimuli were generated by two stimulators (Figure 10A). The first stimulator consisted of a reflective liquid crystal display (LCoS-type; i-glasses; EST), coupled in the microscope's optical path. This LCoS-display was alternately illuminated by two band-pass filtered (blue, 400 BP 10; green, 578 BP 10; AHF) LEDs, to project spatio-temporally structured stimuli through the objective lens onto the retinal slice (Euler et al., 2009). This stimulator was used for the surround illumination experiments (see stimulus protocols (b) and (c) in 3.5). The second stimulator was mounted below the recording chamber, and consisted of two band-pass filtered (UV, 360 BP 12; green, 578 BP 10; AHF) LEDs, driven by an open-source microprocessor board (http://arduino.cc) and synchronized with the microscope's galvo scanners. The light from the LEDs was combined by a beam-splitter (400 DCLP, AHF) and focused by a condenser lens (0.8 NA, H DIC, Zeiss) through the bottom of the recording chamber. This stimulator was used to apply full field stimuli.

The light intensity generated by each of the stimulating LEDs was calibrated as described previously (Breuninger et al., 2011; Baden et al., 2013b; Chang et al., 2013) such that equal photoisomerisation rates were elicited for S- and M-cone opsins. Cones were adapted to different background light levels for at least 20 s before stimuli (see protocols in 3.5) were presented. The background intensity of the LEDs ranged from 0.1 $x10^3$ to 7.5 $x10^3$ $P^*cone^{-1}s^{-1}$ for the first stimulator and from 1.0 $x10^3$ to 8.6 $x10^3$ $P^*cone^{-1}s^{-1}$ for the second one. Because both the light of the stimulator LEDs and the excitation laser contributed to the background light level at the slices, the laser was already scanning during this adaptation period. The contribution of the excitation laser to the background illumination was estimated to be $\sim 10^4$ $P^*cone^{-1}s^{-1}$, based on the transient Ca^{2+} response to laser and stimulator background at the beginning of a recording epoch (Wei et al., 2012). For a detailed discussion of potential laser-related stimulus contribution when recording retinal slices, see Baden et al. (2013b). The resulting illumination levels at the slices corresponded to high mesopic/low photopic background light conditions.

3.5 Light stimulation protocols

Since horizontal cell to cone feedback could be dependent on the type of light stimulus, I used different protocols:

(a) A "colour protocol" consisting of alternating UV and green sine wave stimuli. This protocol was presented at the beginning of each recording session to determine the spectral preference of the recorded cones (Baden et al., 2013b).

For the surround stimulation experiments, two different "stepping bar protocols" were used:

(b) A "stepping bar protocol" consisting of two alternating stimuli: a small (40 µm wide) and a large (500 µm wide) bar, both *brighter* than the background light level. First, the small bar was consecutively shifted along the slice (in 10 µm steps at 0.5 s intervals), starting at a position that was at least 200 µm away from the position of the recorded cones (Figure 11A). Then the procedure was repeated with the large bar (using the same starting position as for the small bar). The contrasts used were 16%, 26%, 35% and 72% (all contrasts given as Weber contrast).

(c) Same protocol as in (b) but with bars *darker* than the background light level (Figure 12). For technical reasons, we used only the green LED channel and therefore this protocol was only tested for dorsal (dominantly M-opsin expressing) cones. The contrast used was -71%.

For the pharmacology experiments, four different full-field flash protocols were used (Figure 13). Full-field means that the stimulus diameter was ~2 mm and therefore usually covered the whole slice.

(d) The "high bright contrast protocol" included stimulation with bright flashes (95% contrast).

(e) The "medium bright/dark contrast" protocol included alternating stimulation with dark flashes (-23% contrast) and bright flashes (51% contrast).

(f) The "high dark contrast protocol" included stimulation with dark flashes (-39% contrast).

(g) A saw-tooth ("intensity ramp") stimulus that covered the whole intensity range as in (d-f).

3.6 Pharmacology and drug application

To pharmacologically dissect the different hypothesized feedback mechanisms from horizontal cells to cones, I used both bath application and local puff application. For bath application, drugs were incubated for at least 5 min and then washed out for at least 10 min. The volume of the recording chamber was

~1 ml and the perfusion rate was ~2 ml/min. For puff application, drugs were puffed onto the recorded photoreceptor axon terminal region (distance of the electrode tip from recorded region: 15-20 µm) for 20-60 s using a glass pipette (resistance 5-8 MΩ) and a pressure application system (Sigmann Elektronik GmbH, Germany; pressure: 0.3-1.0 bar). By adding the fluorescent dye sulforhodamine 101 (Sigma-Aldrich, Steinheim, Germany), we verified that the puffing area on the tissue did not exceed a lateral width of ~100 µm. Puffing extracellular solution had no effect on cone Ca^{2+} signals.

The following drug concentrations were used for bath application (in µM): 100 CBX ((3β,20β)-3-(3-Carboxy-1-oxopropoxy)-11-oxoolean-12-en-29-oic acid disodium), 100 CoCl2 hexahydrate, 0.2 PD168077 maleate, 20,000 HEPES (4-(2-hydroxyethyl)piperazine-1-ethanesulfonic acid), 10 SR-95531/Gabazine (Gz, 2-(3-Carboxypropyl)-3-amino-6-(4 methoxyphenyl)pyridazinium bromide), 75 TPMPA ((1,2,5,6-Tetrahydropyridin-4-yl)methylphosphinic acid), 50 NBQX (6,7-dinitroquinoxaline-2,3-dione), 50 AMPA (α-amino-3-hydroxy-5-methyl-4-isoxazolepropionic acid), and 25 kainic acid. For puff application, the following concentrations were used (in µM): 100 or 500 CBX, 500 GABA (γ-aminobutyric acid), 50 AMPA (α-amino-3-hydroxy-5-methyl-4-isoxazolepropionic acid), and 25 kainic acid. All drugs were purchased from Tocris Bioscience except for CBX, HEPES and CoCl2 (Sigma-Aldrich). All drug solutions were carboxygenated before application. HEPES was added to the carboxygenated extracellular solution, which was then again carboxygenated for 15 minutes, and finally adjusted to pH 7.4 using 1 M NaOH. To exclude osmotic effects in the case of the HEPES application, we used osmolarity-corrected extracellular solution for some of the HEPES experiments. However, we did not see any differences compared to the recordings with HEPES in standard solution.

3.7 Ca^{2+} imaging data analysis

For analysing light-evoked Ca^{2+} signals, custom-written scripts for IgorPro (Wavemetrics) were used. Regions of interest (ROIs) were positioned on the cone axon terminals and the (background-subtracted) ratio acceptor/donor between the fluorescence signal of the FRET donor/acceptor pair eCFP and citrine, respectively, was calculated. A ratio increase represents an elevation in intracellular Ca^{2+} concentration. Because we focused on relative changes in Ca^{2+} levels, we did not attempt to calibrate the setup and give the fluorescence ratio as a proxy of Ca^{2+} level. Only cells that showed reliable light responses during the control condition were selected for further analysis (for response quality criterion, see Baden et al. (2013a)). Several response parameters were determined using boxcar-filtered average traces (typically the average of 10 but minimally 3 stimulus trials; box-width: 160 ms).

For the surround stimulation experiments, we used an approach (see light stimulation protocols (b) and (c) in 3.5) that activated cones in a recording field at different time points within a trial. To determine the time point of the response onset for each cone, its response to the small bar (i.e. the receptive field "centre" response) was fitted with a sigmoid. As response onset we defined the time point when the Ca^{2+} signal level exceeded a threshold of 1 SD below or above the baseline for bright and dark stimuli, respectively. This response onset was used as a "reference" to determine the following parameters: First, we analysed how surround stimulation modulated the cone's Ca^{2+} baseline (R_{base}) during a time period of 0.5 s before response onset (Figure $11C_1$, Figure $12B_1$). At this time point, the bar stimulus was still in the cone's surround (10 µm away from the cone's position). Second, we analysed how surround stimulation modulated the response amplitude (R_{amp}) relative to R_{base} with the bar stimulus just inside the cone's receptive field centre (for details, see Figure $11C_2$, Figure $12B_2$).

For the full-field flash stimulation experiments, we also determined R_{base} (Figure 13C), but – instead of R_{amp} – used the response area under the trace (R_A) as a measure of response size. Finally, we determined the "peakedness index" (*PI*), which was defined as $\frac{A_{peak} - A_{plateau}}{A_{peak} + A_{plateau}}$, with A_{peak} being the amplitude of the response peak, and $A_{plateau}$ the amplitude of the response plateau (Figure 13D).

The drug effects on the different response parameters were statistically evaluated using the Wilcoxon rank-sum test and the Wilcoxon signed-rank test. Alpha was 0.05 and p-values <0.05 were considered as significant (*), <0.01 (**), and <0.001 (***). Using the stimulation protocols described in 3.5, we did not find any significant differences of drug effects between functional S- and M-cones (Baden et al., 2013b) and therefore decided to pool data from both cone types for analysis. If not indicated otherwise, errors are given as standard error of the mean (SEM).

3.8 Immuno-electron microscopy

Immuno-electron microscopy was carried out by Konrad Schultz and Karin Dedek (Department of Neurobiology, University of Oldenburg).

Immuno-electron microscopy was performed as described by Janssen-Bienhold et al. (2009). Retinas were fixed for 40 min in 3% paraformaldehyde in 0.1 M phosphate buffer (PB), pH=7.4. After rinsing and cryoprotection (30% sucrose in PB overnight), tangential sections (60 µm) were cut on a cryotome (Bright Instrument, Huntingdon, UK). Unspecific binding was blocked with 10% normal goat serum in PB for 2 hours, followed by incubation with the primary polyclonal antibodies directed against the $GABA_A$

receptor subunit α1 (1:400 in PB; SYnaptic SYstems, Germany) and the $GABA_C$ receptor subunit ρ (1:250 in PB; provided by R. Enz/S. Haverkamp) for 4 days at 4°C. After several washes in PB, sections were incubated with biotinylated goat-anti-guinea pig IgG (1:250 in PB) and biotinylated goat-anti-rabbit IgG (1:250 in PB), respectively, overnight at 4°C. Binding sites were detected by the Vectastain Elite ABC-Kit (Vector Laboratories Inc., Burlingame, CA). Sections were postfixed (2.5% glutaraldehyde, 1% paraformaldehyde, 1 hour) and subjected to silver intensification, followed by an additional fixation with 1% OsO_4 in PB for 1 hour. Sections were dehydrated by increasing acetone concentrations (50–100%), before being embedded in Agar 100 resin (Agar Scientific Ltd., Essex, UK). Ultrathin sections were collected on copper grids and were photographed and analysed with a Zeiss 902 electron microscope. Intensity and contrast were adjusted using Adobe Photoshop CS6 extended.

4 Results

4.1 Surround stimulation modulates light-evoked Ca^{2+} responses in individual cone axon terminals

Somatic whole-cell patch-clamp recordings strongly suggest that horizontal cells provide feedback to cones by changing the activation level of the VGCCs in the cone terminal (see 2.7.2) (Verweij et al., 1996; Kraaij et al., 2000; Hirasawa and Kaneko, 2003; Fahrenfort et al., 2009). To more directly assess its effect on the VGCC activity in cones, we studied how horizontal cell feedback modulates presynaptic Ca^{2+} levels in cone axon terminals – as a proxy for glutamate release and therefore cone output (Thoreson, 2007; Jackman et al., 2009). We used the transgenic *HR2.1:TN-XL* mouse line (Wei et al., 2012), in which cones selectively express the Ca^{2+} indicator TN-XL (Mank et al., 2006), and recorded light-evoked Ca^{2+} signals in cone axon terminals in retinal slices using two-photon microscopy (Figure 10).

Before pharmacologically dissecting the different hypothesized horizontal cell feedback mechanisms, we investigated how light stimulation in a cone's surround affects its Ca^{2+} response. A classical experiment to study horizontal cell feedback is to stimulate a cone with light spots of different diameters, i.e. a small-diameter spot to evoke mainly the receptive field centre response and a large-diameter spot to evoke the receptive field's combined centre/surround response. The effect of horizontal cell feedback on the cone can then be isolated by subtracting the responses to large and small spots (Baylor et al., 1971). Here, we modified this stimulus paradigm to allow for recording from many cones in a slice simultaneously: We first presented a small bright bar (40 µm wide) at different consecutive positions (10 µm step width) along the slice while recording the Ca^{2+} signals in 5-10 cone terminals (Figure 11A). Then this sequence was repeated but using a large bright bar (500 µm wide). Our sequential approach eliminated the need for recording time-consuming precise alignment of the small spot with a cone. The responses to the two bars can then be extracted for each cone (Figure 11B) and, after appropriate alignment of the Ca^{2+} traces for cone position, compared between the recorded cones.

We analysed how large bright stimuli in the surround modulate the resting Ca^{2+} level (R_{base}) (Figure $11C_1$) and the relative amplitude of the cone response (R_{amp}) (Figure $11C_2$). We found that large bright stimuli in the surround reduced R_{base} (by 3.4 ± 0.8%, n=24, $p<0.001$) and R_{amp} (by 6.2 ± 3.3%, $p=0.03$) (Figure 11D), suggesting that cones in our slice preparation are modulated by lateral interactions consistent with horizontal cell feedback. Note that due to the stimulus design the large bar covered only approximately

half of the cone's surround when R_{base} and R_{amp} were determined. Therefore, the measurements likely represent an underestimate of the surround effect. To exclude the possibility of "flooring" the cone Ca^{2+} levels (or the leaving the sensitivity range of the biosensor), both of which would appear like a reduction in R_{amp}, only data of responses to low contrast stimuli were pooled (16% and 26% Weber contrast) and a brighter test stimulus was used to verify that Ca^{2+} levels can be further decreased (see arrow in Figure 11B). Next, we analysed how increasing the contrast alters the surround effect on R_{base}. Already at 16% Weber contrast, R_{base} was significantly reduced by 1.8 ± 0.7% (n=14, p=0.02); at 72% contrast – the highest contrast tested – R_{base} was reduced by 8.1 ± 1.1% (n=23, p<0.001), suggesting that stimulating the horizontal cell network with higher contrasts leads to larger feedback effects on cone Ca^{2+} signals (Figure 11E). Carbenoxolone (CBX), a commonly used blocker of (ephaptic) horizontal cell feedback (Kamermans et al., 2001), significantly reduced the surround effects on R_{base} by 45% (ctr: -0.073 ± 0.008, CBX: -0.04 ± 0.012, absolute ratio values, n=10, p=0.004) (Figure 11F), supporting that horizontal cell feedback is responsible for the observed surround effects.

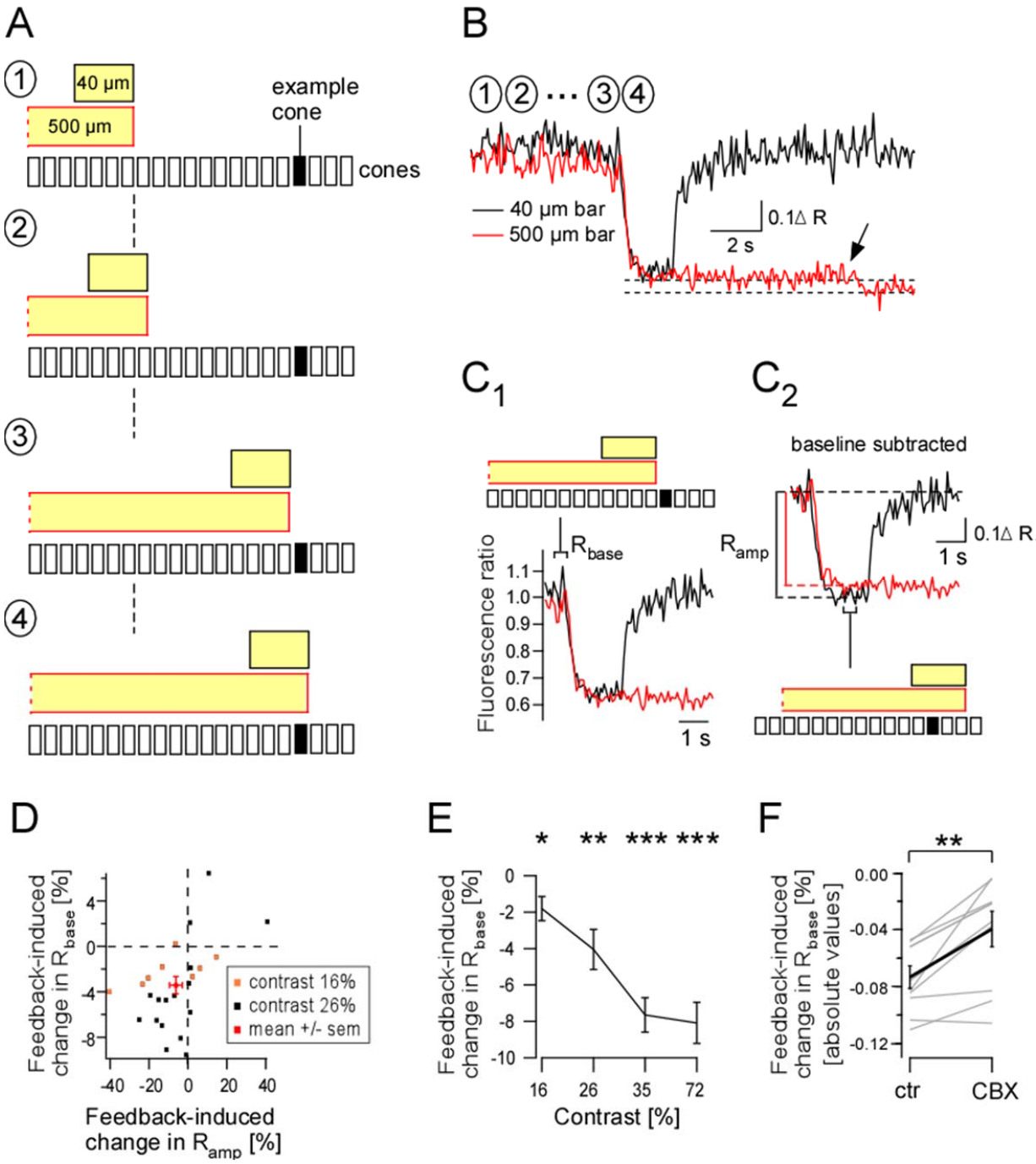

Figure 11: Bright stimulus in cone surround reduces Ca^{2+} level and relative response amplitude

A Illustration of the stimulus paradigm: a small bright bar was shifted step-wise along a retinal slice (with the row of boxes representing cones) towards the centre of an exemplary cone (black box) by 10 µm every 0.5 s. The procedure was then repeated with a large bright bar. ***B*** Ca^{2+} responses (as change in ratio between the fluorescence signals of the FRET donor/acceptor pair eCFP and citrine, average of n=6 trials) of the example cone (from *A*) to the small (black trace) and large bar (red trace); the numbers refer to the different stimulus phases as illustrated in (*A*). Initially, the bars were about 100 µm distant from

the exemplary cone (position 1); the decrease in Ca^{2+} indicates when the edge of the bar entered the receptive field centre of the cone (position 4). The Ca^{2+} signal was not "floored" by the contrast used, as the Ca^{2+} level could be further reduced by further increasing the light intensity (arrow). ***C₁*** The baseline signal R_{base} was determined in a time window of 0.5 s before the response onset (see 3.7). ***C₂*** The response amplitude R_{amp} was determined for the duration of the small bar response after subtraction of R_{base}. ***D*** Surround stimulation-induced effects on R_{base} and R_{amp} quantified as difference between the large and the small bar stimulation conditions and visualized as a scatter plot (ΔR_{base} as a function of ΔR_{amp}; average (red marker) pooled from low contrast data only). ***E*** Surround stimulation-induced reduction of R_{base} as function of stimulus contrast. ***F*** Effect of CBX on surround stimulation-induced reduction of R_{base} (n=10; for this analysis, only cones that showed a feedback-induced reduction in R_{base} >5% were used). Note that absolute ratio values are shown (same units as in C_1). Error bars: SEM.

We also asked how darker-than-background bar stimuli affect cone Ca^{2+} signals (Figure 12). Small and large dark bars elicited responses of opposite polarity compared to those upon stimulation with bright bars (Figure 12A *vs.* Figure 11B). Other than bright bars, dark stimuli presented to the surround led to an increase in R_{base} (by 5.3 ± 0.8%, n=15, p<0.001) as well as in R_{amp} (by 23.0 ± 7.3%, p=0.003) (Figure 12C).

In summary, presenting bright and dark stimuli in the surround of a cone modulated both its baseline Ca^{2+} level and relative response amplitude. Cone Ca^{2+} responses were *smaller* when a bright stimulus was presented to the surround, as expected for "classical" lateral inhibition and contrast enhancement (reviewed in Thoreson and Mangel, 2012). However, when a dark stimulus was present in the surround, cone Ca^{2+} responses became *larger*, a finding that is consistent with the excitatory horizontal cell feedback recently described in different species (Jackman et al., 2011).

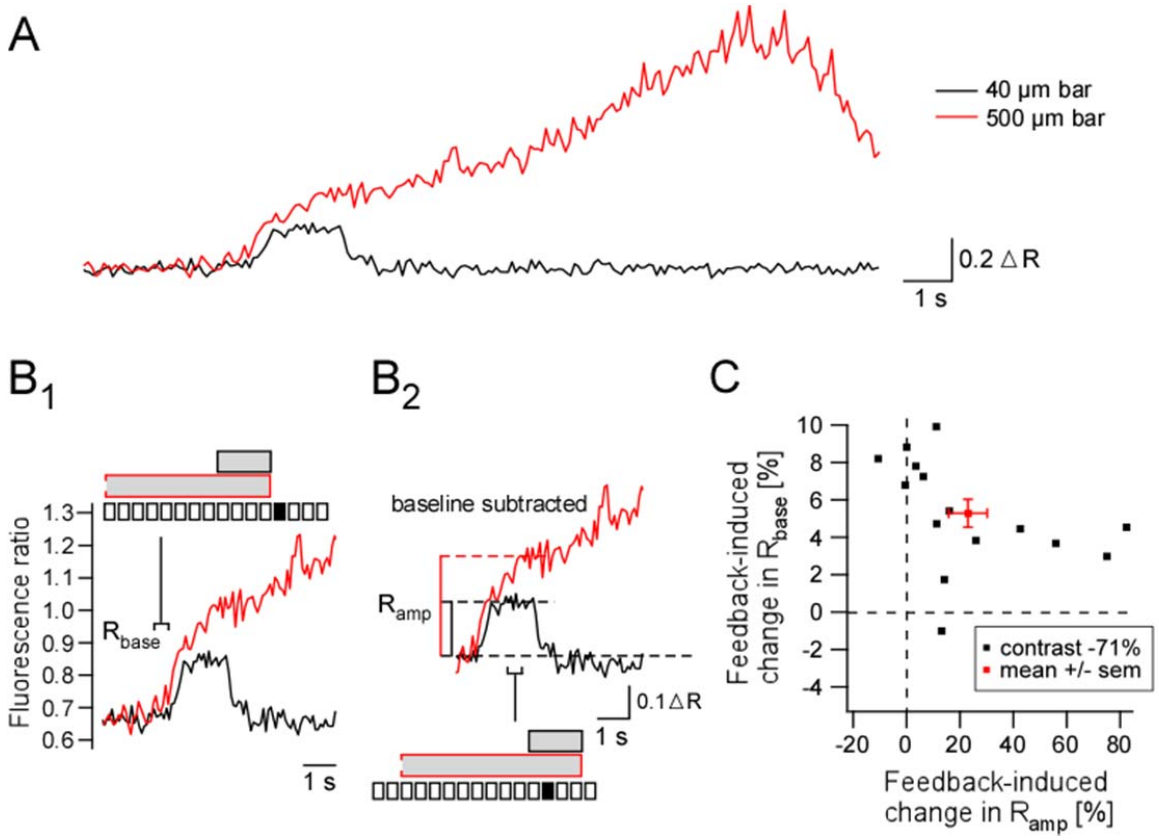

Figure 12: Dark stimulus in cone surround increases Ca^{2+} level and relative response amplitude
A Ca^{2+} responses of an exemplary cone to a small (black trace) and a large dark bar (red trace). Except for the inversed contrast, the stimulus paradigm is the same as is illustrated in Figure 11A. ***B*** R_{base} and R_{amp} were determined analogue to Figure 11C. ***C*** Surround stimulation-induced effects on R_{base} and R_{amp} quantified and visualized analogue to Figure 11D. Error bars: SEM.

4.2 Pharmacological dissection of hypothesized feedback mechanisms

For pharmacological dissection of the different hypothesized feedback mechanisms from horizontal cells to cones (Figure 13A), we used full-field flash protocols. While the three stimulation protocols (Figure 13B) had somewhat different background levels, the differences were within a single log unit and, thus, we assumed similar retinal adaptation states (for details, see 3.4). The responses to the full-field flashes (~2 mm in diameter) are expected to contain a combination of the cone receptive field centre and surround component – the latter mediated by horizontal cell feedback. To dissect the feedback that modulates cone Ca^{2+}, we blocked, selectively or in combination, the three proposed feedback

mechanisms (ephaptic, pH-mediated and GABAergic), or modulated horizontal cell activity in general. We analysed the pharmacological effects on R_{base} and the response area under the trace R_A (Figure 13C), and in addition on the "peakedness index" *PI* (see 3.7) to capture the ratio between transient and sustained response components (Figure 13D).

Based on our bar stimulus experiments, we expected that pharmacologically blocking feedback should: (*i*) increase R_{base} because eliciting feedback by bright stimuli (= hyperpolarizing horizontal cells) in the cone's surround resulted in a decrease of the Ca^{2+} level (Figure 11), (*ii*) increase R_A to bright flashes, as we observed "lateral inhibition" for bright stimuli (Figure 11), and (*iii*) reduce R_A to dark flashes, as we observed "lateral excitation" for dark stimuli (Figure 12).

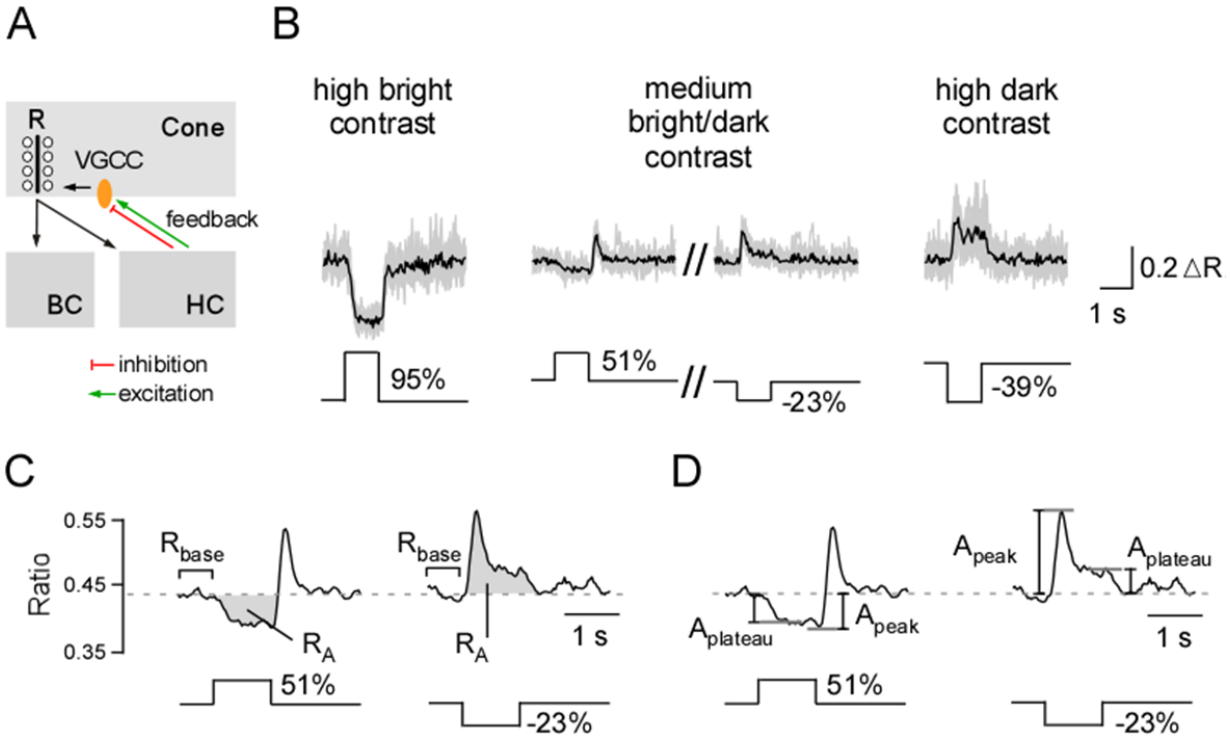

Figure 13: Quantification of light flash-evoked Ca^{2+} responses in cone axon terminals
A Schematic of the local circuitry between a cone, a horizontal cell (HC) and a bipolar cell (BC). Cones were stimulated with full-field flashes and thus their flash-evoked responses contained a centre and a surround component – the latter mediated by horizontal cell feedback. Blocking horizontal cell feedback is expected to block the surround component in the cone's response mediated by inhibitory feedback (red line). In addition, excitatory feedback is indicated as a green arrow. R, ribbon. ***B*** Ca^{2+} responses (average in black, single trials in grey) of different cones to different full-field stimulation protocols: "high bright contrast" (left), "medium bright/dark contrast" (middle) and "high dark contrast" (right) stimulation. ***C*** Quantification of the resting Ca^{2+} level (R_{base}) and the area under the trace (R_A). ***D*** Quantification of the peakedness index (*PI;* see 3.7 for details).

4.3 Ephaptic feedback modulates Ca^{2+} levels and light-evoked Ca^{2+} signals in cone axon terminals

Ephaptic feedback modulating the VGCC activity in cones requires conductances at horizontal cell dendrites to effectively change the local cone membrane potential (reviewed in Kamermans and Fahrenfort, 2004). In fish retina, both hemichannels (~60%) and iGluRs (~40%) contribute to ephaptic feedback (Fahrenfort et al., 2009). Fish retinal hemichannels are formed by Connexin 55.5 (Shields et al., 2007; Klaassen et al., 2011) and Pannexin 1 (Prochnow et al., 2009). In the mouse retina, the connexins that form functional hemichannels in horizontal cell dendrites have not yet been identified (Deans and Paul, 2001; Janssen-Bienhold et al., 2009). Recently, it was reported that Pannexin 1 is also present at mouse horizontal cell dendritic tips and thus represents a promising hemichannel candidate (Kranz et al., 2013). Like fish horizontal cells, mouse horizontal cells express iGluRs (Schubert et al., 2006; Ströh et al., 2013) that could contribute to ephaptic feedback.

To investigate whether *hemichannel*-mediated ephaptic feedback (Figure 14A) plays a role in the mouse retina, we used CBX (Kamermans et al., 2001) to block both connexin- and pannexin-formed hemichannels (Bruzzone et al., 2005), and presented the light stimulus protocols (d) – (f) (see 3.5) (Figure 14B-G). Blocking hemichannels affected the light-evoked cone Ca^{2+} signals in several ways: *(i)* R_{base} increased significantly (Figure 14B-H; for statistics see Table 1), *(ii)* R_A increased for bright flashes (Figure 14D,I) but remained unchanged for dark flashes (Figure 14G,K), and *(iii)* the *PI* for dark flash-evoked responses decreased (Figure 14F,L) but remained unchanged for bright flashes (Figure 14J). These results indicate that ephaptic feedback acts on different aspects of cone terminal Ca^{2+}: it adjusts the basal Ca^{2+} level and modulates the bright and dark flash-evoked responses differentially. That the response size is only affected for bright flashes suggests that the effect of ephaptic feedback on the Ca^{2+} signal strongly depends on the contrast polarity. Finally, our results suggest that ephaptic feedback renders the Ca^{2+} signal of dark flash-evoked responses more transient.

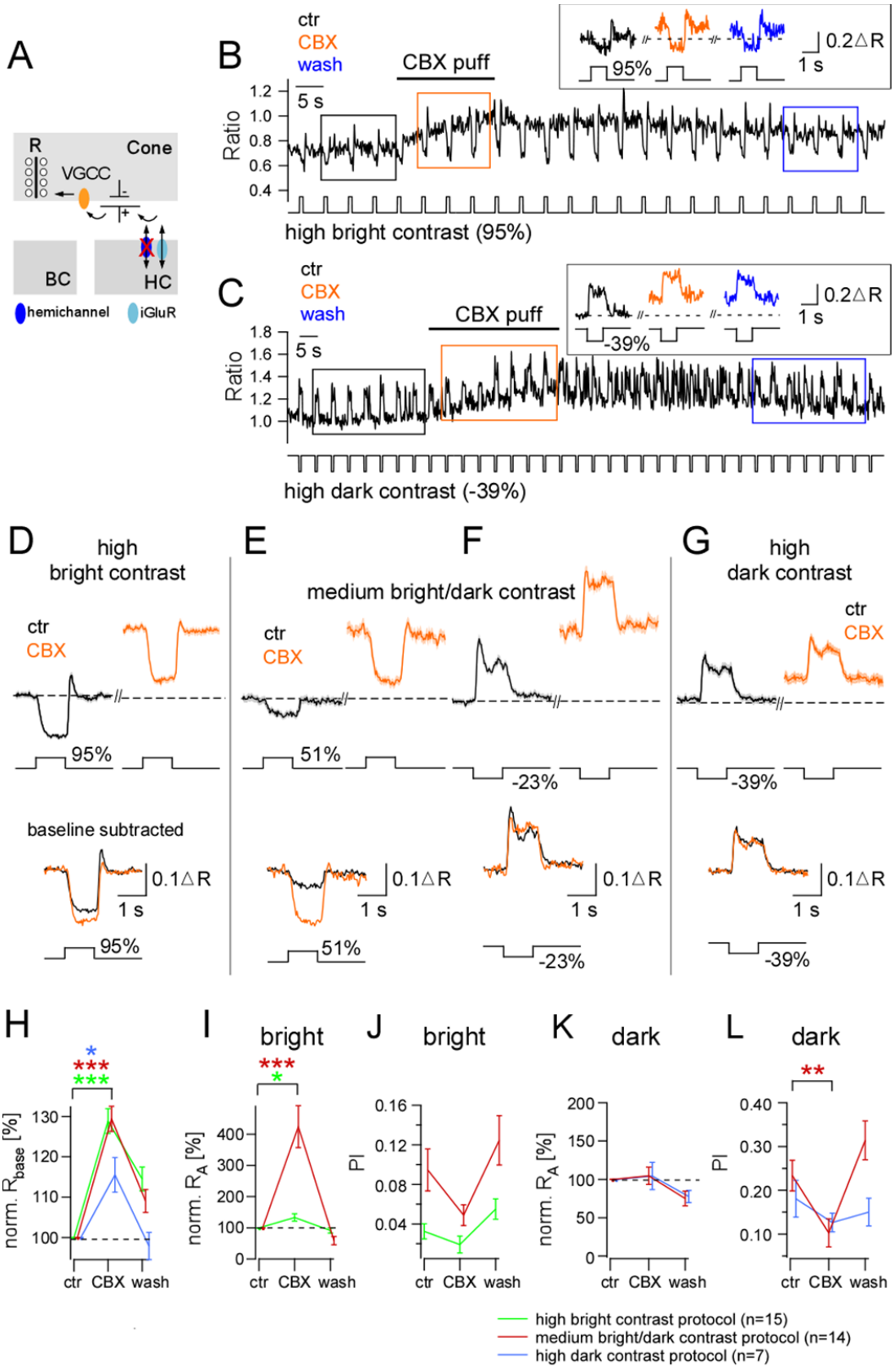
A
R
Cone
VGCC
BC
HC
hemichannel
iGluR
B
ctr
CBX
wash
CBX puff
95%
0.2△R
1 s
5 s
Ratio
high bright contrast (95%)
C
ctr
CBX
wash
CBX puff
-39%
0.2△R
1 s
5 s
Ratio
high dark contrast (-39%)
D
high
bright contrast
ctr
CBX
95%
baseline subtracted
0.1△R
1 s
95%
E
medium bright/dark contrast
ctr
CBX
51%
-23%
0.1△R
1 s
51%
0.1△R
1 s
-23%
F
G
high
dark contrast
ctr
CBX
-39%
0.1△R
1 s
-39%
H
norm. Rbase [%]
ctr CBX wash
I
bright
norm. RA [%]
ctr CBX wash
J
bright
PI
ctr CBX wash
K
dark
norm. RA [%]
ctr CBX wash
L
dark
PI
ctr CBX wash
high bright contrast protocol (n=15)
medium bright/dark contrast protocol (n=14)
high dark contrast protocol (n=7)

Figure 14: Blocking hemichannels with CBX modulates cone Ca^{2+} levels and light-evoked Ca^{2+} responses
A Schematic of the local circuitry between cones and horizontal cells, showing hemichannels (blue) at horizontal cell dendritic tips as proposed key elements in ephaptic feedback. ***B*** Exemplary cone Ca^{2+} responses to bright contrast flashes before (black box), during (orange box) and after (blue box) puff of the hemichannel blocker carbenoxolone (CBX) onto the recorded cone terminals. Inset: Ca^{2+} signals averaged from the three boxes. ***C*** Exemplary cone Ca^{2+} responses to dark contrast flashes. ***D-G*** Effect of bath-applied CBX on the cone Ca^{2+} signal for the "high bright contrast" protocol (*D*, average of n=15 cones), the "medium bright/dark contrast" (*E,F;* average of n=14 cones) and the "high dark contrast" protocol (*G*, average of n=7 cones). ***H-L*** Quantification of CBX effects on R_{base} (*H*), R_A (*I,K*) and *PI* (*J,L*) for the indicated stimulus protocols. Error bars: SEM.

To confirm the presence of ephaptic feedback in the mouse retina, we applied cobalt, which was also shown to block hemichannels (Fahrenfort et al., 2004). At a concentration of 100 µM, cobalt reduced R_{base} (Figure 15A-C) as well as R_A for both bright and dark flashes (Figure 15D,F), which was likely due to cobalt directly inhibiting VGCCs (Corey et al., 1984; Liu et al., 2013). When the cobalt concentration decreased during the first 30 seconds of wash out, both R_{base} (Figure 15C) and R_A increased for bright flashes (Figure 15D) compared to the pre-cobalt control, reminiscent of the CBX condition (compare with Figure 14H,I). A possible interpretation of these results is that at lower cobalt concentrations the blocking effect on hemichannels outweighs the direct inhibition of VGCCs, in line with a recent study showing that cobalt concentrations lower than 100 µM increase Ca^{2+} signals in rat photoreceptors (Liu et al., 2013). Why the peakedness index *PI* did not change significantly remained unclear (Figure 15E,G).

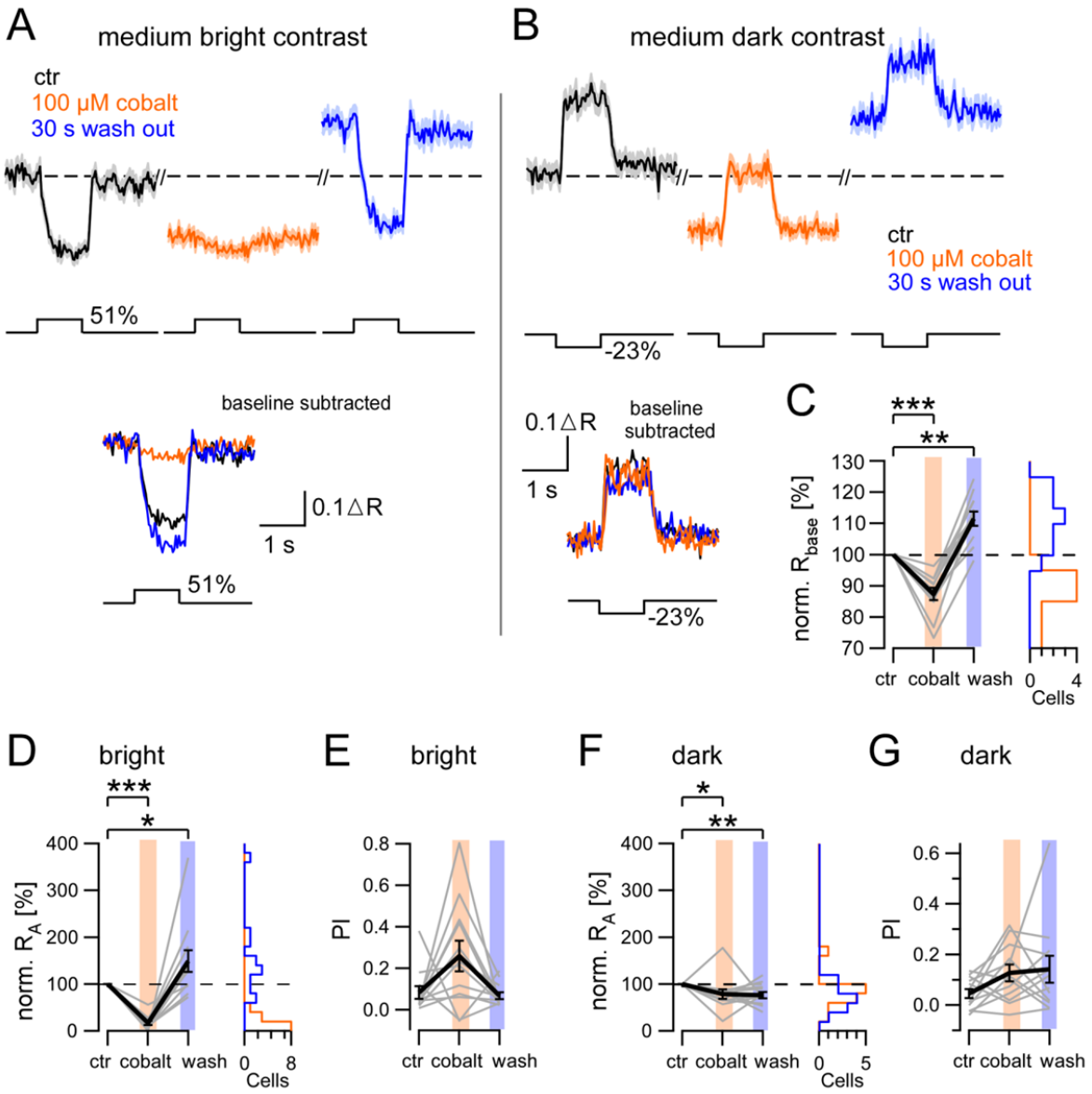

Figure 15: Blocking hemichannels with cobalt at concentrations lower than 100 µM recapitulates most of the effects observed for CBX

A Cone Ca^{2+} responses (n=12 cones averaged) to the "medium bright contrast" protocol before (ctr, black), during application of cobalt (orange) and during wash-out (blue). ***B*** Cone Ca^{2+} responses (n=12 cones averaged) to the "medium dark contrast" protocol before (ctr, black), during application of cobalt (orange) and during wash-out (blue). ***C-G*** Quantification of cobalt effects on R_{base} (*C*), R_A (*D,F*) and *PI* (*E,G*) for the indicated stimulus protocols. Error bars: SEM.

Blocking hemichannels increased the basal Ca^{2+} level in mouse cones, a finding that is in contrast to studies in fish cones. In the fish retina, under resting conditions, the current flow through hemichannels leads to a reduction of the transmembrane voltage at the cone axon terminal (see 2.7.3), thus leading to a local depolarization of the terminal and an increase in Ca^{2+} level (reviewed in Kamermans and Fahrenfort, 2004). Blocking hemichannels should abolish this reduction of the transmembrane voltage at the terminal, thereby hyperpolarizing the cone axon terminal. Consequently, the result would be a decrease in basal Ca^{2+} level and not an increase as observed in our experiments. To test if a current through iGluRs is related to the unexpected effect of CBX on R_{base} observed in mouse cones, we blocked iGluRs with NBQX and co-applied CBX (Figure 16A). However, as for CBX alone, blocking both hemichannels and iGluRs resulted in an increase in R_{base} (Figure 16B-D) and in R_A to bright flashes (Figure 16E), whereas R_A to dark flashes did not change (Figure 16G); moreover, there was no effect on *PI* (Figure 16F,H). The effects of NBQX and CBX on R_{base} were apparently additive: R_{base} for CBX alone (1.29 ± 0.03; n=14) was significantly smaller (p=0.049) than for CBX and NBQX together (1.43 ± 0.05; n=9), arguing against substantial side-effects of CBX on horizontal cell iGluRs (Tovar et al., 2009).

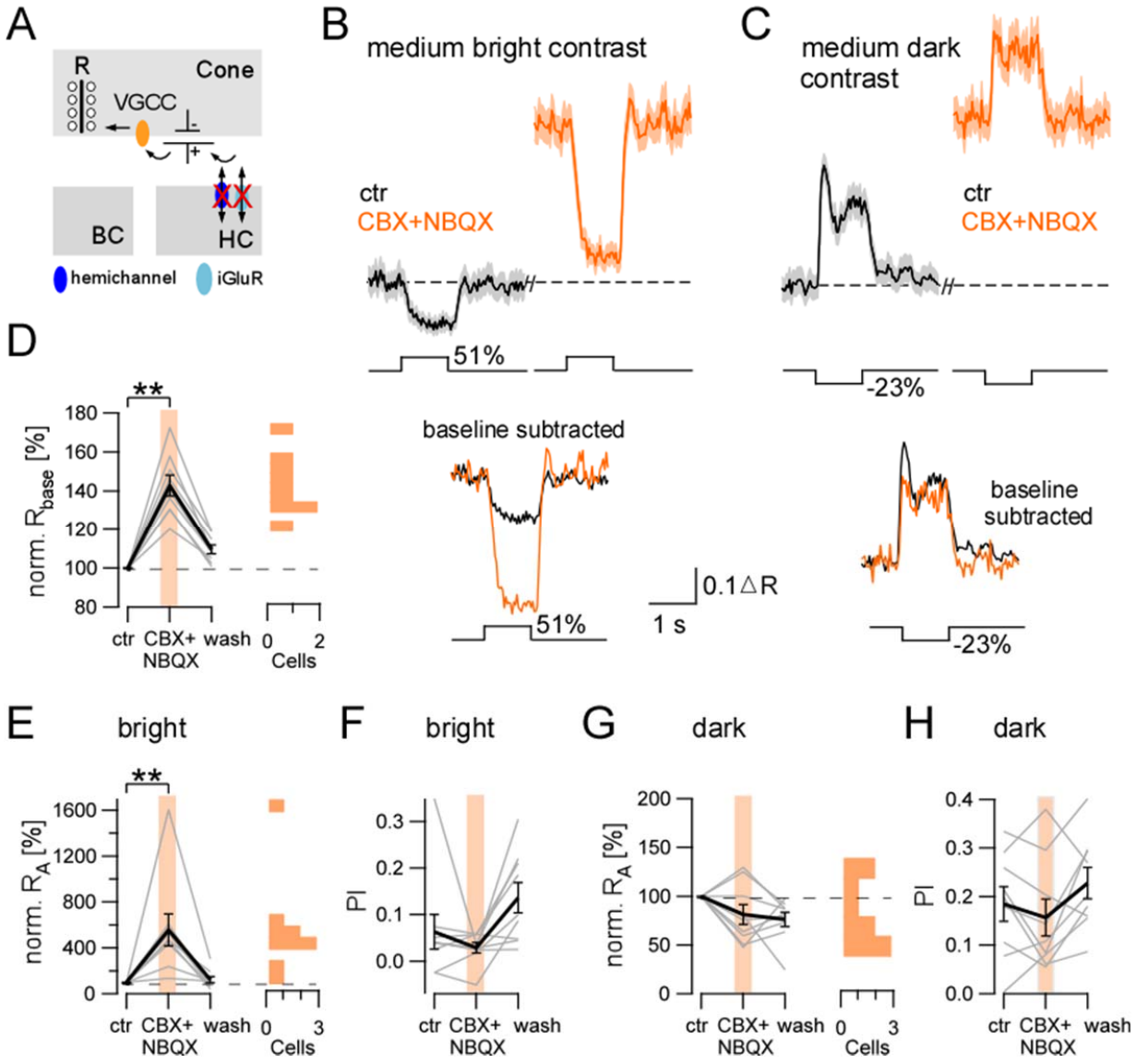

Figure 16: Blocking both hemichannels and ionotropic glutamate receptors on horizontal cells modulates cone Ca^{2+} levels and light-evoked Ca^{2+} responses

A Schematic of the local circuitry between cones and horizontal cells, showing both hemichannels (blue) and ionotropic glutamate receptors (iGluRs, light blue) at horizontal cell dendritic tips mediating ephaptic feedback. ***B,C*** Co-application of CBX and the AMPA/kainate-type iGluR antagonist NBQX had similar effects on light-evoked cone Ca^{2+} signals (n=9 cones averaged) as CBX (compare with Figure 14). ***D-H*** Quantification of CBX+NBQX effects on R_{base} *(D),* R_A (*E,G*) and *PI* (*F,H*) for the indicated stimulus protocols. Error bars: SEM.

To exclude the possibility that the CBX-induced increase in R_{base} was due to disruption of the gap junctionally-coupled rod-cone network (Tsukamoto et al., 2001), we reduced photoreceptor coupling by applying the dopamine receptor 4 (DR4) agonist PD168077 for ≥ 1 hour (Li et al., 2013) and then applied

CBX. In the presence of the DR4 agonist, the CBX-induced increase in R_{base} was comparable to the CBX-only condition (p=0.89, n=29 for ctr and n=6 for PD168077, see Table 1), suggesting that the coupling state of the rod-cone network was not affected by CBX in a way that it changed the cone Ca^{2+} signals in our experiments. Thus, the increase in R_{base} upon blocking hemichannels in the mouse retina cannot be explained by uncoupling of the rod-cone network or a change in current through iGluRs. In fact, that CBX increased R_{base} with full-field flashes is consistent with our surround stimulation experiments (Figure 11), where the reduction in R_{base} by light in the surround is counteracted by CBX.

In summary, blocking hemichannels and thereby modulating ephaptic horizontal cell feedback in the mouse retina resulted in an increase in cone Ca^{2+} level and larger bright flash-evoked responses, whereas the size of dark flash-evoked responses was less affected. The kinetics of dark-flash-evoked responses, however, was affected by modulating ephaptic feedback.

4.4 pH-mediated feedback modulates light-evoked Ca^{2+} signals in cone axon terminals in a contrast dependent way

To test the pH-mediated feedback hypothesis (Figure 17A), we buffered pH changes in the synaptic cleft with HEPES (Hirasawa and Kaneko, 2003; Vessey et al., 2005; Fahrenfort et al., 2009). Except for the stimulus protocol with the lowest background intensity ("high bright contrast", Figure 17B,F), HEPES did not affect R_{base} (Figure 17C-F; for statistics see Table 2). For bright flashes, HEPES had differential effects on R_A depending on the stimulus contrast: responses to high contrast bright flashes increased (Figure 17B,G), whereas responses to medium contrast bright flashes decreased (Figure 17C,G). HEPES did not affect *PI* of bright flash-evoked responses (Figure 17H). These findings point at different roles for pH-mediated feedback in shaping cone responses to bright flashes: attenuation for high contrast and amplification for low contrast stimuli. For dark responses, HEPES did not significantly change R_A (Figure 17I) but affected the response kinetics by decreasing the *PI* (Figure 17J).

In summary, clamping pH with HEPES had contrast-dependent effects on bright flash-evoked responses, and affected the kinetics of dark flash-evoked responses. HEPES did not have consistent effects on R_{base} – in contrast to the drugs that affected ephaptic feedback, which consistently increased R_{base}.

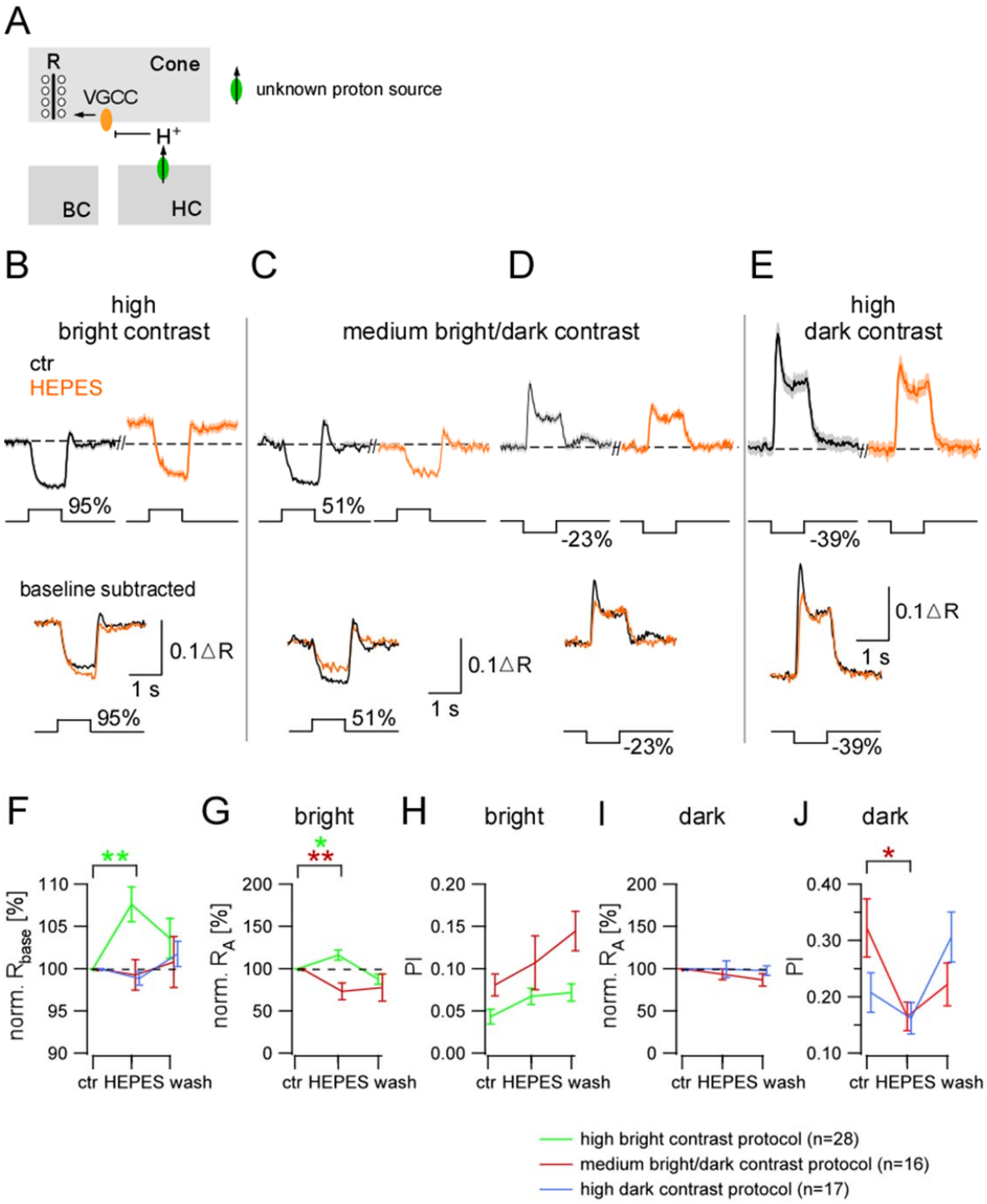

Figure 17: Clamping pH in the synaptic cleft has contrast-dependent effects on cone Ca^{2+} signals
A Schematic of the local circuitry between cones and horizontal cells, illustrating that the activity of voltage-gated calcium channels (orange) in cone terminal depends on the pH in the synaptic cleft. ***B-E*** Effect of the pH buffer HEPES on the cone Ca^{2+} signal for the "high bright contrast" (*B*; average of n=28 cones), the "medium bright/dark contrast" (*C,D*; average of n=16 cones) and the "high dark contrast"

protocol (*E*; average of n=17 cones). ***F-J*** Quantification of HEPES effects on R_{base} (*F*), R_A (*G,I*) and *PI* (*H,J*) for the indicated stimulus protocols. Error bars: SEM.

4.5 GABAergic transmission indirectly modulates cone output

In the OPL, GABA may be released from horizontal cells, which are considered GABAergic in mice (Deniz et al., 2011; Herrmann et al., 2011), and from interplexiform cells (Dedek et al., 2009). To study the effect of GABA on cone Ca^{2+} signals (Figure 18A), we puffed GABA onto the OPL while presenting light flashes (Figure 18B,F). Application of GABA led to a small but significant increase in R_{base} (Figure 18C,G; for statistics see Table 3) and R_A (Figure 18D,H) for both bright and dark flash responses; *PI,* however, was not changed (Figure 18E,I). The increase in R_{base} and R_A is in contrast to what is expected from the classical hypothesis of inhibitory GABAergic feedback mediated by GABA receptors expressed on photoreceptors (Wu, 1986). Nevertheless, in the light of a recent study by Liu et al. (2013), our data suggests a more complex role for GABA in the outer mouse retina: GABA is unlikely acting *directly* at the cone terminal, but instead may modulate cone output by controlling other feedback mechanisms.

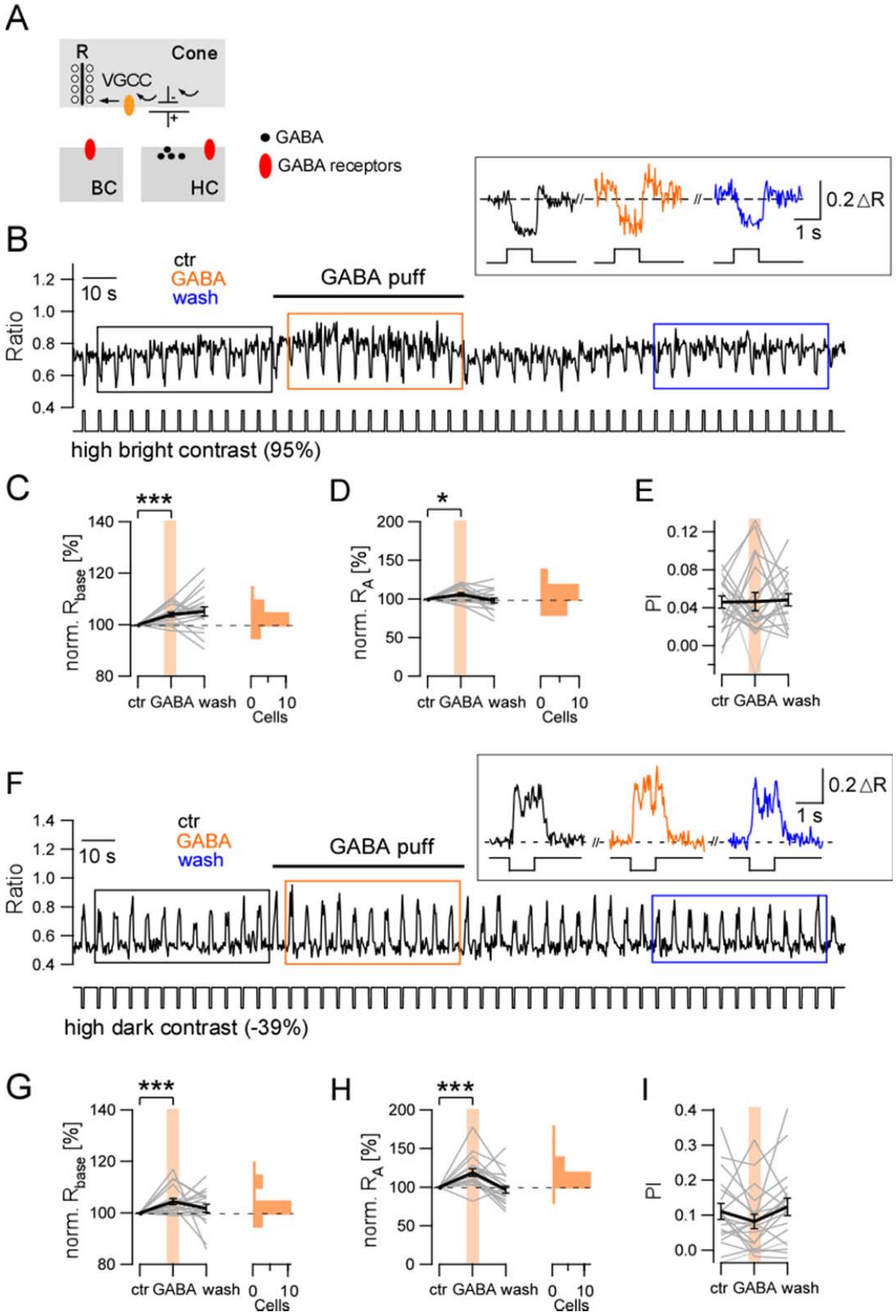
A
R
Cone
VGCC
BC
HC
GABA
GABA receptors
0.2 ΔR
1 s
B
ctr
GABA
wash
GABA puff
10 s
Ratio
high bright contrast (95%)
C
***
norm. Rbase [%]
ctr GABA wash
Cells
D
*
norm. RA [%]
E
PI
F
high dark contrast (-39%)
G
H
I

Figure 18: GABA modulates cone Ca^{2+} signals
A Schematic of the local circuitry between cones and horizontal cells, showing horizontal cells releasing GABA into synaptic cleft. ***B*** Exemplary cone Ca^{2+} response to repetitive "high bright contrast" stimulation before, during and after a GABA puff onto the cone terminals. Inset: averaged Ca^{2+} signals for different time windows (as indicated by the boxes). ***C-E*** Quantification of GABA effects on R_{base} (*C*), R_A (*D*) and *PI* (*E*) for bright contrast-evoked responses. ***F-I*** Same experiment as in (*B-E*) but for the "high dark contrast" protocol. Error bars: SEM.

To determine which cell types in the outer mouse retina express ionotropic GABA receptors and therefore may receive GABAergic input, we employed electron microscopy (Figure 19A,B) in cooperation with the Department of Neurobiology from the University of Oldenburg (see 2.8). In earlier studies, the α1 subunit (but not α2 or α3 subunits) of the $GABA_A$ receptor (Haverkamp and Wässle, 2000) and ρ subunits of $GABA_C$ receptors (Enz et al., 1996) were found to be present in the rodent OPL. Our electron microscopy data shows that none of the examined mouse cone terminals (n=73) expressed either of these GABA receptor subunits (Figure 19A,B), but we detected GABA receptors on the dendrites of cells postsynaptic to cones (horizontal cells and ON-cone bipolar cells) as expected from functional studies (Feigenspan and Weiler, 2004; Duebel et al., 2006). The distribution of GABA receptors in the mouse OPL (the lack thereof on cone terminals but their presence on horizontal cells) supports the conclusion from our functional data: It argues against a direct inhibitory GABAergic feedback pathway acting at the cone terminal and supports the hypothesis of GABA auto-reception-mediated effects on horizontal cells (Liu et al., 2013). It is noteworthy that the $GABA_A$ and $GABA_C$ receptor antagonists Gz and TPMPA, respectively, did not affect R_A and R_{base} (Figure 19C-H), which may point at a lack of endogenous GABA in the retinal slice preparation.

Taken together, GABAergic transmission appears to contribute to modulating cone output in the mouse retina, however, rather through indirect action (possibly auto-reception in horizontal cells) and not directly via ionotropic GABA receptors on cone terminals.

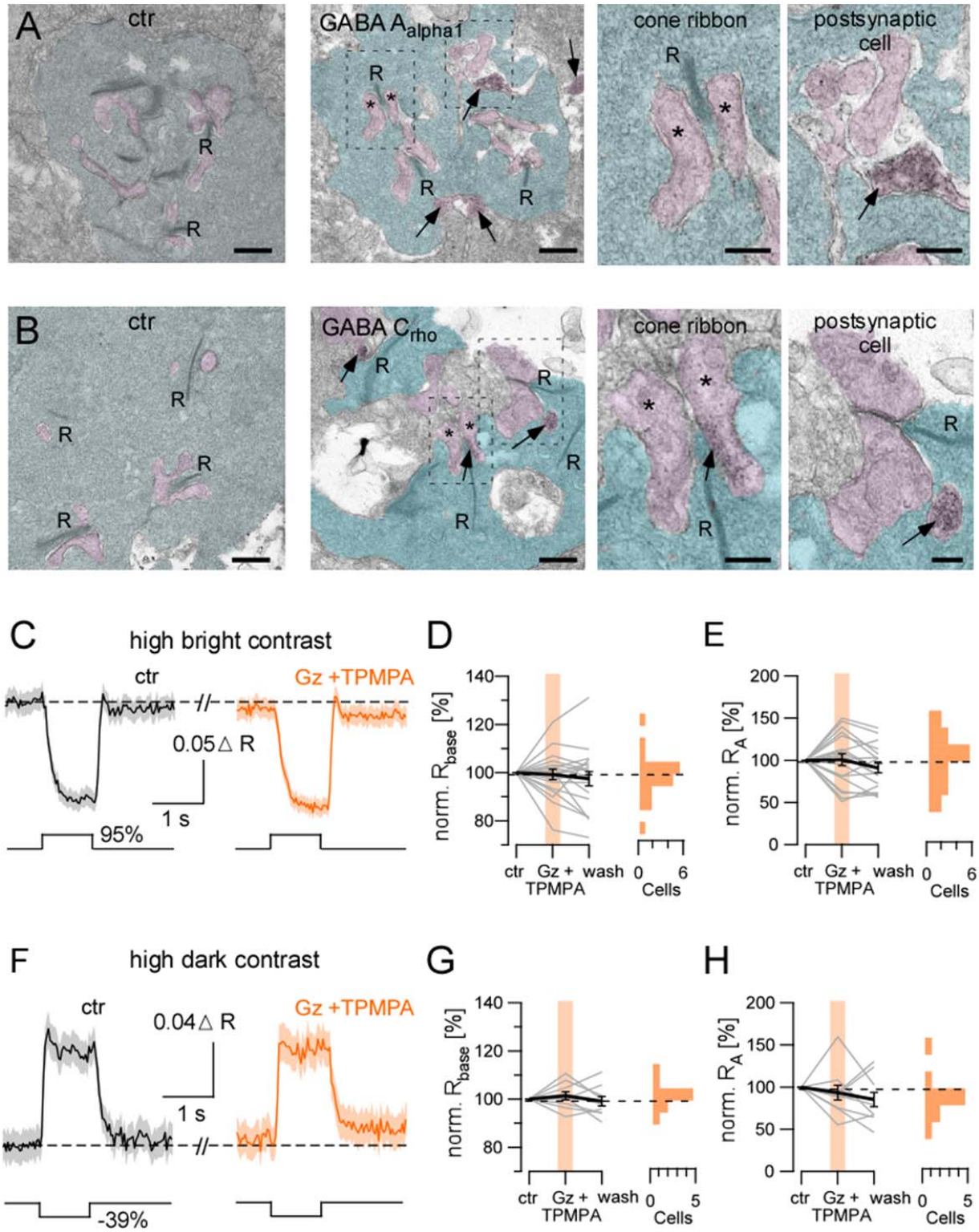

Figure 19: Cone axon terminals do not express ionotropic GABA receptors

A,B Electron microscopy images showing immunolabeling for the α1 subunit of $GABA_A$ (*A*) and ρ subunits of $GABA_C$ (*B*) receptors at cone ribbon synapses. Left: immunolabeling without antibodies as control

(ctr). Middle left: GABA receptor labelling. Middle right: magnified ribbon synapse region. Right: GABA receptors on ON-bipolar cell/horizontal cell dendrites (green, cone pedicle; purple, postsynaptic ON-bipolar cells/horizontal cells; asterisks, horizontal cell dendrites; arrows point at GABA receptor labelling on dendrites of postsynaptic cells; R, ribbon). Bars = 500 nm for left panels and 200 nm for right panels. ***C,F*** Co-application of the GABA receptor antagonists Gz and TPMPA did not affect cone Ca^{2+} responses to bright (*C*; n=19 cones averaged) nor dark stimuli (*F*; n=10 cones averaged). ***D,E,G,H*** Quantification of Gz+TPMPA effects on R_{base} (*D,G*) and R_A (*E,H*) for the indicated stimulus protocols. Error bars: SEM.

4.6 Local and global pharmacological manipulation of horizontal cell activity affect cone Ca^{2+} levels differently

All three feedback mechanisms from horizontal cells to cones can be simultaneously affected by clamping the input of horizontal cells via AMPA/kainate-type glutamate receptors (Schubert et al., 2006; Ströh et al., 2013) either with antagonists (NBQX) or agonists (AMPA/kainate). Hyperpolarization of horizontal cells by bath application of NBQX strongly increased R_{base} (Figure 20A-C), whereas depolarizing horizontal cells with AMPA/kainate tended to reduce R_{base} (Figure 20D,E). Both effects were consistent over the whole light stimulation range used. We then measured the effects of NBQX and AMPA/kainate on the bright flash-evoked cone Ca^{2+} responses and found the same effects on R_{base} (Figure 20F,G,I,J; for statistics see Table 4) as with the intensity ramp protocol (Figure 20A-E). In addition, while NBQX had no effect on R_A (Figure 20F,H), AMPA/kainate decreased R_A (Figure 20I,K).

The effects of blocking glutamatergic input to horizontal cells (by bath application) appear to be in conflict with our surround stimulation data, where hyperpolarizing horizontal cells (by presenting bright stimuli in the surround, Figure 11) and depolarizing horizontal cells (by presenting dark stimuli in the surround, Figure 12) decreased and increased R_{base}, respectively. However, when we puffed AMPA/kainate onto the recorded cones, locally "bathing" a tissue area of ~100 µm in width, we found R_{base} to increase, which is the opposite effect compared to (global) bath application (Figure 20L,M *vs.* J) but consistent with the effect of presenting a dark stimulus in the surround (Figure 12). The differential effects of local and global application are reminiscent of the findings by Jackman et al. (2011) in that horizontal cell feedback on cones appears to depend on the spatial scale of stimulation: local activation of horizontal cells predominantly triggered (spatially restricted) positive feedback, whereas global horizontal cell activation strengthened the contribution of (laterally operating) negative feedback (see *Discussion*).

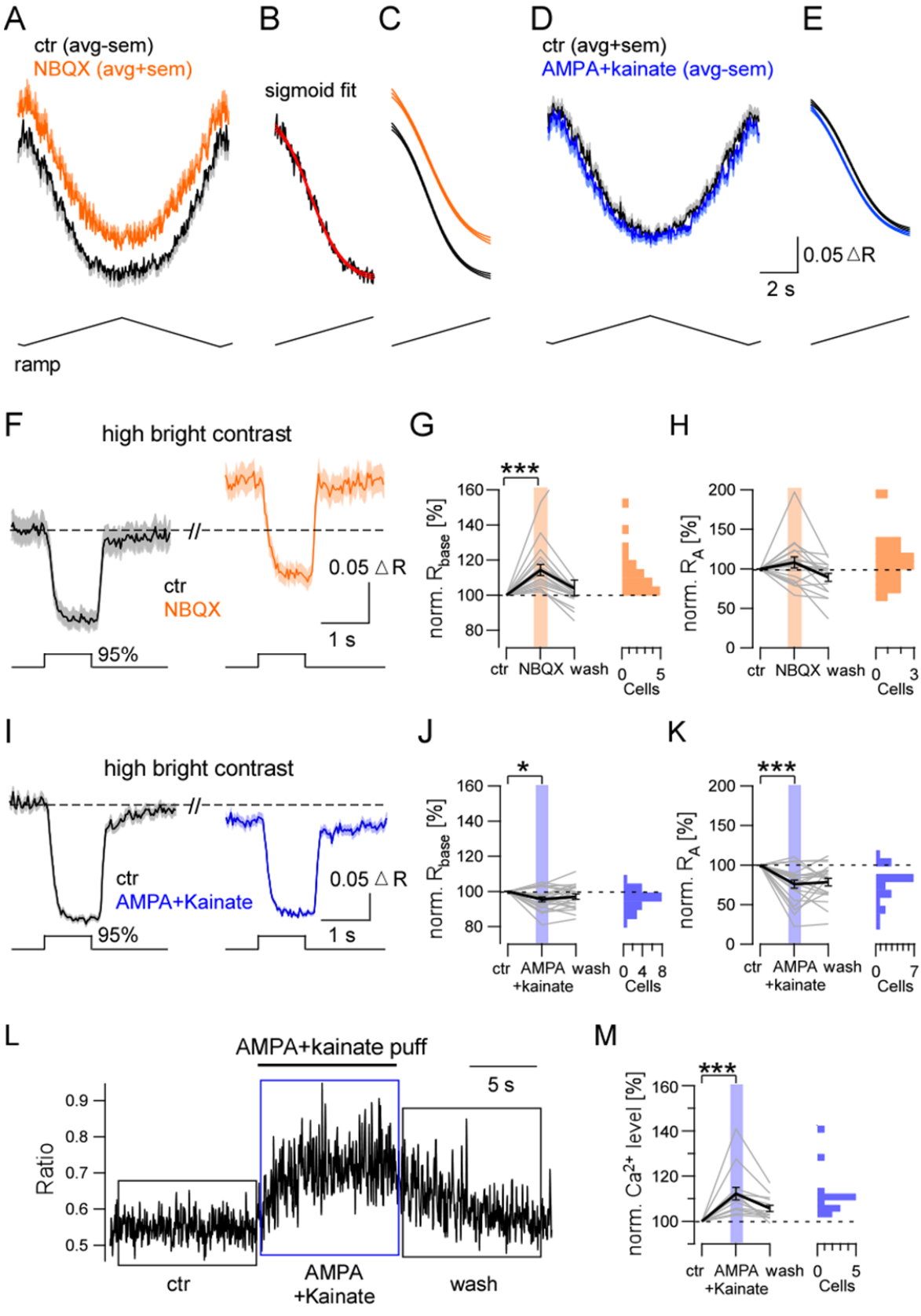
A
ctr (avg-sem)
NBQX (avg+sem)
B
sigmoid fit
C
D
ctr (avg+sem)
AMPA+kainate (avg-sem)
E
0.05 △R
2 s
ramp
F
high bright contrast
ctr
NBQX
0.05 △R
1 s
95%
G
***
norm. R_{base} [%]
160
140
120
100
80
ctr NBQX wash
0 5
Cells
H
norm. R_A [%]
200
150
100
50
0
ctr NBQX wash
0 3
Cells
I
high bright contrast
ctr
AMPA+Kainate
0.05 △R
1 s
95%
J
*
norm. R_{base} [%]
160
140
120
100
80
ctr AMPA wash
+kainate
0 4 8
Cells
K
***
norm. R_A [%]
200
150
100
50
0
ctr AMPA wash
+kainate
0 7
Cells
L
AMPA+kainate puff
5 s
Ratio
0.9
0.8
0.7
0.6
0.5
ctr
AMPA
+Kainate
wash
M
***
norm. Ca^{2+} level [%]
160
140
120
100
ctr AMPA wash
+Kainate
0 5
Cells

Figure 20: Clamping synaptic input to horizontal cells modulates cone Ca^{2+} signals depending on the spatial scale of drug application

A-C Effect of the AMPA/kainate-type GluR antagonist NBQX on cone Ca^{2+} level (n=12 cones averaged) before (ctr, black) and during NBQX application (orange) while presenting an intensity ramp stimulus. First part of averaged response (black) fitted with a sigmoid (red) (*B*) and corresponding fits of control (ctr, black) and NBQX traces (orange), with 95% confident intervals (*C*). ***D*** Effect of agonists AMPA/kainate on cone Ca^{2+} level (n=21 cones averaged) before (ctr, black) and during AMPA/kainate application (blue) while presenting an intensity ramp stimulus. ***E*** Analysis analogue to (*B,C*). ***F*** Cone Ca^{2+} responses to the "high bright contrast" stimulus (n=18 cones averaged) before (ctr, black) and during bath application of NBQX (orange). ***G,H*** Quantification of NBQX effect (bath application) on R_{base} *(G)* and R_A *(H)*. ***I*** Cone Ca^{2+} responses to the "high bright contrast" stimulus (n=21 cones averaged) before (ctr, black) and during bath application of AMPA/kainate (blue). ***J,K*** Quantification of AMPA/kainate effect (bath application) on R_{base} *(J)* and R_A *(K)*. ***L*** Puffing AMPA/kainate locally onto photoreceptor terminals increased cone Ca^{2+} level (n=14 cones) (boxes indicate time windows for calculating Ca^{2+} levels for control, AMPA/kainate and wash out conditions; no light flashes were applied, but the background light level was the same as for (*I*)). ***M*** Quantification of AMPA/kainate effect (local puff) on cone Ca^{2+} level. Error bars: SEM.

5 Discussion

This thesis represents the first study that directly compares different horizontal cell feedback mechanisms in the mouse retina. We show that cone output is dominantly regulated by ephaptic and pH-mediated feedback and that these two mechanisms modulate different aspects of the cone Ca^{2+} response: ephaptic feedback modulates the cone resting Ca^{2+} level, the response size to bright flashes, as well as the response kinetics to dark flashes. In contrast, pH-mediated feedback does not affect the cone resting Ca^{2+} level, but modulates – as the ephaptic pathway – the response size to bright flashes and the response kinetics to dark flashes. GABA also modulates cone output, but the observed effect is inconsistent with direct GABAergic inhibition at cone terminals as proposed earlier (Wu, 1986). Instead, GABA appears to affect the other two feedback pathways, possibly via GABA auto-receptors on horizontal cells (Liu et al., 2013).

5.1 Imaging Ca^{2+} levels in cone axon terminals as a proxy for cone output

Previous studies measured horizontal cell feedback at the level of cones, horizontal cells and ganglion cells using electrical recordings from the respective cell soma (reviewed in Thoreson and Mangel, 2012). In the present study, we monitored horizontal cell feedback by optically recording light-evoked Ca^{2+} signals directly in cone axon terminals. While Ca^{2+} imaging lacks the temporal resolution of electrical techniques (i.e. to resolve potential fast aspects of horizontal cell feedback kinetics), it allows for a more direct measurement of the consequences that horizontal cell feedback has on cone output: All feedback mechanisms are thought to directly act on the cone synaptic terminal by affecting the activation of VGCCs (reviewed in Kamermans and Fahrenfort, 2004). Because the cone membrane potential is only weakly modulated by horizontal cell feedback (Kraaij et al., 2000), assessing the horizontal cell feedback based on electrical recordings from the soma requires sophisticated analysis tools to extract the relevant Ca^{2+} currents (Fahrenfort et al., 1999). Imaging local Ca^{2+} changes directly in the cone pedicle using the *HR2:1:TN-XL* biosensor mouse line (Wei et al., 2012) circumvents these potential problems and is also less invasive compared to electrical cone recordings (e.g. no dialysis). Furthermore, transmitter release from cones was shown to directly depend on presynaptic Ca^{2+} (Thoreson, 2007; Jackman et al., 2009), therefore cone terminal Ca^{2+} is an excellent proxy for cone synaptic output. It is noteworthy that the measured terminal Ca^{2+} is thought to be a combination of (largely) Ca^{2+} entry through VGCCs and Ca^{2+}-induced release from stores like the endoplasmic reticulum (Figure 6) (Wei et al., 2012). Physiologically,

Ca^{2+}-induced release of Ca^{2+} in photoreceptors might be important for shaping synaptic transmission (Babai et al., 2010).

5.2 Is feedback from horizontal cells to cones inhibitory or excitatory?

Conceptually, horizontal cell feedback is thought of as inhibitory (Baylor et al., 1971). However, recently, evidence for excitatory horizontal cell feedback was presented (VanLeeuwen et al., 2009; Jackman et al., 2011). Like the "classical" inhibitory feedback, this excitatory feedback relies on glutamatergic transmission from cones to horizontal cells, but it acts at a more local scale (Jackman et al., 2011). Jackman and co-workers proposed that such excitatory feedback could preserve signal strength by counteracting the detrimental effects of the inhibitory feedback. Here, we asked whether in the mouse retina both inhibitory and excitatory effects of horizontal cell feedback on cone Ca^{2+} signals could be observed. To this end, we first analysed the effects of presenting bright or dark stimuli in a cone's receptive field surround on its Ca^{2+} responses: the cone Ca^{2+} responses were attenuated by more light (Figure 21A) but increased by less light in the surround (Figure 21C). From that we hypothesized that the effects of horizontal cell feedback are inhibitory for bright stimuli and excitatory for dark stimuli – in line with the earlier observations that *(i)* the effects of (inhibitory) horizontal cell feedback decrease substantially at more depolarized cone membrane potentials (Verweij et al., 1996), and that *(ii)* depolarizing horizontal cells has excitatory effects on cone Ca^{2+} levels (Jackman et al., 2011).

In the second part of our study we aimed at dissecting the different hypothesized horizontal cell feedback mechanisms using full-field stimuli in combination with pharmacology. We showed that drugs blocking ephaptic and pH-mediated feedback generally increased the size of cone Ca^{2+} responses to bright flashes (Figure 21B), pointing at inhibitory effects of horizontal cell feedback for light presented to the surround, as expected from the surround stimulation experiments. For dark flashes, however, most of these drugs mainly affected the kinetics (*PI*) and had no effect on the size of cone Ca^{2+} responses (Figure 21D). Thus, the excitatory effect of horizontal cell feedback on cone Ca^{2+} levels observed when presenting dark stimuli in a cone's surround may be mediated by a feedback mechanism that is little affected by the drugs used in this study. Notably, also Jackman et al. (2011) failed to unanimously identify the underlying mechanism of the excitatory feedback in their study. Nevertheless, our data confirms their results in that this excitatory horizontal cell feedback mechanism works on a more local scale, since we observed excitatory effects only when depolarizing horizontal cells pharmacologically

with local puff application, but not with global bath application (Figure 20). When we globally changed the activity state of horizontal cells, we observed inhibitory effects on cone Ca^{2+} signals, suggesting that under this condition the effects of (laterally operating) inhibitory feedback exceeded those of excitatory feedback.

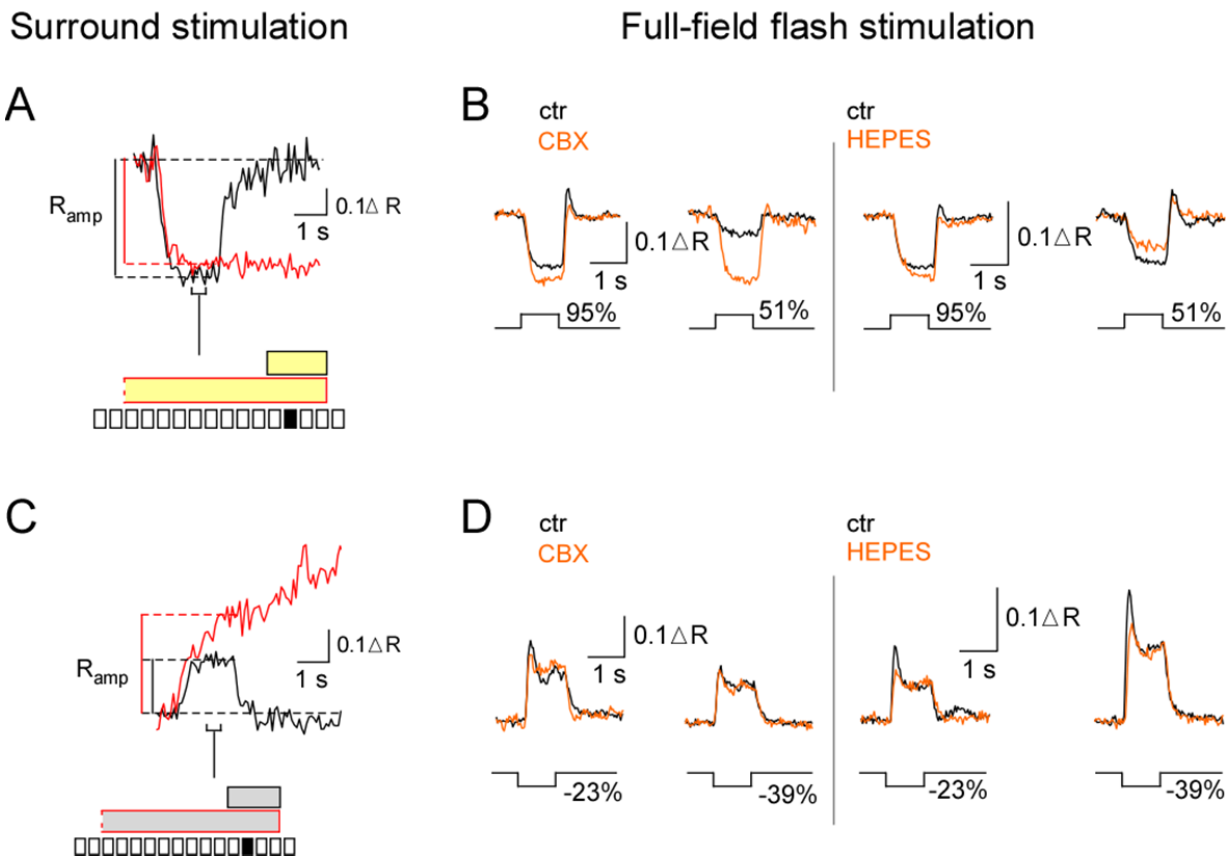

Figure 21: Inhibitory and excitatory effects of horizontal cell feedback
A Bright contrast-evoked Ca^{2+} responses were reduced by surround stimulation ("lateral inhibition"). ***B*** Blocking ephaptic feedback with CBX or pH-mediated feedback with HEPES, respectively, generally increased the size of the bright-contrast-evoked Ca^{2+} responses in cones, indicative of blocked inhibitory feedback. ***C*** Dark contrast-evoked Ca^{2+} responses were increased by surround stimulation ("lateral excitation"). ***D*** Blocking ephaptic and pH-mediated feedback, respectively, did not affect the size of the dark contrast-evoked Ca^{2+} responses, suggesting that excitatory feedback involves a mechanism that cannot be abolished using "conventional" inhibitory feedback blockers (see text). Figure consists of extracts from Figure 11, Figure 12, Figure 14 and Figure 17.

5.3 Ephaptic and pH-mediated feedback regulate different aspects of cone synaptic output

Our pharmacological data suggest that both ephaptic and pH-mediated feedback are functional in the mouse retina. Blocking hemichannels/iGluRs and clamping pH in the synaptic cleft resulted in some common but also some substantially different effects on light-evoked cone Ca^{2+} signals. Together with previous studies (reviewed in Thoreson and Mangel, 2012), the here observed effects indicate that both mechanisms may represent two sides of a complex feedback system that ensures reliable information transfer from cones to bipolar cells.

We propose that ephaptic feedback is involved in controlling the cone terminal's resting Ca^{2+}, as presenting light in a cone's receptive field surround reduced the Ca^{2+} level – an effect that was attenuated by CBX. Also with full-field stimulation, blocking ephaptic feedback with CBX or cobalt (Kamermans et al., 2001; Fahrenfort et al., 2004) increased the cone resting Ca^{2+} level. In contrast, blocking pH-mediated feedback with HEPES (Hirasawa and Kaneko, 2003) did not have consistent effects on the cone resting Ca^{2+} level. We think that the observed CBX effects on the cone Ca^{2+} level reflect modulation of ephaptic feedback because we could exclude other potential routes of CBX action, such as the disruption of the gap-junctionally coupled rod-cone network (Tsukamoto et al., 2001) or the direct or indirect modulation of iGluR-mediated currents. Also, because CBX increased Ca^{2+} levels, an unspecific inhibitory effect on VGCCs (Vessey et al., 2004) is unlikely. Moreover, CBX also increased the bright flash-evoked responses in cones (Figure 21B, left), consistent with blocking inhibitory feedback (Kamermans et al., 2001). Functionally, ephaptic feedback may be important for setting the gain of cone excitability, and thus keeping the cones responsive at different background light adaptation states.

In comparison, the effects of pH-mediated feedback were much more diverse and strongly depended on the stimulus protocol (Figure 21B, right): for instance, when high contrast bright flashes were presented, the cone Ca^{2+} response increased in the presence of HEPES, pointing at "conventional" inhibitory pH-mediated feedback, whereas with lower contrast bright flashes the cone Ca^{2+} response decreased in the presence of HEPES, indicative of excitatory feedback. This suggests that pH-mediated feedback results in a "compression" of the cones' response range to bright flashes: high contrasts attenuate, whereas low contrasts accentuate the responses. The pH of the synaptic cleft is controlled by a large number of pH-regulating mechanisms, including proton or bicarbonate-permeable channels and exchangers, the activity of which strongly depends on the horizontal cell membrane potential (reviewed in Chesler,

2003). Therefore, depending on the stimulus contrast, one or the other pH-regulating mechanisms may dominate, potentially resulting in net pH changes of different polarity for lower and higher contrast, and leading to the respective (opposite) effects on the cone Ca^{2+} responses.

Taken together, this work suggests that in the mouse retina both ephaptic and pH-mediated feedback may act together and form a complex feedback system: *(i)* the ephaptic feedback sets the cone's output gain by adjusting the cone resting Ca^{2+} level, thereby adapting the cone output to the overall background light intensity. *(ii)* the pH-mediated feedback compresses the cone output depending on the light stimulus contrast, possibly to maintain the cone response within its dynamic range. *(iii)* interestingly, both mechanisms appear to also affect the kinetics of the cone's dark response.

5.4 What role does GABA play in the outer mouse retina?

The first hypothesis forwarded about horizontal cell feedback involved a direct GABAergic pathway in the salamander retina (Wu, 1986): GABA released by horizontal cells inhibits cones via GABA receptors on their pedicles. Over the years and, in particular recently (Endeman et al., 2012; Liu et al., 2013), our view of the role of GABA in horizontal cell feedback became more differentiated. The data presented here confirm that GABAergic transmission plays a role in modulating cone output signals, but not via the classical pathway: No ionotropic GABA receptors were detected on cone terminals and GABA receptor blockers did not affect the cone light response, arguing against a direct action of GABA at cone terminals. Yet, application of GABA resulted in larger cone light responses. How can this GABA effect be explained?

One possibility is that GABA acts on horizontal cells, which have been functionally shown to express $GABA_A$ receptors (Feigenspan and Weiler, 2004), thereby increasing the horizontal cell membrane conductance and shunting of the cation current flow through hemichannels (Endeman et al., 2012). This way, GABA would reduce ephaptic feedback, resulting in an elevated cone Ca^{2+} level and larger light-evoked Ca^{2+} signals – similar to what we observed in our CBX experiments. Alternatively, GABA activating auto-receptors on horizontal cells could also affect the pH-mediated feedback mechanism – as recently proposed by Liu and co-workers in the rat retina (Liu et al., 2013): GABA receptors are permeable for both chloride and bicarbonate (Bormann et al., 1987; Kaila et al., 1993; Liu et al., 2013), and release of GABA by horizontal cells and opening of GABA auto-receptors induces an outflow of bicarbonate from horizontal cells into the synaptic cleft, when the membrane potential is more negative than the equilibrium potential for bicarbonate (at physiological pH usually ~0 mV, Dallwig et al., 1999). Synaptic cleft alkalinisation by bicarbonate increases the activity of cone VGCCs and disinhibits cones (Liu et al.,

2013). Under our experimental conditions with horizontal cells very likely below 0 mV, it is therefore conceivable that GABA receptor activation increases VGCC activity via the aforementioned pathway. However, since direction and strength of the bicarbonate current critically depend on both the bicarbonate reversal potential and the horizontal cell's polarization state, it is difficult to ultimately ascribe our GABA findings to the pathway proposed by Liu et al. (2013) or, alternatively, to a shunting effect (Endeman et al., 2012). Noteworthy, apart from horizontal cells, also GABAergic interplexiform cells could be the source of GABA release in the outer retina (Dedek et al., 2009). Since this type of amacrine cell connects the inner with the outer retina, inner retinal signal processing could affect the processing at the photoreceptor synapse by GABA release.

Taken together, in the mouse retina, GABAergic transmission likely modulates ephaptic and/or pH mediated feedback rather than providing direct feedback to cones.

5.5 Outlook

In this project, we used pharmacology to dissect the different horizontal cell feedback mechanisms thought to form the basis of the synaptic control of neurotransmitter release from photoreceptors. Based on the different effects on light-evoked Ca^{2+} signals in cones observed when different feedback mechanisms were selectively blocked, we concluded that ephaptic and pH-mediated feedback may fulfil distinct functions in shaping cone output, and we hypothesized that this might be important to adjust the photoreceptor output to changing ambient light levels and stimulus contrasts. In future, it will be interesting to use the same experimental approach like in this study but with substantially different background light levels (e.g. mesopic *vs.* high photopic) to test if specific aspects of light adaptation, i.e. sensitivity and operating range, in cones are compromised when ephaptic and/or pH-mediated feedback are pharmacologically blocked.

Pharmacological intervention, however, has the disadvantage that it requires the use of many drugs with (ideally) different mechanisms of action to exclude most of the potential unspecific effects of individual drugs – as was the case in this study. A "cleaner" and therefore more reliable approach to block feedback would be to genetically interfere with different components that are thought to be required for feedback, e.g. Pannexin 1 hemichannels (Kranz et al., 2013). Ideally, these cellular components should be either genetically silenced using AAVs or knocked out after the animal has completed its development (conditional knock out) to exclude confounding effects, such as compensatory expression of other channels, frequently encountered using "simple" knock out animals. This way, recordings from the

output neurons of the retina, the ganglion cells, or even behavioural experiments could be employed to explore the role(s) of horizontal cell to cone feedback for mammals like the mouse. Such an approach has been recently demonstrated in zebrafish by Klaassen and co-workers, who genetically interfered with the hemichannels, the key elements of ephaptic feedback, and found reduced contrast sensitivity at the behavioural level (Klaassen et al., 2011). Performing similar genetic experiments to investigate mainly the pH-mediated feedback, however, would be more challenging, since pH-mediated feedback is probably mediated by many different pH-regulating mechanisms (see 2.7.4). Importantly, because both ephaptic and pH-mediated feedback may be interconnected – hemichannels are pH-sensitive (Trexler et al., 1999) and maybe permeable to protons (Zaniboni et al., 2003; Wang et al., 2014) – it will be necessary to further physiologically characterize potential feedback candidates to estimate their relative contribution to the ephaptic and pH-mediated mechanism within this complex feedback system.

It will be also exciting to explore if similar feedback systems like that at the photoreceptor synapse can be found in other parts of the central nervous system. Knowing other examples for such an intricate feedback system may help understanding why neurotransmitter release from photoreceptors is controlled in this peculiar manner. Is it because the output of these cells has to be adjusted to function over a broad range of ambient light levels covering more than ten orders of magnitude (Rodieck, 1998), or is it because the output of these cells has to be precisely controlled over time by feedback mechanisms with different time constants? These questions might represent tasks that probably cannot be accomplished by, for instance, a simple inhibitory GABAergic feedback. The prerequisites for both ephaptic and pH-mediated feedback are present in many parts of the brain. In case of the ephaptic mechanism, these are current sinks on dendrites, a high intersynaptic resistance and voltage-sensitive channels on the opposing cell (Vroman et al., 2013) – necessities that are e.g. met by the large synapse between mossy fibres and CA3 pyramidal cell dendrites in the hippocampus (Berretta et al., 2000). For the pH-mediated mechanism, pH-regulating channels, ion exchangers and pumps are necessary – most of the components which are expressed by every neuron because pH regulation is critical for homeostasis (reviewed in Chesler, 2003). In this light, it is therefore well possible that also at other synapses in the central nervous system feedback pathways turn out to be more sophisticated than previously thought.

6 Tables

6.1 Pharmacology to test the ephaptic feedback hypothesis

	Number of mice/slices/cells	Control	Drug	Wash
CBX, bath application				
Bright responses (95% contrast)				
Normalized R_{base}	2/2/15	1.0	1.289±0.031 (***)	1.145±0.030 (***)
Normalized R_A	2/2/15	1.0	1.329±0.119 (*)	0.913±0.086
PI	2/2/15	0.033±0.008	0.019±0.009	0.055±0.010
Bright responses (51% contrast)				
Normalized R_{base}	2/3/14	1.0	1.293±0.031 (***)	1.090±0.0284(*)
Normalized R_A	2/3/14	1.0	4.244±0.669 (***)	0.588±0.129 (**)
PI	2/3/14	0.094±0.021	0.048±0.010	0.124±0.024
Dark responses (-23% contrast)				
Normalized R_A	2/3/14	1.0	1.04±0.11	0.75±0.09 (*)
PI	2/3/14	0.234±0.035	0.103±0.032 (**)	0.314±0.044
Dark responses (-39% contrast)				
Normalized R_{base}	1/2/7	1.0	1.155±0.042 (*)	0.979±0.033
Normalized R_A	1/2/7	1.0	1.044±0.176	0.775±0.079
PI	1/2/7	0.180±0.041	0.126±0.021	0.150±0.031
CBX, puff application				
Bright responses (95% contrast)				
Normalized R_{base}	3/3/32	1.0	1.154±0.013 (***)	1.071±0.013 (***)
Normalized R_A	3/3/32	1.0	1.395±0.122 (*)	1.287±0.090 (**)
PI	3/3/32	0.074±0.010	0.067±0.011	0.043±0.006 (*)
Dark responses (-39% contrast)				
Normalized R_{base}	1/1/5	1.0	1.090±0.023	1.030±0.039
Normalized R_A	1/1/5	1.0	0.952±0.037	0.956±0.049
PI	1/1/5	0.167±0.042	0.090±0.040	0.154±0.033
cobalt, bath application				
Bright responses (51% contrast)				
Normalized R_{base}	1/4/12	1.0	0.872±0.018 (***)	1.114±0.023 (**)
Normalized R_A	1/4/12	1.0	0.168±0.043 (***)	1.487±0.231 (*)
PI	1/4/12	0.082±0.030	0.258±0.074	0.066±0.016
Dark responses (-23% contrast)				
Normalized R_A	1/4/12	1.0	0.783±0.104 (*)	0.761±0.066 (**)
PI	1/4/12	0.046±0.018	0.127±0.033	0.141±0.053
CBX + NBQX, bath application				
Bright responses (51% contrast)				
Normalized R_{base}	2/3/9	1.0	1.427±0.053 (**)	1.096±0.022 (**)
Normalized R_A	2/3/9	1.0	5.561±1.399 (**)	1.226±0.267
PI	2/3/9	0.063±0.037	0.028±0.011	0.136±0.032
Dark responses (-23% contrast)				
Normalized R_A	2/3/9	1.0	0.813±0.102	0.763±0.073 (**)
PI	2/3/9	0.185±0.036	0.157±0.038	0.227±0.032

CBX, bath application, with PD168077				
Pooled Data from 2 protocols (95% and 51% contrast)				
Normalized R_{base}	1/4/6	1.0	1.295±0.090 (*)	1.142±0.034 (*)

Table 1: R_{base} and R_A are normalized to 1 in control condition. Results are presented as mean ± SEM. Statistical significance is indicated as *p<0.05, **p<0.01, and ***p<0.001 (control *vs.* drug or wash-out (wash) conditions). CBX, carbenoxolone.

6.2 Pharmacology to test the pH-mediated feedback hypothesis

	Number of mice/slices/cells	Control	Drug	Wash
HEPES, bath application				
Bright responses (95% contrast)				
Normalized R_{base}	4/9/28	1.0	1.076±0.020 (**)	1.035±0.023
Normalized R_A	4/9/28	1.0	1.158±0.059 (*)	0.875±0.058 (**)
PI	4/9/28	0.043±0.008	0.067±0.009	0.071±0.010 (*)
Bright responses (51% contrast)				
Normalized R_{base}	2/8/16	1.0	0.992±0.018	1.007±0.030
Normalized R_A	2/8/16	1.0	0.729±0.097 (**)	0.774±0.159 (**)
PI	2/8/16	0.080±0.013	0.107±0.031	0.144±0.023 (*)
Dark responses (-23% contrast)				
Normalized R_A	2/8/16	1.0	0.935±0.064	0.865±0.075
PI	2/8/16	0.322±0.051	0.165±0.026 (*)	0.222±0.038
Dark responses (-39% contrast)				
Normalized R_{base}	3/3/17	1.0	0.988±0.007	1.017±0.014
Normalized R_A	3/3/17	1.0	0.991±0.098	0.974±0.056
PI	3/3/17	0.207±0.035	0.161±0.028	0.305±0.044 (*)

Table 2: R_{base} and R_A are normalized to 1 in control condition. Results are presented as mean ± SEM. Statistical significance is indicated as *p<0.05, **p<0.01, and ***p<0.001 (control *vs.* drug or wash-out (wash) conditions).

6.3 Pharmacology to test the GABAergic feedback hypothesis

	Number of mice/slices/cells	Control	Drug	Wash
GABA, puff application				
Bright responses (95% contrast)				
Normalized R_{base}	1/2/19	1.0	1.039±0.008 (***)	1.051±0.017 (*)
Normalized R_A	1/2/19	1.0	1.057±0.022 (*)	0.978±0.030
PI	1/2/19	0.045±0.006	0.046±0.009	0.048±0.006
Dark responses (-39% contrast)				
Normalized R_{base}	1/2/19	1.0	1.043±0.012 (***)	1.017±0.015
Normalized R_A	1/2/19	1.0	1.187±0.046 (***)	0.967±0.046
PI	1/2/19	0.110±0.022	0.082±0.020	0.123±0.025
Gz + TPMPA, bath application				
Bright responses (95% contrast)				
Normalized R_{base}	2/4/19	1.0	0.992±0.021	0.974±0.029
Normalized R_A	2/4/19	1.0	1.005±0.070	0.908±0.057
PI	2/4/19	0.040±0.008	0.047±0.005	0.053±0.007
Dark responses (-39% contrast)				
Normalized R_{base}	4/5/10	1.0	1.013±0.016	0.991±0.019
Normalized R_A	4/5/10	1.0	0.933±0.086	0.852±0.084
PI	4/5/10	0.131±0.040	0.090±0.044	0.141±0.042

Table 3: R_{base} and R_A are normalized to 1 in control condition. Results are presented as mean ± SEM. Indicated statistical significance: control *vs.* drug or wash-out (wash) conditions. Statistical significance is indicated as *p<0.05, **p<0.01, and ***p<0.001 (control *vs.* drug or wash-out (wash) conditions). Gz, Gabazine.

6.4 Pharmacology to manipulate the activity state of horizontal cells

	Number of mice/slices/cells	Control	Drug	Wash
NBQX, bath application				
Bright responses (95% contrast)				
Normalized R_{base}	2/5/18	1.0	1.143±0.031 (***)	1.039±0.047
Normalized R_A	2/5/18	1.0	1.080±0.069	0.892±0.050
PI	2/5/18	0.031±0.006	0.043±0.008	0.054±0.011
AMPA/kainate, bath application				
Bright responses (95% contrast)				
Normalized R_{base}	2/7/21	1.0	0.955±0.014 (*)	0.971±0.015
Normalized R_A	2/7/21	1.0	0.758±0.052 (***)	0.784±0.048 (***)
PI	2/7/21	0.027±0.005	0.027±0.005	0.028±0.004

Table 4: R_{base} and R_A are normalized to 1 in control condition. Results are presented as mean ± SEM. Indicated statistical significance: control *vs.* drug or wash-out (wash) conditions. Statistical significance is indicated as *p<0.05, **p<0.01, and ***p<0.001 (control *vs.* drug or wash out (wash) conditions).

7 References

Babai N, Thoreson WB (2009) Horizontal cell feedback regulates calcium currents and intracellular calcium levels in rod photoreceptors of salamander and mouse retina. The Journal of physiology 587:2353-2364.

Babai N, Morgans CW, Thoreson WB (2010) Calcium-induced calcium release contributes to synaptic release from mouse rod photoreceptors. Neuroscience 165:1447-1456.

Baden T, Berens P, Bethge M, Euler T (2013a) Spikes in mammalian bipolar cells support temporal layering of the inner retina. Current biology : CB 23:48-52.

Baden T, Schubert T, Chang L, Wei T, Zaichuk M, Wissinger B, Euler T (2013b) A Tale of Two Retinal Domains: Near-Optimal Sampling of Achromatic Contrasts in Natural Scenes through Asymmetric Photoreceptor Distribution. Neuron 80:1206-1217.

Barlow HB (1953) Summation and inhibition in the frog's retina. The Journal of physiology 119:69-88.

Barlow HB, Levick WR (1965) The mechanism of directionally selective units in rabbit's retina. The Journal of physiology 178:477-504.

Barlow HB, Fitzhugh R, Kuffler SW (1957) Change of organization in the receptive fields of the cat's retina during dark adaptation. The Journal of physiology 137:338-354.

Baylor DA, Fuortes MG, O'Bryan PM (1971) Receptive fields of cones in the retina of the turtle. The Journal of physiology 214:265-294.

Baylor DA, Lamb TD, Yau KW (1979) Responses of retinal rods to single photons. J Physiol 288:613-634.

Berretta N, Rossokhin AV, Kasyanov AM, Sokolov MV, Cherubini E, Voronin LL (2000) Postsynaptic hyperpolarization increases the strength of AMPA-mediated synaptic transmission at large synapses between mossy fibers and CA3 pyramidal cells. Neuropharmacology 39:2288-2301.

Berson DM (2003) Strange vision: ganglion cells as circadian photoreceptors. Trends in neurosciences 26:314-320.

Bloomfield SA, Dacheux RF (2001) Rod vision: pathways and processing in the mammalian retina. Progress in retinal and eye research 20:351-384.

Bloomfield SA, Volgyi B (2009) The diverse functional roles and regulation of neuronal gap junctions in the retina. Nat Rev Neurosci 10:495-506.

Bormann J, Hamill OP, Sakmann B (1987) Mechanism of anion permeation through channels gated by glycine and gamma-aminobutyric acid in mouse cultured spinal neurones. The Journal of physiology 385:243-286.

Breuninger T, Puller C, Haverkamp S, Euler T (2011) Chromatic bipolar cell pathways in the mouse retina. The Journal of neuroscience : the official journal of the Society for Neuroscience 31:6504-6517.

Brockway LM, Zhou ZH, Bubien JK, Jovov B, Benos DJ, Keyser KT (2002) Rabbit retinal neurons and glia express a variety of ENaC/DEG subunits. Am J Physiol Cell Physiol 283:C126-134.

Bruzzone R, Barbe MT, Jakob NJ, Monyer H (2005) Pharmacological properties of homomeric and heteromeric pannexin hemichannels expressed in Xenopus oocytes. Journal of neurochemistry 92:1033-1043.

Burkhardt DA (1995) The influence of center-surround antagonism on light adaptation in cones in the retina of the turtle. Visual neuroscience 12:877-885.

Burns ME, Baylor DA (2001) Activation, deactivation, and adaptation in vertebrate photoreceptor cells. Annu Rev Neurosci 24:779-805.

Byzov AL, Shura-Bura TM (1986) Electrical feedback mechanism in the processing of signals in the outer plexiform layer of the retina. Vision research 26:33-44.

Chang L, Breuninger T, Euler T (2013) Chromatic coding from cone-type unselective circuits in the mouse retina. Neuron 77:559-571.

Chen XH, Bezprozvanny I, Tsien RW (1996) Molecular basis of proton block of L-type Ca2+ channels. The Journal of general physiology 108:363-374.
Chesler M (2003) Regulation and modulation of pH in the brain. Physiological reviews 83:1183-1221.
Cook PB, McReynolds JS (1998) Lateral inhibition in the inner retina is important for spatial tuning of ganglion cells. Nature neuroscience 1:714-719.
Corey DP, Dubinsky JM, Schwartz EA (1984) The calcium current in inner segments of rods from the salamander (Ambystoma tigrinum) retina. The Journal of physiology 354:557-575.
Cueva JG, Haverkamp S, Reimer RJ, Edwards R, Wassle H, Brecha NC (2002) Vesicular gamma-aminobutyric acid transporter expression in amacrine and horizontal cells. The Journal of comparative neurology 445:227-237.
Dacey DM, Lee BB (1994) The 'blue-on' opponent pathway in primate retina originates from a distinct bistratified ganglion cell type. Nature 367:731-735.
Dacheux RF, Miller RF (1981) An intracellular electrophysiological study of the ontogeny of functional synapses in the rabbit retina. I. Receptors, horizontal, and bipolar cells. The Journal of comparative neurology 198:307-326.
Dallwig R, Deitmer JW, Backus KH (1999) On the mechanism of GABA-induced currents in cultured rat cortical neurons. Pflugers Archiv : European journal of physiology 437:289-297.
Davenport CM, Detwiler PB, Dacey DM (2008) Effects of pH buffering on horizontal and ganglion cell light responses in primate retina: evidence for the proton hypothesis of surround formation. The Journal of neuroscience : the official journal of the Society for Neuroscience 28:456-464.
Deans MR, Paul DL (2001) Mouse horizontal cells do not express connexin26 or connexin36. Cell communication & adhesion 8:361-366.
Dedek K, Breuninger T, de Sevilla Muller LP, Maxeiner S, Schultz K, Janssen-Bienhold U, Willecke K, Euler T, Weiler R (2009) A novel type of interplexiform amacrine cell in the mouse retina. The European journal of neuroscience 30:217-228.
Demb JB, Haarsma L, Freed MA, Sterling P (1999) Functional circuitry of the retinal ganglion cell's nonlinear receptive field. The Journal of neuroscience : the official journal of the Society for Neuroscience 19:9756-9767.
Deniz S, Wersinger E, Schwab Y, Mura C, Erdelyi F, Szabo G, Rendon A, Sahel JA, Picaud S, Roux MJ (2011) Mammalian retinal horizontal cells are unconventional GABAergic neurons. Journal of neurochemistry 116:350-362.
Denk W, Strickler JH, Webb WW (1990) Two-photon laser scanning fluorescence microscopy. Science 248:73-76.
DeVries SH (2000) Bipolar cells use kainate and AMPA receptors to filter visual information into separate channels. Neuron 28:847-856.
DeVries SH (2001) Exocytosed protons feedback to suppress the Ca2+ current in mammalian cone photoreceptors. Neuron 32:1107-1117.
Drobizhev M, Makarov NS, Tillo SE, Hughes TE, Rebane A (2011) Two-photon absorption properties of fluorescent proteins. Nature methods 8:393-399.
Duebel J, Haverkamp S, Schleich W, Feng G, Augustine GJ, Kuner T, Euler T (2006) Two-photon imaging reveals somatodendritic chloride gradient in retinal ON-type bipolar cells expressing the biosensor Clomeleon. Neuron 49:81-94.
Eggers ED, Lukasiewicz PD (2011) Multiple pathways of inhibition shape bipolar cell responses in the retina. Visual neuroscience 28:95-108.
Endeman D, Fahrenfort I, Sjoerdsma T, Steijaert M, Ten Eikelder H, Kamermans M (2012) Chloride currents in cones modify feedback from horizontal cells to cones in goldfish retina. The Journal of physiology 590:5581-5595.

Enz R, Brandstatter JH, Wassle H, Bormann J (1996) Immunocytochemical localization of the GABAc receptor rho subunits in the mammalian retina. The Journal of neuroscience : the official journal of the Society for Neuroscience 16:4479-4490.

Ettaiche M, Deval E, Cougnon M, Lazdunski M, Voilley N (2006) Silencing acid-sensing ion channel 1a alters cone-mediated retinal function. The Journal of neuroscience : the official journal of the Society for Neuroscience 26:5800-5809.

Euler T, Schneider H, Wassle H (1996) Glutamate responses of bipolar cells in a slice preparation of the rat retina. The Journal of neuroscience : the official journal of the Society for Neuroscience 16:2934-2944.

Euler T, Detwiler PB, Denk W (2002) Directionally selective calcium signals in dendrites of starburst amacrine cells. Nature 418:845-852.

Euler T, Hausselt SE, Margolis DJ, Breuninger T, Castell X, Detwiler PB, Denk W (2009) Eyecup scope--optical recordings of light stimulus-evoked fluorescence signals in the retina. Pflugers Archiv : European journal of physiology 457:1393-1414.

Fahey PK, Burkhardt DA (2003) Center-surround organization in bipolar cells: symmetry for opposing contrasts. Visual neuroscience 20:1-10.

Fahrenfort I, Habets RL, Spekreijse H, Kamermans M (1999) Intrinsic cone adaptation modulates feedback efficiency from horizontal cells to cones. The Journal of general physiology 114:511-524.

Fahrenfort I, Sjoerdsma T, Ripps H, Kamermans M (2004) Cobalt ions inhibit negative feedback in the outer retina by blocking hemichannels on horizontal cells. Visual neuroscience 21:501-511.

Fahrenfort I, Klooster J, Sjoerdsma T, Kamermans M (2005) The involvement of glutamate-gated channels in negative feedback from horizontal cells to cones. Progress in brain research 147:219-229.

Fahrenfort I, Steijaert M, Sjoerdsma T, Vickers E, Ripps H, van Asselt J, Endeman D, Klooster J, Numan R, ten Eikelder H, von Gersdorff H, Kamermans M (2009) Hemichannel-mediated and pH-based feedback from horizontal cells to cones in the vertebrate retina. PloS one 4:e6090.

Feigenspan A, Weiler R (2004) Electrophysiological properties of mouse horizontal cell GABAA receptors. Journal of neurophysiology 92:2789-2801.

Feigenspan A, Janssen-Bienhold U, Hormuzdi S, Monyer H, Degen J, Sohl G, Willecke K, Ammermuller J, Weiler R (2004) Expression of connexin36 in cone pedicles and OFF-cone bipolar cells of the mouse retina. The Journal of neuroscience : the official journal of the Society for Neuroscience 24:3325-3334.

Fu Y, Yau KW (2007) Phototransduction in mouse rods and cones. Pflugers Archiv : European journal of physiology 454:805-819.

Hampson EC, Weiler R, Vaney DI (1994) pH-gated dopaminergic modulation of horizontal cell gap junctions in mammalian retina. Proceedings Biological sciences / The Royal Society 255:67-72.

Hartline HK, Ratliff F (1957) Inhibitory interaction of receptor units in the eye of Limulus. The Journal of general physiology 40:357-376.

Hartline HK, Wagner HG, Ratliff F (1956) Inhibition in the eye of Limulus. The Journal of general physiology 39:651-673.

Haugh-Scheidt L, Ripps H (1998) pH regulation in horizontal cells of the skate retina. Experimental eye research 66:449-463.

Haverkamp S, Wässle H (2000) Immunocytochemical analysis of the mouse retina. The Journal of comparative neurology 424:1-23.

Haverkamp S, Grunert U, Wassle H (2000) The cone pedicle, a complex synapse in the retina. Neuron 27:85-95.

Haverkamp S, Wassle H, Duebel J, Kuner T, Augustine GJ, Feng G, Euler T (2005) The primordial, blue-cone color system of the mouse retina. The Journal of neuroscience : the official journal of the Society for Neuroscience 25:5438-5445.

He S, Weiler R, Vaney DI (2000) Endogenous dopaminergic regulation of horizontal cell coupling in the mammalian retina. The Journal of comparative neurology 418:33-40.

Herrmann R, Heflin SJ, Hammond T, Lee B, Wang J, Gainetdinov RR, Caron MG, Eggers ED, Frishman LJ, McCall MA, Arshavsky VY (2011) Rod vision is controlled by dopamine-dependent sensitization of rod bipolar cells by GABA. Neuron 72:101-110.

Hirano AA, Brandstatter JH, Morgans CW, Brecha NC (2011) SNAP25 expression in mammalian retinal horizontal cells. The Journal of comparative neurology 519:972-988.

Hirasawa H, Kaneko A (2003) pH changes in the invaginating synaptic cleft mediate feedback from horizontal cells to cone photoreceptors by modulating Ca2+ channels. The Journal of general physiology 122:657-671.

Hodgkin AL, Nunn BJ (1988) Control of light-sensitive current in salamander rods. The Journal of physiology 403:439-471.

Hubel DH, Wiesel TN (1962) Receptive fields, binocular interaction and functional architecture in the cat's visual cortex. The Journal of physiology 160:106-154.

Huberman AD, Niell CM (2011) What can mice tell us about how vision works? Trends in neurosciences 34:464-473.

Ichinose T, Lukasiewicz PD (2005) Inner and outer retinal pathways both contribute to surround inhibition of salamander ganglion cells. The Journal of physiology 565:517-535.

Jackman SL, Babai N, Chambers JJ, Thoreson WB, Kramer RH (2011) A positive feedback synapse from retinal horizontal cells to cone photoreceptors. PLoS biology 9:e1001057.

Jackman SL, Choi SY, Thoreson WB, Rabl K, Bartoletti TM, Kramer RH (2009) Role of the synaptic ribbon in transmitting the cone light response. Nature neuroscience 12:303-310.

Jacobs GH (1993) The distribution and nature of colour vision among the mammals. Biological reviews of the Cambridge Philosophical Society 68:413-471.

Jacobs GH, Neitz J, Deegan JF, 2nd (1991) Retinal receptors in rodents maximally sensitive to ultraviolet light. Nature 353:655-656.

Janssen-Bienhold U, Trumpler J, Hilgen G, Schultz K, Muller LP, Sonntag S, Dedek K, Dirks P, Willecke K, Weiler R (2009) Connexin57 is expressed in dendro-dendritic and axo-axonal gap junctions of mouse horizontal cells and its distribution is modulated by light. The Journal of comparative neurology 513:363-374.

Jefferys JG (1995) Nonsynaptic modulation of neuronal activity in the brain: electric currents and extracellular ions. Physiological reviews 75:689-723.

Jeon CJ, Strettoi E, Masland RH (1998) The major cell populations of the mouse retina. The Journal of neuroscience : the official journal of the Society for Neuroscience 18:8936-8946.

Johnson JE, Jr., Perkins GA, Giddabasappa A, Chaney S, Xiao W, White AD, Brown JM, Waggoner J, Ellisman MH, Fox DA (2007) Spatiotemporal regulation of ATP and Ca2+ dynamics in vertebrate rod and cone ribbon synapses. Molecular vision 13:887-919.

Jonz MG, Barnes S (2007) Proton modulation of ion channels in isolated horizontal cells of the goldfish retina. The Journal of physiology 581:529-541.

Kaila K, Voipio J, Paalasmaa P, Pasternack M, Deisz RA (1993) The role of bicarbonate in GABAA receptor-mediated IPSPs of rat neocortical neurones. The Journal of physiology 464:273-289.

Kamermans M, Spekreijse H (1999) The feedback pathway from horizontal cells to cones. A mini review with a look ahead. Vision research 39:2449-2468.

Kamermans M, Fahrenfort I (2004) Ephaptic interactions within a chemical synapse: hemichannel-mediated ephaptic inhibition in the retina. Current opinion in neurobiology 14:531-541.

Kamermans M, Fahrenfort I, Schultz K, Janssen-Bienhold U, Sjoerdsma T, Weiler R (2001) Hemichannel-mediated inhibition in the outer retina. Science 292:1178-1180.

Kamermans M, Vroman R, Klaassen L, Sjoerdsma T, Smith R, Howlett M (2013) The kinetic properties of negative feedback from horizontal cells to cones. In: Association for Research in Vision and Ophthalmology.

Klaassen LJ, Sun Z, Steijaert MN, Bolte P, Fahrenfort I, Sjoerdsma T, Klooster J, Claassen Y, Shields CR, Ten Eikelder HM, Janssen-Bienhold U, Zoidl G, McMahon DG, Kamermans M (2011) Synaptic transmission from horizontal cells to cones is impaired by loss of connexin hemichannels. PLoS biology 9:e1001107.

Kolb H (1970) Organization of the outer plexiform layer of the primate retina: electron microscopy of Golgi-impregnated cells. Philosophical transactions of the Royal Society of London Series B, Biological sciences 258:261-283.

Kolb H (1974) The connections between horizontal cells and photoreceptors in the retina of the cat: electron microscopy of Golgi preparations. The Journal of comparative neurology 155:1-14.

Kraaij DA, Spekreijse H, Kamermans M (2000) The nature of surround-induced depolarizing responses in goldfish cones. The Journal of general physiology 115:3-16.

Kranz K, Dorgau B, Pottek M, Herrling R, Schultz K, Bolte P, Monyer H, Penuela S, Laird DW, Dedek K, Weiler R, Janssen-Bienhold U (2013) Expression of Pannexin1 in the outer plexiform layer of the mouse retina and physiological impact of its knockout. The Journal of comparative neurology 521:1119-1135.

Kreitzer MA, Collis LP, Molina AJ, Smith PJ, Malchow RP (2007) Modulation of extracellular proton fluxes from retinal horizontal cells of the catfish by depolarization and glutamate. The Journal of general physiology 130:169-182.

Kuffler SW (1953) Discharge patterns and functional organization of mammalian retina. Journal of neurophysiology 16:37-68.

Lankheet MJ, Frens MA, van de Grind WA (1990) Spatial properties of horizontal cell responses in the cat retina. Vision research 30:1257-1275.

Li H, Zhang Z, Blackburn MR, Wang SW, Ribelayga CP, O'Brien J (2013) Adenosine and dopamine receptors coregulate photoreceptor coupling via gap junction phosphorylation in mouse retina. The Journal of neuroscience : the official journal of the Society for Neuroscience 33:3135-3150.

Liu X, Hirano AA, Sun X, Brecha NC, Barnes S (2013) Calcium channels in rat horizontal cells regulate feedback inhibition of photoreceptors through an unconventional GABA- and pH-sensitive mechanism. The Journal of physiology.

Lukasiewicz PD (2005) Synaptic mechanisms that shape visual signaling at the inner retina. Progress in brain research 147:205-218.

Luo D, Kefalov V, Yau K (2008) Phototransduction in rods and cones. San Diego, CA: Academic Press.

Mangel SC (1991) Analysis of the horizontal cell contribution to the receptive field surround of ganglion cells in the rabbit retina. The Journal of physiology 442:211-234.

Mank M, Reiff DF, Heim N, Friedrich MW, Borst A, Griesbeck O (2006) A FRET-based calcium biosensor with fast signal kinetics and high fluorescence change. Biophysical journal 90:1790-1796.

Marc RE, Murry RF, Basinger SF (1995) Pattern recognition of amino acid signatures in retinal neurons. The Journal of neuroscience : the official journal of the Society for Neuroscience 15:5106-5129.

Masland RH (2012) The neuronal organization of the retina. Neuron 76:266-280.

Masu M, Iwakabe H, Tagawa Y, Miyoshi T, Yamashita M, Fukuda Y, Sasaki H, Hiroi K, Nakamura Y, Shigemoto R, et al. (1995) Specific deficit of the ON response in visual transmission by targeted disruption of the mGluR6 gene. Cell 80:757-765.

Matthews HR, Fain GL, Murphy RL, Lamb TD (1990) Light adaptation in cone photoreceptors of the salamander: a role for cytoplasmic calcium. The Journal of physiology 420:447-469.

McMahon MJ, Packer OS, Dacey DM (2004) The classical receptive field surround of primate parasol ganglion cells is mediated primarily by a non-GABAergic pathway. The Journal of neuroscience : the official journal of the Society for Neuroscience 24:3736-3745.

Mills SL, Tian LM, Hoshi H, Whitaker CM, Massey SC (2014) Three distinct blue-green color pathways in a Mammalian retina. The Journal of neuroscience : the official journal of the Society for Neuroscience 34:1760-1768.

Molina AJ, Verzi MP, Birnbaum AD, Yamoah EN, Hammar K, Smith PJ, Malchow RP (2004) Neurotransmitter modulation of extracellular H+ fluxes from isolated retinal horizontal cells of the skate. The Journal of physiology 560:639-657.

Morgans CW, Bayley PR, Oesch NW, Ren G, Akileswaran L, Taylor WR (2005) Photoreceptor calcium channels: insight from night blindness. Visual neuroscience 22:561-568.

Mustafi D, Engel AH, Palczewski K (2009) Structure of cone photoreceptors. Progress in retinal and eye research 28:289-302.

Nakatani K, Yau KW (1988) Calcium and light adaptation in retinal rods and cones. Nature 334:69-71.

Newman E, Reichenbach A (1996) The Muller cell: a functional element of the retina. Trends in neurosciences 19:307-312.

Ölveczky BP, Baccus SA, Meister M (2003) Segregation of object and background motion in the retina. Nature 423:401-408.

Packer OS, Verweij J, Li PH, Schnapf JL, Dacey DM (2010) Blue-yellow opponency in primate S cone photoreceptors. The Journal of neuroscience : the official journal of the Society for Neuroscience 30:568-572.

Peichl L, Gonzalez-Soriano J (1994) Morphological types of horizontal cell in rodent retinae: a comparison of rat, mouse, gerbil, and guinea pig. Visual neuroscience 11:501-517.

Pow DV, Barnett NL (2000) Developmental expression of excitatory amino acid transporter 5: a photoreceptor and bipolar cell glutamate transporter in rat retina. Neuroscience letters 280:21-24.

Prochnow N, Hoffmann S, Vroman R, Klooster J, Bunse S, Kamermans M, Dermietzel R, Zoidl G (2009) Pannexin1 in the outer retina of the zebrafish, Danio rerio. Neuroscience 162:1039-1054.

Pugh EN, Jr., Nikonov S, Lamb TD (1999) Molecular mechanisms of vertebrate photoreceptor light adaptation. Current opinion in neurobiology 9:410-418.

Ratliff F, Hartline HK (1959) The responses of Limulus optic nerve fibers to patterns of illumination on the receptor mosaic. The Journal of general physiology 42:1241-1255.

Rauen T, Kanner BI (1994) Localization of the glutamate transporter GLT-1 in rat and macaque monkey retinae. Neuroscience letters 169:137-140.

Rauen T, Taylor WR, Kuhlbrodt K, Wiessner M (1998) High-affinity glutamate transporters in the rat retina: a major role of the glial glutamate transporter GLAST-1 in transmitter clearance. Cell and tissue research 291:19-31.

Raviola E, Gilula NB (1973) Gap junctions between photoreceptor cells in the vertebrate retina. Proceedings of the National Academy of Sciences of the United States of America 70:1677-1681.

Ribelayga C, Cao Y, Mangel SC (2008) The circadian clock in the retina controls rod-cone coupling. Neuron 59:790-801.

Rodieck R (1998) The first steps in seeing. Sunderland, MA: Sinauer Ass. Inc.

Schmitz Y, Witkovsky P (1997) Dependence of photoreceptor glutamate release on a dihydropyridine-sensitive calcium channel. Neuroscience 78:1209-1216.

Schubert T, Euler T (2010) Retinal processing: global players like it local. Current biology : CB 20:R486-488.

Schubert T, Weiler R, Feigenspan A (2006) Intracellular calcium is regulated by different pathways in horizontal cells of the mouse retina. Journal of neurophysiology 96:1278-1292.

Schubert T, Huckfeldt RM, Parker E, Campbell JE, Wong RO (2010) Assembly of the outer retina in the absence of GABA synthesis in horizontal cells. Neural development 5:15.

Shelley J, Dedek K, Schubert T, Feigenspan A, Schultz K, Hombach S, Willecke K, Weiler R (2006) Horizontal cell receptive fields are reduced in connexin57-deficient mice. The European journal of neuroscience 23:3176-3186.

Shields CR, Klooster J, Claassen Y, Ul-Hussain M, Zoidl G, Dermietzel R, Kamermans M (2007) Retinal horizontal cell-specific promoter activity and protein expression of zebrafish connexin 52.6 and connexin 55.5. The Journal of comparative neurology 501:765-779.

Smith R (2008) Contributions of horizontal cells. San Diego, CA: Academic Press.

Steinberg RH (1985) Interactions between the retinal pigment epithelium and the neural retina. Doc Ophthalmol 60:327-346.

Stenkamp RE, Filipek S, Driessen CA, Teller DC, Palczewski K (2002) Crystal structure of rhodopsin: a template for cone visual pigments and other G protein-coupled receptors. Biochimica et biophysica acta 1565:168-182.

Sterling P, Matthews G (2005) Structure and function of ribbon synapses. Trends in neurosciences 28:20-29.

Ströh S, Sonntag S, Janssen-Bienhold U, Schultz K, Cimiotti K, Weiler R, Willecke K, Dedek K (2013) Cell-specific cre recombinase expression allows selective ablation of glutamate receptors from mouse horizontal cells. PloS one 8:e83076.

Sun Z, Risner ML, van Asselt JB, Zhang DQ, Kamermans M, McMahon DG (2012) Physiological and molecular characterization of connexin hemichannels in zebrafish retinal horizontal cells. Journal of neurophysiology 107:2624-2632.

Tatsukawa T, Hirasawa H, Kaneko A, Kaneda M (2005) GABA-mediated component in the feedback response of turtle retinal cones. Visual neuroscience 22:317-324.

Taylor WR, Morgans C (1998) Localization and properties of voltage-gated calcium channels in cone photoreceptors of Tupaia belangeri. Visual neuroscience 15:541-552.

Teranishi T, Negishi K, Kato S (1983) Dopamine modulates S-potential amplitude and dye-coupling between external horizontal cells in carp retina. Nature 301:243-246.

Thoreson WB (2007) Kinetics of synaptic transmission at ribbon synapses of rods and cones. Molecular neurobiology 36:205-223.

Thoreson WB, Mangel SC (2012) Lateral interactions in the outer retina. Progress in retinal and eye research 31:407-441.

Thoreson WB, Babai N, Bartoletti TM (2008) Feedback from horizontal cells to rod photoreceptors in vertebrate retina. The Journal of neuroscience : the official journal of the Society for Neuroscience 28:5691-5695.

Tovar KR, Maher BJ, Westbrook GL (2009) Direct actions of carbenoxolone on synaptic transmission and neuronal membrane properties. Journal of neurophysiology 102:974-978.

Toyoda J, Kujiraoka T (1982) Analyses of bipolar cell responses elicited by polarization of horizontal cells. The Journal of general physiology 79:131-145.

Trexler EB, Bukauskas FF, Bennett MV, Bargiello TA, Verselis VK (1999) Rapid and direct effects of pH on connexins revealed by the connexin46 hemichannel preparation. The Journal of general physiology 113:721-742.

Trümpler J, Dedek K, Schubert T, de Sevilla Muller LP, Seeliger M, Humphries P, Biel M, Weiler R (2008) Rod and cone contributions to horizontal cell light responses in the mouse retina. The Journal of neuroscience : the official journal of the Society for Neuroscience 28:6818-6825.

Tsukamoto Y, Morigiwa K, Ueda M, Sterling P (2001) Microcircuits for night vision in mouse retina. The Journal of neuroscience : the official journal of the Society for Neuroscience 21:8616-8623.

Van Essen D (2004) Organization of visual areas in macaque and human cerebral cortex. Cambridge, MA: MIT press.

VanLeeuwen M, Fahrenfort I, Sjoerdsma T, Numan R, Kamermans M (2009) Lateral gain control in the outer retina leads to potentiation of center responses of retinal neurons. The Journal of neuroscience : the official journal of the Society for Neuroscience 29:6358-6366.

Vanleeuwen MT, Joselevitch C, Fahrenfort I, Kamermans M (2007) The contribution of the outer retina to color constancy: a general model for color constancy synthesized from primate and fish data. Visual neuroscience 24:277-290.

Verweij J, Kamermans M, Spekreijse H (1996) Horizontal cells feed back to cones by shifting the cone calcium-current activation range. Vision research 36:3943-3953.

Verweij J, Hornstein EP, Schnapf JL (2003) Surround antagonism in macaque cone photoreceptors. The Journal of neuroscience : the official journal of the Society for Neuroscience 23:10249-10257.

Vessey JP, Lalonde MR, Mizan HA, Welch NC, Kelly ME, Barnes S (2004) Carbenoxolone inhibition of voltage-gated Ca channels and synaptic transmission in the retina. Journal of neurophysiology 92:1252-1256.

Vessey JP, Stratis AK, Daniels BA, Da Silva N, Jonz MG, Lalonde MR, Baldridge WH, Barnes S (2005) Proton-mediated feedback inhibition of presynaptic calcium channels at the cone photoreceptor synapse. The Journal of neuroscience : the official journal of the Society for Neuroscience 25:4108-4117.

Voronin LL (2000) Intrasynaptic ephaptic feedback in central synapses. Neuroscience and behavioral physiology 30:575-585.

Vroman R, Klaassen LJ, Kamermans M (2013) Ephaptic communication in the vertebrate retina. Frontiers in human neuroscience 7:612.

Wang TM, Holzhausen LC, Kramer RH (2014) Imaging an optogenetic pH sensor reveals that protons mediate lateral inhibition in the retina. Nature neuroscience.

Wässle H (2004) Parallel processing in the mammalian retina. Nature reviews Neuroscience 5:747-757.

Wei T, Schubert T, Paquet-Durand F, Tanimoto N, Chang L, Koeppen K, Ott T, Griesbeck O, Seeliger MW, Euler T, Wissinger B (2012) Light-driven calcium signals in mouse cone photoreceptors. The Journal of neuroscience : the official journal of the Society for Neuroscience 32:6981-6994.

Werblin FS (1978) Transmission along and between rods in the tiger salamander retina. The Journal of physiology 280:449-470.

Werblin FS, Dowling JE (1969) Organization of the retina of the mudpuppy, Necturus maculosus. II. Intracellular recording. Journal of neurophysiology 32:339-355.

Wu SM (1986) Effects of gamma-aminobutyric acid on cones and bipolar cells of the tiger salamander retina. Brain research 365:70-77.

Wu SM (1992) Feedback connections and operation of the outer plexiform layer of the retina. Current opinion in neurobiology 2:462-468.

Wu SM, Gao F, Maple BR (2000) Functional architecture of synapses in the inner retina: segregation of visual signals by stratification of bipolar cell axon terminals. The Journal of neuroscience : the official journal of the Society for Neuroscience 20:4462-4470.

Xin D, Bloomfield SA (1999) Dark- and light-induced changes in coupling between horizontal cells in mammalian retina. The Journal of comparative neurology 405:75-87.

Yang XL, Wu SM (1991) Feedforward lateral inhibition in retinal bipolar cells: input-output relation of the horizontal cell-depolarizing bipolar cell synapse. Proceedings of the National Academy of Sciences of the United States of America 88:3310-3313.

Yau KW, Nakatani K (1984) Cation selectivity of light-sensitive conductance in retinal rods. Nature 309:352-354.

Zaniboni M, Rossini A, Swietach P, Banger N, Spitzer KW, Vaughan-Jones RD (2003) Proton permeation through the myocardial gap junction. Circulation research 93:726-735.

Zhang AJ, Wu SM (2009) Receptive fields of retinal bipolar cells are mediated by heterogeneous synaptic circuitry. The Journal of neuroscience : the official journal of the Society for Neuroscience 29:789-797.